UNIVERSITY
OF
JOHANNESBURG

How to cite this thesis

Surname, Initial(s). (2012). Title of the thesis or dissertation (Doctoral Thesis / Master's Dissertation). Johannesburg: University of Johannesburg. Available from: http://hdl.handle.net/102000/0002 (Accessed: 22 August 2017).

Optimised orthogonal frequency-division multiplexing based communication systems for wireless environments

by

Martin Trollip

A dissertation submitted to the

Faculty of Engineering and the Built Environment

for the partial fulfilment of the requirements for the degree

Magister Ingeneriae

in

Electrical and Electronic Engineering Science

at the

University of Johannesburg

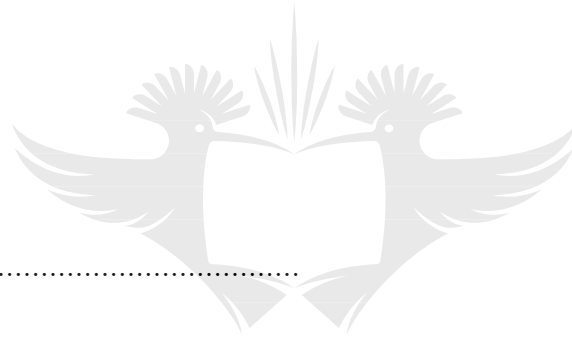Supervisor: Prof. Khmaies Ouahada

October 2018

To my loving mother, Theresa

Declaration

I, *Martin Trollip*, declare that this dissertation is my own work and material used from other sources has been acknowledged and referenced. This work has not been submitted for the purpose of another degree at any university other than the University of Johannesburg.

....

Signature   Date

Abstract

The demand for wireless access to the internet is constantly increasing and the applications such as social media, gaming and video require a high bandwidth connections. Mobile technologies are becoming more affordable and accessible. Existing telecommunications systems can be improved to ensure that it is sustainable for future generations.

Orthogonal Frequency Division Multiplexing (OFDM) is a good candidate which is already used widely in wireless applications. It is robust against many of the multipath effects commonly encountered in wireless channels. It also makes efficient use of the limited radio spectrum.

Certain parameters of the OFDM system have been investigated and recommendations on the optimal parameters are made in order to achieve the best bit error rate (BER) performance. These investigations have been conducted by designing a comprehensive and configurable simulation of the OFDM system, including an adapted modulator and demodulator and an accurate channel model.

The guard interval is an important design consideration as it counters Inter Symbol Interference (ISI). The optimal length of the guard interval should be less than 25% of the total symbol length. As shorter guard interval results in more usable bandwidth. The choice of quadrature amplitude modulation (QAM) scheme to use is also an important one and the optimal design depends on the throughput requirements of the system. The number of subcarriers depends on the available bandwidth and the subcarrier spacing.

A fundamental problem with OFDM is the high Peak to Average Power Ratio (PAPR). A high PAPR results in more expensive amplifiers, requiring more power, resulting in more power consumption and a reduced battery life on mobile devices. A simple, yet effective, PAPR reduction technique called clipping and filtering, making the system more relevant for modern day applications, was implemented.

A method of combining OFDM with spectral shaping techniques such as spectral null codes, is investigated. These codes can shape the power spectral density (PSD) of the system to have spectral null at desired frequencies. It has been shown that the PSD of OFDM systems can be shaped by making use of these techniques. Applications of this includes the usage of spectral nulls as a sensor for the quality of the channel. The transmitter and receiver was modified by adding a PSD detector at the modulator and demodulator. The results have shown that the spectrum can be shaped and that narrowband signals introduced in the channel will destroy the shaping, indicating that corruption occurred. The usage of spectral null codes did not degrade the system's performance.

Acknowledgements

I wish to express my gratitude towards everyone with whom I crossed paths during this journey and to all who ultimately enabled me to complete this work. Thanks to my family and friends for providing me with the continuous support and motivation, making this possible. Thanks to everyone who lend a helping hand in reviewing the content, language and grammar.

I thank my study leader Prof. Khmaies Ouahada, for his continued support, dedication and guidance. I am truly inspired by his knowledge and vigour.

Thanks to my employer and managers, Pheello, Pranen and Jamie for granting me the necessary study leave and support in order to focus on my dissertation and research. It would certainly have been impossible to complete this otherwise.

Thanks to my brother, Brendan for his support, proof reading and suggestions. Thanks to Gabriel and Heystek for their suggestions.

Thanks to my father, Eugene, who is always supportive and encouraging. *Dankie dat Pa altyd in my glo en my ondersteun.*

Finally, I wish to express my gratitude towards the staff of the Department of Electrical and Electronic Engineering at the University of Johannesburg.

Contents

List of Abbreviations

3G	Third Generation of Mobile Telecommunications Technology
3GPP	Third Generation Partnership Project
3GPP LTE	Third Generation Partnership Project Long Term Evolution
4G	Fourth Generation of Mobile Telecommunications Technology
ADC	Analogue to Digital Conversion
ADSL	Asymmetric Digital Subscriber Line
ASK	Amplitude Shift Keying
AWGN	Additive White Gaussian Noise
BER	Bit Error Rate
BPKS	Binary Phase-Shift Keying
BSS	Binary Symmetric Information Source
CCDF	Complementary Cumulative Distribution Function
CD	Compact Disc
CDMA	Code Division Multiple Access
CP	Cyclic Prefix
DAB	Digital Audio Broadcasting
DAC	Digital to Analogue Conversion
DFT	Discrete Fourier Transform
DSP	Digital Signal Processing
DSSS	Direct Sequence Spread Spectrum
DVB - H	Digital Video Broadcasting - Handheld
DVB - T	Digital Video Broadcasting - Return Channel Terrestrial
DVD	Digital Versatile Disc
ECC	Error Correctional Codes
ECSA	Engineering Council of South Africa
EMI	Electromagnetic Interference
FCC	Federal Communications Commission
FDM	Frequency Division Multiplexing
FFT	Fast Fourier Transform
FIR	Finite Impulse Response
FPGA	Field-Programmable Gate Array
FSK	Frequency Shift Keying
GDS	Gradient Decent Search
GUI	Graphical User Interface
GSM	Digital cellular radio (Global System for Mobile communication)
HPA	High Powered Amplifiers
IC	Integrated Circuit
ICASA	Independent Communications Authority of South Africa
ICI	Inter Carrier Interference
IDFT	Inverse Discrete Fourier Transform
IEEE	Institute for Electrical and Electronic Engineers
IFFT	Inverse Fast Fourier Transform

ISI	Inter symbol interference
LAN	Local Area Network
LHS	Left Hand Side
LOS	Line of Sight
LPF	Low Pass Filter
LTAS	Long-Term Average Spectrum
LTE	Long Term Evolution
LT	Luby Transform
MIMO	Multiple-Input and Multiple-Output
MU-MIMO	Multiple-user MIMO
NBI	Narrowband Interference
NLOS	Non Line-of-Sight
OFDM	Orthogonal Frequency Division Multiplexing
OFDMA	Orthogonal Frequency-Division Multiple Access
OOP	Object Oriented Programming
PAPR	Peak-to-Average Power Ratio
PDF	Probability Density Function
PEC	Piecewise Exponential Companding
PLC	Power Line Communication
PSD	Power Spectral Density
PSK	Phase Shift Keying
PTS	Partial Transmit Sequence
QAM	Quadrature Amplitude Modulation
QPSK	Quadrature Phase-Shift Keying
RHS	Right Hand Side
RSD	Robust Soliton Distribution
SCM	Single Carrier Modulation
SISO	Single-Input and Single-Output
SLM	Selective Mapping
SNR	Signal to Noise Ratio
VLC	Visible Light Communication
Wi-Fi	Wireless Interoperability by making use of IEEE 802.11.x standards
WiMAX	Worldwide Interoperability for Microwave Access
WLAN	Wireless Local Area Network
XP	Extreme Programming

List of Symbols

Symbol	Description	Units
Δf_{error}	Frequency shift in individual subcarriers	Hz
Δf	Subcarrier spacing ($1/T_u$)	Hz
τ_p	Time delay associated with path p	s
φ_p	Phase shift associated with path p	Radians
$\varphi_p(t)$	Set of orthogonal functions where ($x_1 \cdot x_2 = 0$) due to orthogonality	
a	Amplitude	
a_p	Amplitude of the path p	
b	Number of bits per symbol	
B	Bandwidth	Hz
BER	BER for the case when the input and output can be compared readily	
$C_b(M,N)$	Codebook with codeword length M and N nulls	
C_s	Cardianality of codebook S	
d	Distance	m
d_0	Reference Distance	m
$\frac{E_b}{N_0}$	Ratio of bit energy to noise spectral density	dB/bit
f	Frequency	Hz
$f_{\text{D,p}}$	Doppler frequency associated with path p	Hz
$H(\omega)$	Power Spectral Deinsity	
$h(\tau, t)$	Impulse arriving a the receiver	
I_k	Periodogram (k^{th})	
j	$0 \cdots L-1$ (segment index)	
$J_0(\cdot)$	Zeroth order Bessel function of the first kind	
k	Integer where $k \geq 1$	
K_R	Rician Factor	
κ	Clipping thereshold	
l_{input}	Length of the system input	Bits
L	Equal segments in Welch's method	
L_p	Path loss	dB
$L(d)$	Path loss at a distance d from the receiver	dB
$L(d_0)$	Path loss at a reference distance d_0 from the receiver	dB
M	Number of symbols in modulation scheme	
M	Length of codeword	
n	Integer $n = 1, 2, \ldots, N_c$. Unless otherwise stated	
N	Number of spectral null groupings	
N_c	Number of subcarriers	
N_p	Number of distinct propagation paths. Subscript p identifies the path	
P_b	Bit error probability	%
P_e	Symbol error probability	%
ω or ϕ $Q(\cdot)$	Standard Q-function	

S	Codebook of codewords	
$\left(\frac{S}{N}\right)_{\text{loss, CP}}$	Loss in SNR due to adding a cyclic prefix	dB
σ^2	Variance	$[\text{Units}]^2$
T	Symbol Duration ($T = T_u + T_{\text{cp}}$)	s
T_{cp}	Cyclic prefix period	s
T_{zp}	Zero padding period	s
T_u	Useful symbol data period	s
τ	Clipping threshold ratio	
X	Loss due to Shadowing (unless otherwise stated)	dB
$X_l[k]$	The l-th symbol multiplied with the k-th subcarrier	
$x_l[n]$	Discrete-time OFDM symbol	
$Y_l[k]$	The l-th received symbol on the k-th carrier	
$\mathcal{Y}$	Fourier Fransform	

List of Figures

List of Tables

Chapter 1

Introduction

1.1   Background of the study

Telecommunication is a way of communication which is not limited by the proximity of
the parties involved. It has been around for centuries. Smoke signals, carrier pidgins and
foot messengers formed part of early ancient communication systems. In terms of modern
telecommunications, the use of an optical telegraph in 1794 was the first step towards a rev-
olutionary development telecommunications. A system of towers within sight of each other
was constructed, each with a telegrapher who looked through a telescope at another tower
in the chain. Messages were relayed from tower to tower until the distant destination of the
message was reached. Next, the Von Soemmerring telegraph created in 1809, relied on a
voltaic pile to create Hydrogen bubbles on a cathode placed in acid. The cathode on which
bubbles formed, indicated a particular letter of the alphabet. The electrical telegraph was
demonstrated soon after and Morse developed a method for writing telegraphic messages.
As the technology evolved, the distances over which it operated became wider, even crossing
the Atlantic. In 1876 the patent for the first telephone was submitted making voice teleg-
raphy possible. The next achievement was the implementation of radio telegraphy at the
end of the 19th century. The invention of pulse code modulation made digital communica-
tions possible. In 1962 television broadcasts via satellite started and cellular radio became
commercially available. Next, long distance underwater optical fibres connected continents.
At the end of the 20th century the World Wide Web was already invented and consumers

had access to digital cellular radio, the Global System for Mobile communication (GSM) networks and millions of telephones and Internet users existed. The technology continues to evolve as the demand increase and the applications thereof becomes ever more complex [1].

Kleiner Perkins partners has published the Internet Trends report annually and consistently observed an increase in Internet users around the world. A reported 3.4 billion people now have access to the Internet, with an expected year on year growth of 10% [2]. Figure 1.1 shows the trends observed since 2009 [2]. The demand for wireless access and communications is steadily increasing and new methodologies and technology needs to be researched to ensure that this demand is met.
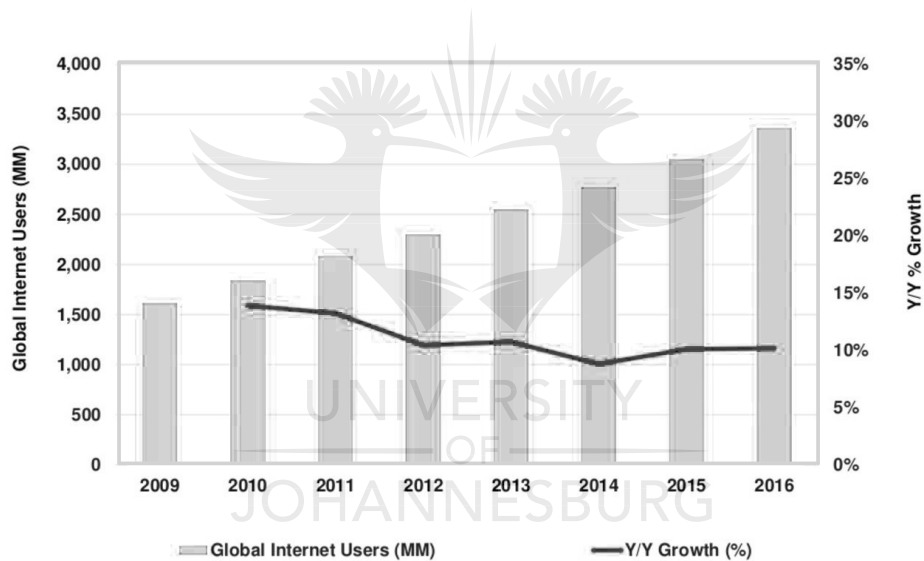
Figure 1.1: Internet Trends - Global Internet Users (MM), 2009 - 2016. 3.4B users with 46% market penetration and 10% year on year increase in users

Numerous developments in information theory and telecommunications made word-wide and terrestrial communications possible. These systems has developed over the past decades to provide more bandwidth, faster throughputs and to be more reliable and cheaper. Small and efficient solid state circuits developed in the 1960s made mobile communications affordable. The popularity of mobile communication has seen exponential growth since then. More users than ever now rely on wireless communications, and the infrastructure and technology implemented becomes insufficient. The increasing demand for broadband wireless access

motivates the development of more reliable and efficient techniques and methodologies to be used in the next generation of communication systems, beyond the 4$^{\text{th}}$ generation of mobile communications (4G) and Long Term Evolution (LTE) [3].

In principle the basic communication system consists of a transmitter and a receiver with the channel in which the signal propagates. The transmitter will take some forms of input and modulate it according to the particular application. The modulation technique has an important role in the performance and other characteristics of the communication system. Source coding and error correcting codes may also be applied in order to improve performance. Error correcting codes allows data which was lost during transmission to be recovered. It still forms the basis of many academic papers and conferences. The modulated signal is then added onto the channel. Typically noise is present in any real word example of a channel. It corrupts the data and places limitations on the capacity of the channel. Various techniques may be used in order to mitigate or recover from the effects of noise. Finally the transmitted signal arrives at the receiver and is decoded in order to obtain the message.

The characteristics of the wireless channel makes the transmission of data challenging compared to wired mediums. These includes signal attenuation as a function of distance, other wireless sources causing interference and multipath propagation. The limited radio spectrum also poses a problem. Only a small amount of the radio spectrum is unallocated. This is the part of the electromagnetic spectrum suitable for wireless communications and falls within 300 kHz to 300 GHz range [4]. See Figure C.2 in Appendix C.

Orthogonal Frequency Division Multiplexing (OFDM) is a good choice for usage in modern day applications, given the constraints on the wireless spectrum and increasing demand. It was developed in the 1960s for military applications. It overcomes many challenges presented by the environment today, such as the limited bandwidth available and interference caused by other systems present. OFDM a multicarrier modulation scheme. It provides a high bandwidth efficiency because of its overlapping subcarriers, and it is robust against

noise introduced in the communication channels. OFDM can be used in wireless, wired and optic mediums. Recent developments in integrated circuits (IC) makes the use of multicarrier modulation methods like OFDM more economical and feasible. OFDM makes optimal use of the radio spectrum due to the overlapping of subcarriers. It is robust against many of the multipath effects and corruption typically introduced by the wireless channel [5]. The close spacing of orthogonal subcarriers however, makes OFDM susceptible to Narrowband Interference (NBI) which degrades the system performance. Further, the out-of-band (OOB) emissions present in OFDM makes it less usable in future applications such as the 5th generation of wireless communication (5G) [6]. OOB emissions is transmissions on a frequency which lies outside of the allocated bandwidth for the specific OFDM system [7].

OFDM can be combined with source coding for reasons other than error correction.One such example is spectral null codes. These codes allows the power spectral density (PSD) of the signal to be shaped according to specifications. The PSD simply indicates the amount of power a signal has at a given frequency. Historically spectral null codes were used to allow for pilot tones on magnetic storage devices [8].

1.2 Problem statement

Existing technologies may be improved in order to make it more efficient and reliable. Current methods employed in telecommunications can be improved to better fulfil the requirements of society and the billions of users with access to the internet. In particular, a good candidate for efficient and reliable communications is a modulation called OFDM.

As with any communication channel the problem remains the noise naturally present. The major challenge is transmitting data efficiently with minimal loss whilst taking constraints such as the crowded radio spectrum into account as well. OFDM proved to be a good candidate in this environment since it is robust and makes efficient use of the spectrum due to its overlapping subcarriers. It is important to note that the transmission does not take place in an isolated environment. The available bandwidth is crowded with many other

transmissions for hundreds of different applications such as radio and television. These can introduce noise into the OFDM system. This can be in the form of Additive White Gaussian Noise (AWGN), Rayleigh fading and Narrowband Interference (NBI). NBI is common in the wireless channel and it is caused by interference from other radio sources such as Bluetooth transceivers and WiFi. OFDM is extra susceptible to corruption caused by NBI because of the close spacing of subcarriers. It usually affects only a few subcarriers at a given instance, but it can drastically degrade the performance of the system in terms of its bit error rate (BER).

Remember that OFDM has numerous carriers each spanning a small range of frequencies. Similarly NBI also spans a small range of frequencies. Now, consider NBI present in the OFDM channel. NBI causes one or more of the subcarriers to become corrupt, degrading the performance of the system as a whole [9]. Previously forward error correction schemes was used as an inter-subcarrier encoding scheme where all carriers was analysed at the same time. This implementation required OFDM subcarriers to be switched off manually in an attempt to avoid the degrading effects of narrowband interference [10].

Investigations are aimed at how NBI may be detected by making use of a technique called spectral shaping which may be combined with OFDM in an attempt to improve system performance by detecting NBI and attempting to cancel its effects.

Spectral shaping techniques used to shape the PSD, combined with channel sensing, may be used in order to mitigate the effects of narrowband interference present in the channel. The transmitted data may be shaped in such a way as to create a spectral nulls at the narrowband interference's frequency. This may be equivalent to switching off the OFDM subcarriers manually and mitigating the effect of NBI. The PSD can also act as a sensor or indicator for the integrity of the channel. It becomes possible to derive some of the channel's characteristics by observing the PSD. The PSD may be used as a metric to apply cancellation and adjustments to the OFDM subcarriers. It becomes important to consider how to predict or to sense the condition of the channel.

1.3   Objectives

Given the need for more reliable and efficient communication systems and how OFDM is a good candidate for future applications, the aim is to introduce a different method of using OFDM in combination with existing spectral shaping techniques in order to achieve improved performance.

The goal of this project is to firstly understand the relevant theory and mathematics describing spectral null codes and spectral shaping technique. This will be done by studying work previously conducted. Secondly, simulations will be implemented based on theoretical descriptions of the wireless environment and finally research will also be conducted into the feasibility of using these spectral coding techniques with OFDM and determining the effectiveness thereof when attempting to mitigate the effects of narrowband interference. The possibility of using spectral null codes as a means to determine or estimate the channel integrity will also be investigated. This implies that the channel needs to be sensed or predicted, and the spectral null code must be applied to the data in such a way as to create nulls at the location of the narrowband interference and might yield an improved system performance.

In short the aim is to develop an optimised and new OFDM coding scheme where subcarriers are loaded with spectral shaped codes. The observation of the spectrum can give insightful information into the state and quality of the channel. Further an attempt will be made to detect and cancel NBI by making use of the same technique. This will prove beneficial in future applications and will ensure that OFDM remains a suitable candidate for modern communications systems. An optimised OFDM system in terms of the spectral properties and system parameters will be proposed. This system will also make use of PAPR reduction techniques to make it viable for real world applications.

The OFDM system can be modified including the multiplexer, the modulator and demodulator needs to be adapted in order to achieve the aforementioned objectives. The system will employ an optimal set of parameters and the implementation thereof will be economic and efficient.

1.4 Methodology and tools

A literature study will be conducted in order to understand the problem, possible solutions and theory describing the system and its properties. The overarching objective is to propose an improved OFDM system with optimal parameters and spectral properties which will be suitable for future applications. The system design will be improved by investigating the optimal design in terms of the OFDM system's parameters. These includes the cyclic prefix (or other guard interval) length, the subcarrier count and the modulation schemes used. Results and applications for the findings in this section will be documented and analysed. The reduction of peak to average power ratio (PAPR) will also be incorporated into this section. The aim here is to provide a simulation and give recommendations on the optimal OFDM parameter for a given environment and application.

The spectrum of the system, designing the power spectral density (PSD) and reducing the PAPR is considered as separate branches of this investigation. This section is concerned with designing the optimal spectrum for the OFDM system in question. Results and applications for the findings in this section will be documented and analysed. Finally the optimised parameters and spectral design will be incorporated in a single application where is will be possible to draw conclusions on the applicability of using OFDM in future applications.

MATLAB and the digital signal processing toolbox (DSP) add-on will be used to facilitate the implementation of various simulations. The implementation of the simulation will be approached as a software engineering problem and the extreme programming (XP) method will be applied as described in Figure 1.2 [11]. The process starts with identifying and eliciting the requirements for the simulation software and designing a solution. The

implementation phase is iterative and one requirement will be developed, implemented and tested at a time [11].
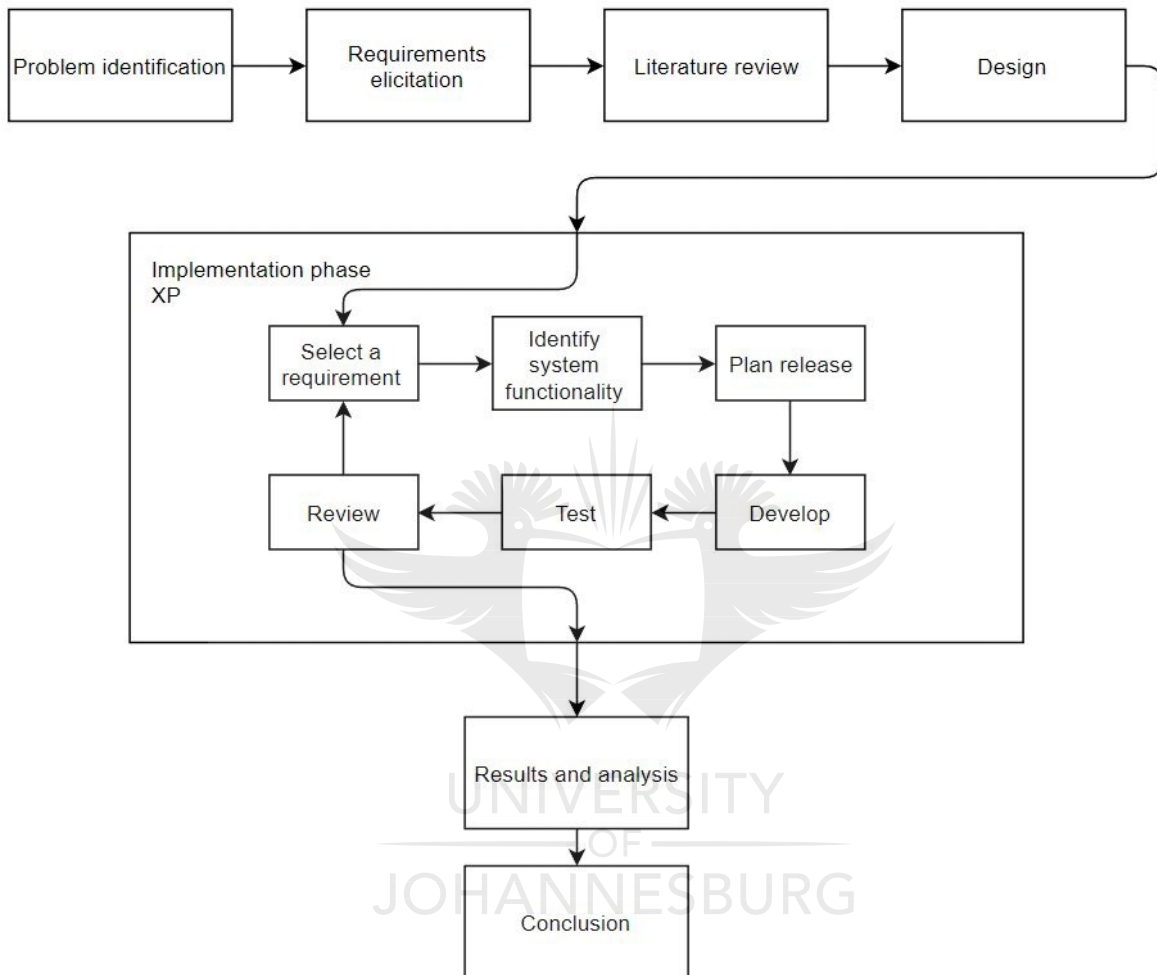
Figure 1.2: Outline of methodology used for the development of simulations. The development strategy is called extreme programming

Previously simulations aimed at the OFDM system and its parameters was implemented [12]. These simulations can be extended to include spectral shaping codes based on the channel sensing or predictions. It will provide insight into the applicability and effectiveness of spectral null codes and spectral shaping in combination with OFDM. Conclusions can be drawn on the system performance. Further the use of spectral analysis to detect NBI will be investigated.

1.5   Research contribution

The output of this research will propose optimal system configurations in terms of the design of OFDM parameters such as cyclic prefix lengths, subcarrier counts and the modulation scheme. Further, the applications of spectral shaping in combination with OFDM will also be investigated.

The key outcomes of this investigation

1. Optimal OFDM system parameters for a given implementation. This includes the CP length, subcarrier count and modulation scheme to use

2. Applications for applying spectral shaping techniques such as spectral null codes in combination with OFDM

3. Reducing PAPR in order to make the application suitable for low-energy devices

4. Using the design of the PSD in order to draw conclusions on the channel quality and the integrity of the transmission

5. Constructing a more robust and self-aware OFDM system suitable for modern day applications

6. The OFDM parameter optimisation will be combined with the PAPR reduction technique as well as employing spectral shaping techniques in order to make a system which is sustainable for usage in future generations of telecommunications

The result of this research will propose optimal system configurations when using spectral shaping and spectral null codes combined with channel sensing. It will provide insight into the applicability of combining spectral shaping codes with OFDM and adjusting the PSD to be null at the frequencies of narrowband interference. Simulation studies will be used in order to determine the feasibility of this solution in order to reduce the effect of NBI on the transmitted signal. Finally a definitive answer will be provided regarding the performance improvement when using the relevant coding techniques in conjunction with OFDM.

The aim is to design an optimised OFDM system with reduced PAPR which will employ spectral shaping techniques.

1.6 Research output

1. M. Trollip, K. Ouahada and L. Gqiba, "Optimised ofdm based communication systems for wireless environments," submitted to *Digital Communications and Networks.* 2018.

2. M. Trollip, K. Ouahada, "Effects of spectral null codes on papr and ber performance in ofdm systems," submitted to *7th International Conference on Adaptive Science and Technology (ICAST).* IEEE, 2018.

3. M. Trollip, K. Ouahada, "Effects of spectral shaping techniques on the papr of ofdm applications," submitted to *2nd International Conference on Signals and Systems (IC-SigSys).* IEEE, 2018

4. M. Trollip, K. Ouahada and T. Imoto, "Narrowband signal detection in ofdm systems using spectral shaping techniques," in *Proceedings of the 13th IEEE AFRICON Conference.* IEEE, 2017, pp. 232-237. [13]

5. M. Trollip, K. Ouahada, "Simulation Study on the Performance of OFDM in Different Environments" for *2nd African Winter School On Information Theory And Communications.* 2015.

6. M. Trollip, K. Ouahada, "NarrowBand Interference Signal Detection with Spectral Shaping Technique" for *2nd African Winter School On Information Theory And Communications.* 2015.

1.7 Overview of the dissertation

Figure 1.3 outlines the format and flow of this document.

The characteristics of the wireless environment makes modern telecommunication challenging and there is a need for more reliable wireless technologies since the demand has been constantly increasing over the past decade and it will continue to do so for the foreseeable future. The problem is the limited amount of radio spectrum available for communication purposes. New designs needs to take this constraint into account whilst preserving the robustness of the system. Throughput and reliability should also be considered.

The objective is to simulate an optimised OFDM system fit for future applications. It will have an optimal design in terms of the system parameters and performance. In addition
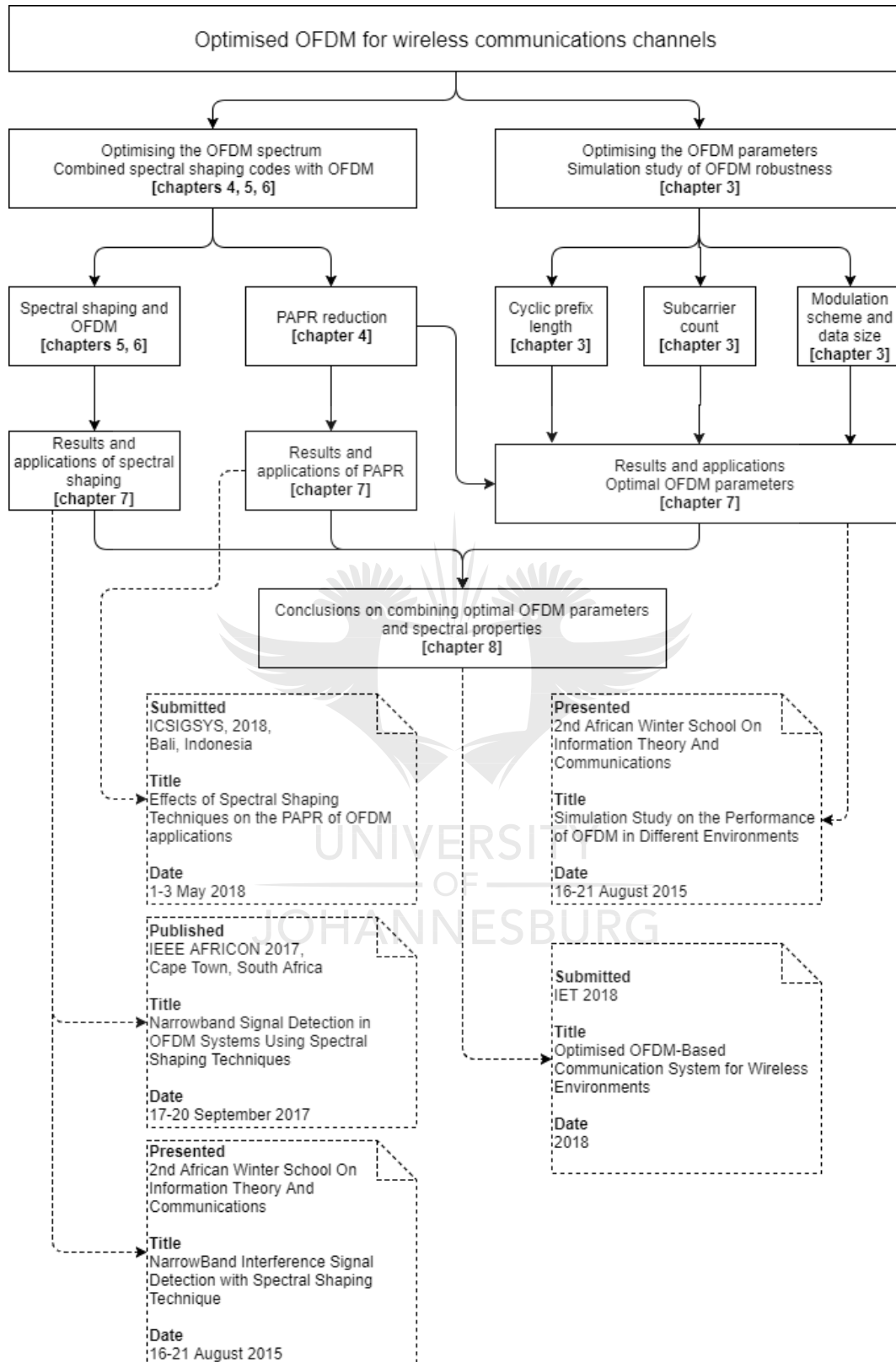
Figure 1.3: Outline of this dissertation including research output, presentations and conference publications

to the design, investigations on how spectral shaping techniques and spectral analysis may be used in order to further improve the system performance will be conducted. This will be achieved by implementing comprehensive simulations using MATLAB and the DSP toolbox add-on.

This research is aimed at the spectral null codes and spectral shaping. Firstly a good mathematical description thereof will be defined. Then by making use of simulations, the applicability of combining these coding schemes with OFDM will be investigated. The simulation will make proper provision for noise present in the channel and the model will represent a real world channel as closely as possible. This concludes with a proposal for optimal OFDM parameters, making use of spectral shaping to further improve the system, reducing PAPR, sensing the quality of the channel and constructing a robust OFDM system fit for future applications.

The next chapter presents a review of the relevant literature and related work which forms the foundation for the rest of the dissertation. Chapter 3 presents the optimised OFDM system and important parameters to be taken into account. Chapter 4 follows, introducing a common problem with any OFDM system called the high peak to average power ration (PAPR) and how it might be mitigated. A technique to combine spectral shaping codes with the conventional OFDM system is investigated in Chapter 6. Chapter 7 combines the principles investigated in earlier chapters and presents a smart OFDM-based system which can sense NBI in wireless channels. The final chapter presents the analysis of the results and a summary of the findings of this dissertation.

Chapter 2

Literature Review

2.1 Introduction

In this chapter the literature review is conducted. Relevant theory supporting findings in upcoming chapters is documented here. Information theory and its importance is introduced. The characteristics of the communications channel, specifically the wireless environment is discussed along with the physical phenomena present within the environment. We briefly look at how spectral sensing is implemented for cognitive radio applications. It has some important applications when choosing the bit length of the null codes. Welch's method of estimating the PSD for a transmission is introduced as it forms an integral part to analysing and understanding the results of the simulation study. An comprehensive description of NBI is presented and a model for NBI in the wireless environment is defined which will be used in conjunction with the model for wireless environments in order to accurately simulate a real word wireless channel. Finally a study on similar and related work is conducted in order to anticipate possible road blocks and to determine key area where more research and investigations will be required.

2.2 Information theory

Information theory defines the term information and how it can be modelled [14].

Information theory was introduced in 1948 when Claude Shannon published his paper on the mathematics making communications possible [15]. Shannon described entropy and how it relates to the uncertainty in any message. He further made the statement that a message can be transmitted over a noisy channel with great accuracy, even in the presence of noise.

The key components of a communication system is the information source and its transmitter which will encode and modulate the message, making it suitable for transmission. This is then passed onto the channel, which also introduces some noise which will degrade the system accuracy. And finally to the receiver will pass the message on the its final destination [16].

Since then the world has been transformed by electronic communications with faster and more accurate methods emerging. Messages are encoded in order to achieve the accuracy Shannon mentioned in his paper. Coding schemes still remains a vastly popular research topic within the field of communications and information theory.

2.2.1 Information sources and entropy

Consider any binary digital signal which represents data. It takes on a discrete amplitude and period, making it possible to identify the information it represents. In a binary system data is represented by a 1 or zero or some *on* and *off* state. It can be the presence or absence of a magnetic field, a positive and negative voltage, an optical signal or any other state indicating 1's and 0's. The input of a communication system is some information in analogue or digital form. The information is prepared by modulating it before it is transmitted over the channel. Finally the received signal is converted back to its digital representation and information may be reconstructed after the channel corrupted its original form. Shannon defined a measure of information called entropy, in the case of binary data, entropy is defined as $H(U)$ [14]

$$H(U) = -\sum_{i=1}^{r} p_i \log_2 p_i \tag{2.1}$$

where U is a random process with r outcomes, each with a probability of p_i. If the

probability of an event $p_i = 1$, equation (2.1) becomes $H(U) = 0$. This event is certain and therefore it provides no additional information when it occurs. The less probable an event is, the more information is gained when it occurs.

Consider an example of entropy, as commonly used by academics to convey its meaning. Let's take the weather tomorrow as being an information source U. Lets assume that it will have two possible outcomes, so $r = 2$ which is

1. Clear skies and a light breeze with a low chance of precipitation

2. A blizzard causing havoc and snow country wide

In South Africa, the probability of having clear skies is highly probable and that outcome contains little information. A blizzard on the other hand is highly unlikely and South Africans rarely see snow. This event will contain a considerable amount of information. The information source is the probability distribution assigned to a set of possible outcomes. The more unlikely an outcome is, the more information it contains. The weather in South Africa is a binary symmetric source (BSS) of information. The probability of clear skies is $p_0 = p$ and by definition the probability of a blizzard is $p_1 = 1 - p$. Substituting these into (2.1) gives

$$H(U) = -p \log_2 p - (1 - p) \log_2(1 - p) \tag{2.2}$$

Figure 2.1 shows the Entropy vs Probability for the above example. When $p = 0$ or when $p = 1$ the function is zero. It is at a maximum when $p = 1 - p$ or $p = 0.5$. In the BSS the maximum information is gained when the two outcome are equally probable. Entropy is measured in bits/symbol and allows us to define the information, on average, contained by each bit 0 or 1.

2.2.2 Channel coding

A way to increase the reliability of a channel is by employing a method named channel coding [17]. Coding is also used in order to reduce the length of codewords used to transmit
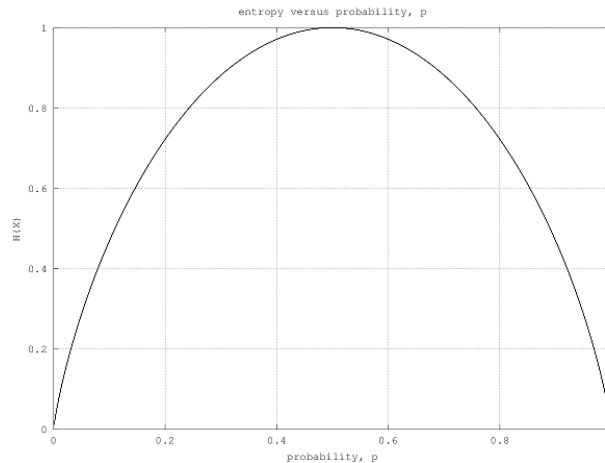
Figure 2.1: Entropy vs Probability for a binary symmetric information source

information and in order to detect and correct or recover from errors.

Block codes

By adding redundant information, the performance of a system can be improved. Consider an encoder which outputs code words c. A block code may be applied to a set of data bits with length K such that the block $b = (b_1, \ldots, b_K)^T$ is encoded to produce a code word $c = (c_1, \ldots, c_N)^T$ with N code bits [17]. The code rate is defined as

$$R_C = \frac{K}{N} \tag{2.3}$$

The application of error correctional codes is used in order to recover from errors during transmission. The redundancy added will be used at the receiver in order to detect and correct the corrupted bits.

An example of this is the Hamming code (usually referred to as the (7,4) Hamming code) which was developed in 1950 by R. Hamming in order to eliminate errors in a computing system [18]. This type of error correctional code represents each codeword by exactly 7 bits, even though only 4 bits is required to code the message. The remaining 3 bits is parity check bits and can be used in order to recover information lost during transmission. Consider the following example where a (7,4) Hamming code is constructed.

Example 2.1   Consider an arbitrary input

$$\mathbf{x} = \begin{bmatrix} x_0 \\ x_1 \\ x_2 \\ x_3 \end{bmatrix} = \begin{bmatrix} 0 & 1 & 0 & 0 \\ 0 & 1 & 0 & 0 \\ 0 & 1 & 1 & 1 \\ 1 & 0 & 0 & 1 \end{bmatrix} \tag{2.4}$$

The (7,4) Hamming encoder generator matrix $\mathbf{G}$ is given as

$$\mathbf{G} = \begin{bmatrix} \mathbf{P} & | \mathbf{I}_k \end{bmatrix} = \begin{bmatrix} 1 & 1 & 0 & 1 & 0 & 0 & 0 \\ 0 & 1 & 1 & 0 & 1 & 0 & 0 \\ 1 & 1 & 1 & 0 & 0 & 1 & 0 \\ 1 & 0 & 1 & 0 & 0 & 0 & 1 \end{bmatrix} \tag{2.5}$$

where $\mathbf{P}$ is the parity matrix and k denotes the message length and n denotes the block length. For the given $\mathbf{G}$, $n = 7$ and $k = 4$. The Parity Check matrix $\mathbf{H}$ is also constructed for future use [19]:

$$\mathbf{H} = \begin{bmatrix} \mathbf{I}_{n-k} | \mathbf{P}^T \end{bmatrix} = \begin{bmatrix} 1 & 0 & 0 & 1 & 0 & 1 & 1 \\ 0 & 1 & 0 & 1 & 1 & 1 & 0 \\ 0 & 0 & 1 & 0 & 1 & 1 & 1 \end{bmatrix} \tag{2.6}$$

The encoded message is

$$\mathbf{y} = \mathbf{xG} = \begin{bmatrix} y_0 \\ y_1 \\ y_2 \\ y_3 \end{bmatrix} = \begin{bmatrix} 0 & 1 & 0 & 0 \\ 0 & 1 & 0 & 0 \\ 0 & 1 & 1 & 1 \\ 1 & 0 & 0 & 1 \end{bmatrix} \begin{bmatrix} 1 & 1 & 0 & 1 & 0 & 0 & 0 \\ 0 & 1 & 1 & 0 & 1 & 0 & 0 \\ 1 & 1 & 1 & 0 & 0 & 1 & 0 \\ 1 & 0 & 1 & 0 & 0 & 0 & 1 \end{bmatrix} \tag{2.7}$$

$$= \begin{bmatrix} 0 & 1 & 1 & 0 & 1 & 0 & 0 \\ 0 & 1 & 1 & 0 & 1 & 0 & 0 \\ 0 & 0 & 1 & 0 & 1 & 1 & 1 \\ 0 & 1 & 1 & 1 & 0 & 0 & 1 \end{bmatrix} \tag{2.8}$$

The encoded binary sequence containing a total of 28 bits can be represented as a serial stream; 0110100 0110100 0010111 0111001. In contrast to block codes, convolutional codes operates on a continuous stream of bits [20].

$\square$

2.2.3 Channel capacity

The channel is simply the environment in which the signal is transmitted. Typical examples include copper cables, optic fibres and electromagnetic spectrum or wireless transmissions [16].

The channel capacity C is proportional to the probability of obtaining a bit error, or a data bit becoming corrupted. If the probability of obtaining a bit error is zero, the channel capacity will be at a maximum. Interestingly C will also be a maximum when the probability of a bit error is certain. If every bit is certain to be corrupted, the receiver can simply invert every bit in order to retrieve the original information. C will be at a minimum when the probability of a bit error is 0.5. The Hartley-Shannon law states that the maximum capacity C of a channel with bandwidth B is [16]

$$C = B \log_2 \left(1 + \frac{S}{N_0} \right) \quad \text{bits/sec} \tag{2.9}$$

This is the optimal performance for a channel with Gaussian noise present. This is the theoretical optimal performance of the channel. Shannon however, did not make any recommendations as how to achieve this performance. Observe that C tends to infinity as SNR tends to infinity, meaning there is no noise is present in the channel. This is not true when B tends to infinity as seen in (2.11) [16, 21]

$$\lim_{\frac{S}{N_0} \to \infty} C = \lim_{\frac{S}{N_0} \to \infty} B \log_2 \left(1 + \frac{S}{N_0} \right) \approx \infty \tag{2.10}$$

$$\lim_{B \to \infty} C = \lim_{B \to \infty} B \log_2 \left(1 + \frac{S}{N_0} \right) = \frac{1}{\ln 2} \left(\frac{S}{N_0} \right) \tag{2.11}$$

Lee derived the channel capacity for a Rayleigh fading channel, on average. He found that C in Rayleigh environments is lower than in a Gaussian channel [21]

$$C_{\text{avg}} = B \int_0^\infty \log_2 \left(1 + \frac{S}{N_0} \right) \delta \left(\frac{S}{N_0} = \left(\frac{S}{N_0} \right)_{\text{avg}} \right) d\frac{S}{N_0} \tag{2.12}$$

It is important to consider the Rayleigh fading channel since it is used to represent a wireless environment and all of the physical effects present therein [5, 22].

2.3 Channel characteristics

The phenomena present in the wireless channel is random and mostly unpredictable, making the modelling of the channel a challenging task. This section aims to define the phenomena present in the channel and how to represent them mathematically. The signal to noise ratio (SNR) of a given system is the ratio between the signal's power and the noise's power at the receiver. It indicates the efficiency of the given system [23].

Typically in a wireless channel a signal will propagate via more than one distinct paths. Each with a different time delay, phase offset and interference. The signal may arrive at the receiver a number of times at different times or at the same time. Figure 2.2 illustrates how a single transmission can reach the receiver via a number of distinct paths which is called multipath propagation [5]. This section will consider the impact of multipath propagation on the system performance and design.
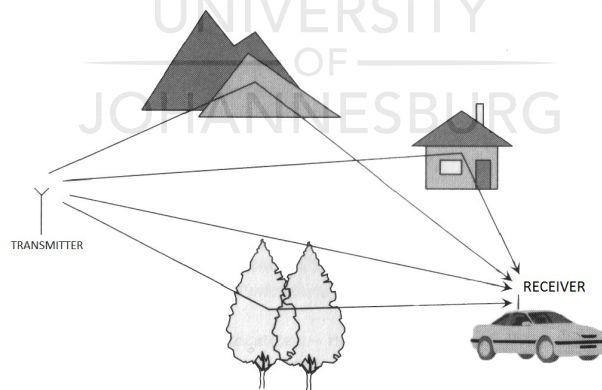
Figure 2.2: Basic illustration of multipath propagation in the wireless environment

2.3.1 Propagation loss

Propagation loss is an attenuation due to the distance d between the transmitter and receiver. The choice of model depends on the assumptions made for the wireless environment.

Path and shadow loss

Path loss is a loss in power during propagation. This depends largely, but not exclusively, on the distance between the transmitter and receiver. For a free space system (for example a vacuum), the free-space model may be employed [23]:

$$L_p = 147.56 - 20\log(f_c) - 20\log(d) \tag{2.13}$$

where L_p is the path loss in dB, f_c the carrier frequency and d the distance. Another model where reflections are taken into account, is called the plane-earth model [23]:

$$L_p = 10\log(a) + 20\log(h_t) + 20\log(h_r) - 40\log(d) \tag{2.14}$$

where a is a factor of correction, h_t and h_r is the height of the transmitter and receiver respectively. Various other models for path loss exist, both analytical and empirical [23].

Shadowing is the result of obstacles encountered during propagation such as buildings or cars and other objects. It results in the signal power to fluctuate over large distances, also called slow fading [23,24]. This is generally modelled by a lognormal distribution. Both path and shadow loss can be corrected by increasing the transmitter power [23,25]. Figure 2.3 shows the effects of fading on the system [5].

Multipath fading

A electromagnetic wave propagating through a channel will undergo physical phenomena such as reflection (when encountering relatively large flat surfaces), scattering (rough surfaces) and diffraction (pass through narrow aperture). The collective result is multipath propagation, namely the transmitted signal arrives at the receiver via multiple distinct paths [12].

In many cases a direct line of sight (LOS) path between the transmitter and receiver does not exist. A direct line of site path is simply a path where the transmitter and the receiver has an unobstructed view of each other. This means that if someone was to stand next to
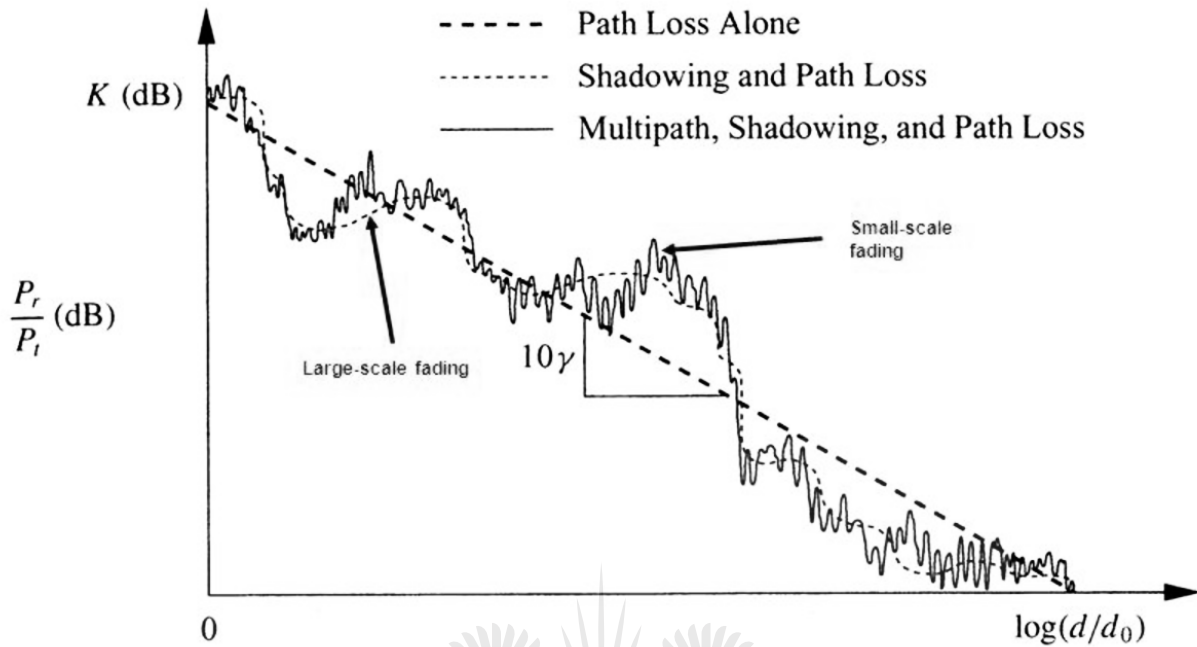
Figure 2.3: Small and Large scale fading showing the effects of path loss, shadowing, and shadowing on the signal power as a function of transmitted distance

the transmitter they would be able to see the receiver. If the receiver is too far away the person might require some binoculars, but it will still be a direct line of sight path. If a tree obstructs the view, or a car drives in between the person and the receiver, it will no longer be a direct line of sight path, but rather a non-line of sight path (NLOS).

Consider the example where a mobile phone is used indoors. A LOS path does not exist between the mobile phone and base station, but the reception is still reliable. A signal can propagate through the wireless channel via N_p distinct paths before arriving at the receiver. Each path with a different amplitude, phase, frequency and time. These paths interfere and constructive or destructive interference results in a fluctuating signal power at the receiver [23, 25]. This is also known as fast fading since it acts on small distances. The received power is Rayleigh distributed. The impulse at the receiver is described by [25]

$$h(\tau, t) = \sum_{p=0}^{N_p-1} a_p e^{j(2\pi f_{D,p} t + \phi_p)} \delta(\tau - \tau_p) \tag{2.15}$$

where N_p is the number of distinct propagation paths, $p = 0, 1, \ldots, N_p - 1$, a_p is the amplitude of path p, $f_{D,p}$ is the Doppler shift experienced by path p, φ_p is the phase offset of path p and τ_p is the time delay. δ is defined by

$$\delta(\tau - \tau_p) = \begin{cases} 1, & \text{if } \tau = \tau_p \\ 0, & \text{otherwise} \end{cases} \tag{2.16}$$

In the wireless environment it can easily be assumed that the receiver and transmitted will move with respect to one another and therefore experience a Doppler shift. The Doppler effect is discussed in more detail in Sub-Section 2.3.3

Consider a large amount of paths p arriving at the receiver. Cho *et al.* [5] described this process as being Gaussian with a zero mean and variance σ^2. The simplifying assumption is made that this is a Non-line of sight NLOS environment and therefore the average power of each path is equal. The amplitude of the process is [5]

$$f_X(x) = \frac{x}{\sigma^2} e^{-x^2/\sigma^2} \tag{2.17}$$

In the case of a LOS environment, the LOS path will have a factor K_R power when compared to other paths. The process at the receiver is then described by the Rician distribution [5, 23, 25].

2.3.2 Multipath delay spread

From the multipath equation (2.15), a time delay τ_p is present. This is due to the simple fact that each path p has a different length. The LOS path is an unobstructed path between the transmitter and receiver. It will be a straight line and it is the shortest possible path. Let the time a signal takes to propagate be τ_1, for the first signal (p_1) to arrive at the receiver. If the next signal arrives at τ_2, the time difference is $\tau_\Delta = \tau_2 - \tau_1$. If τ_Δ is large, the symbol will interfere with either the next or previously transmitted symbol, causing ISI [23].

2.3.3 Doppler shift

The Doppler shift is a change in the observed frequency of a source when the source moves relative to the receiver. A typical example of the Doppler effect is the change in the observed pitch in an Ambulance's sirens when it rushes past a stationary bystander on the sidewalk.

A change in frequency occurs when two objects move relative to each other. This is true for electromagnetic waves such as light. For example, the redshift in light from stars allowed scientists to study the expansion of the universe. When the transmitter or receiver moves relative to each other, a Doppler shift will also be present [5, 23]:

$$f_D, p = -v\frac{f_c}{c}\cos\phi \tag{2.18}$$

where $v = v_r - v_t$, the velocity of the transmitter relative to the receiver. ϕ indicates the direction of movement relative to the receiver. The Doppler shift results in orthogonality between subcarriers to vanish, resulting in ICI.

2.4 Performance metrics

For the purpose of this investigation the concern is with the system's performance in terms of the quality and integrity of the transmission. Metrics such as the throughput is less important, at least in the context of this paper. Hence the bit error rate will be used in order to assess the performance of the design.

2.4.1 Bit error rate

A simple way to compare the performance of any communications system is the bit error rate (BER), which is the ratio of errors to the total number of bits. It is a common metric used to measure the performance of any communication channel. It may be used with any application and communications channel. The BER can therefore be used to compare the performance of any given communication systems with each other, even if they are significantly different.

BER is given by

$$BER = \frac{\text{number of errors}}{\text{total number of bits}} \tag{2.19}$$

BER makes the comparison of different systems trivial. Programmatically the BER can be calculated efficiently by making use of the exclusive-or `xor` and counting the number of non-zero matrix elements `nnz` [26, 27].

Listing 2.1: Code for calculating BER

```matlab
1  % FILE: calcBER.m
2  % AUTH: Martin Trollip
3  % DATE: 2016/06/01
4  % DESC: Effeciently calculate the BER for the given input and output
5  function [BER, num_err] = calcBER(serial_input, serial_output)
6      [r_in, c_in] = size(serial_input);
7      [r_out, c_out] = size(serial_output);
8      difference = xor(serial_input, serial_output);
9      num_err = nnz(difference);
10     BER = num_err / c_in;
11 end
```

2.5 Spectral sensing in cognitive radio

Cognitive radio (CR) applications makes efficient use of the radio spectrum by employing a method known as spectral sensing. It continuously sense which part of the spectrum is in use and what data it contains. It is aware of the relevant parameters of the radio spectrum including the power and data being transmitted. Unused spectrum can also be detected. This allows for multiple users (primary and secondary) to make use of the spectrum. The primary user will not utilise its allocated spectrum continuously. By sensing the spectrum, secondary, unlicensed users can make use of the channel as well. The primary user can then be granted opportunistic use of the channel when no other transmission is taking place on the same frequency. These techniques is promising given the radio crowdeness and the ever

increasing demand for faster and higher quality communication services [28, 29].

Cognitive radio is particularly useful in situations where the available bandwidth is limited and multiple users makes use of the system [30, 31]. The transmitted signal has properties which will be known, such as the modulation, guard intervals and frequency amongst others [32]. The spectral sensing algorithm is key to the successful implementation of the CR and detection time should be short [33]. Various methods may be applied in order to sense the channel including energy detection, waveform-based sensing and matched filtering [34, 35]. Challenges with sensing includes uncertainty due to noise, fading and conflicting CR systems operating in the same band [28]. Other studies also proposed channel sensing with Multiple-Input and Multiple-Output Orthogonal Frequency Division Multiplexing (MIMO-OFDM) by using the shrink and match algorithm [36].

Consider waveform-based sensing. Predetermined sequences of bits is commonly used in order to provide synchronisation in digital communications. This happens in the time domain. The correlation between the received bits and a known sequence of bits allows waveform-based sensing to work. When a pattern of bits received correlates to the known pattern, it means that the channel was sensed. The sensing error floor was defined by Tang as the probability of a false detection or the probability of a loss detection (PDF or PLD) at an optimal detection threshold. This threshold occurs where the PLD is equal to the PDF.

$$\text{SEF} = Q\left(\sqrt{N_B}\frac{\sqrt{\text{SNR}}}{\sqrt{(\alpha-1)\text{SNR}+1/2}+\sqrt{1/2}}\right) \tag{2.20}$$

with

$$\alpha = \frac{E\left[|x(n)|^4\right]}{\left\{E\left[|x(n)|^2\right]\right\}^2} \tag{2.21}$$

where $x(n)$ is the signal and α is related to its randomness [37]. SEF may be approximated as

$$\text{SEF} \approx \begin{cases} Q\left(\sqrt{N_B}\sqrt{\frac{\text{SNR}}{2}}\right) & \text{SNR} \ll 1 \\ Q\left(\sqrt{N_B}/\sqrt{\alpha - 1}\right) & \text{SNR} \gg 1 \end{cases} \tag{2.22}$$

This shows that a longer signal pattern length N_B improves the performance of the waveform-based algorithm [34, 37]. The observations of this section will be important later on.

2.6 Welch's method for power spectra estimation

P. D. Welch, a researcher at the IBM Thomas J. Watson Research Center, proposed a simplified method for performing an estimation on power spectra at given frequencies by making use of segmented periodograms [38, 39].

Consider the random process divided into equal segments with length L, $X(j)$ where $j = 0 \cdots L - 1$.

Segments are defined as follows

$$X_1(j) \;\; = \;\; X(j) \tag{2.23}$$

$$X_2(j) \;\; = \;\; X(j + D) \tag{2.24}$$

$$X_k(j) \;\; = \;\; X(j + (k-1)D) \tag{2.25}$$

where k is the number of segments and D is the distance between segments. It is important to note that segments may be overlapping.

The method of estimation takes a window $W(j)$ such that the process is

$$X_1(j)W(j), X_2(j)W(j) \cdots X_k(j)W(j) \tag{2.26}$$

For each of the windows, the DFT (or equivalently FFT) is performed to obtain [38]

$$A_k(n) = \frac{1}{L} \sum_{j=0}^{L-1} X_k(j) W(j) e^{-2kijn/L} \tag{2.27}$$

From here periodograms $I_k(f_n)$ are obtained and the estimation of the spectra is the average thereof [38]

$$\hat{P}(f_n) = \frac{1}{K} \sum_{k=1}^{K} I_k(f_n) \tag{2.28}$$

This estimation is an integral part of the investigations into how spectral null code affects the spectrum for an OFDM system.

2.7   Narrowband interference

In this section narrowband interference is introduced. A large portion of this document will focus on detecting and cancelling NBI. This type of noise is given special consideration due to the degrading effect it has on OFDM in particular. NBI is a type of impulse interference with a spectrum much smaller than the transmitted signal. It occurs when two different systems is operating in the same frequency range [40].

OFDM will be covered extensively in Chapter 3. Assume that NBI has a small bandwidth spanning at most a few subcarriers with a magnitude which can be an order of magnitude greater than that of the transmitter. It degrades the system performance and the demodulator becomes saturated. Cancellation of NBI is important in broadband systems such as OFDM since the environment in which it is employed typically presents noise with characteristics different from that as Additive White Gaussian Noise (AWGN). OFDM has delivered good performance in the wireless and power line communications (PLC) environments but the effect of narrowband or impulse noise present in these channels makes the usage of OFDM impossible without implementing some narrowband cancellation techniques [41].

2.7.1   **Sources of narrowband interference**

The wireless environment is volatile and numerous factors plays a role in the degree of noise present in the channel. OFDM is a broadband broadcasting method making it more susceptible to NBI than other methods. A broader band means more room for NBI to interfere with. The interfering impulse or narrowband signal is called the interferer. It may be caused by any radio transmission present in the same band as the OFDM subcarriers. These range from microwaves through to Bluetooth and many other radio broadcasts [41, 42]. In the PLC network electrical devices connected to the grid and the alternating switching frequency may also cause NBI. This may spill over into the wireless environment via electromagnetic interference (EMI). Numerous other rogue radio transmissions may also be an interferer. These include remote controls for vehicle alarm systems, two way radios and the unauthorised usage of radio transmitters.

2.7.2   **Characteristics and model**

Noise determines the theoretical capacity of the channel and it translates to the number of errors received in practice during transmission. Noise is random and unpredictable. Therefore noise is usually described with a probability density function (PDF). Narrowband and impulse signals are estimated to span the length of a single carrier and have an energy which can be an order of magnitude greater than that of the modulator [43, 44].

Let us consider an interference in the channel. It may be modelled by making use of the Poisson distribution P_k since a certain number of interferers will interact with the system over the given bandwidth

$$P_k = \frac{\lambda^k e^{-\lambda}}{k!} \tag{2.29}$$

where λ is the number of interferers η acting on the given spectrum of the system (For OFDM this is $B = \Delta f N_c$) with Δf the subcarrier spacing and N_c the number of subcarriers. Then $\lambda = \frac{\eta}{\Delta f N_c}$ and P_k is the probability of k interferences on the OFDM bandwidth [42, 45].

Consider the general form for any transmission system as show in Figure 2.4. The received symbol $r(k)$ can be defined as [41]

$$r(k) = s_t(k)h(k) + n(k) + i_n(k) \tag{2.30}$$
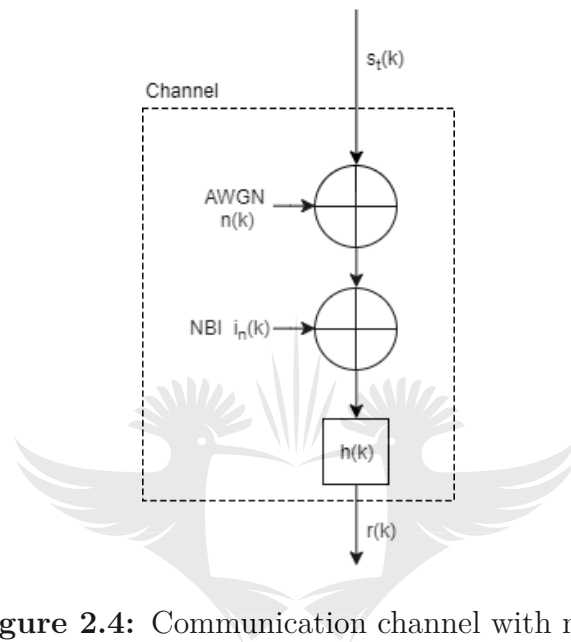
Figure 2.4: Communication channel with noise

where s_t is the transmitter output, $h(k)$ is the channel response, $n(k)$ is thermal noise or AWGN in this example and $i_n(k)$ represents the noise caused by the presence of NBI and distributed according to (2.29). $i_n(k) = \sqrt{10}R_{\mathrm{nbi}}(k)$, assuming the NBI is uniformly distributed [42]. R_{nbi} generates a random number. (2.30) in the discrete form is

$$R_{k,n} = S_{k,n}H_{k,n} + N_{k,n} + I_{k,n} \tag{2.31}$$

Where $k = 0, 1 \ldots, N_C - 1$ is the subcarrier and $n = 0, 1 \ldots, \infty$ is the transmitted symbol. NBI and additive white Gaussian noise (AWGN) will be added to the channel during simulations [40]. In the simplest form the interference can be represented as a single sinusoid

$$i_n(k) = ae^{(j2\pi f\tau + \phi)} \tag{2.32}$$

The sinusoid is acceptable where the NBI is assumed to be a small portion of the total

OFDM spectrum. If the NBI has a wider range of impact a different approach is required and the narrowband interference will take the form of a summation of sinusoids [46]. For the purpose of this investigation (2.32) is sufficient.

2.7.3 Effects of NBI in OFDM channels
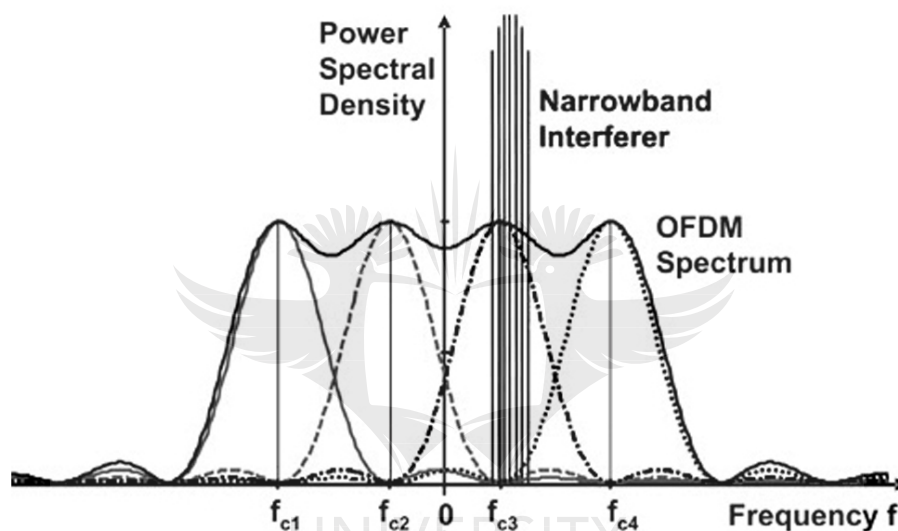
Figure 2.5: The effect of NBI in an OFDM system showing the spectrum of NBI [47]. See Figure 3.2 for the unaffected OFDM spectrum.

Suppose NBI is present in the channel where the OFDM signal is transmitted as illustrated in Figure 2.5. It may be caused by a variety of factors such as radio frequency interference emitted by devices such as microwaves or Bluetooth transponders [49]. In the case of PLC the impulse noise is caused as a result of alternating current. NBI usually has a power far greater than that of the transmitter and it affects only a few individual subcarriers. NBI will cause the data carried on the affected subcarrier to become corrupted completely since the power of NBI is far greater.
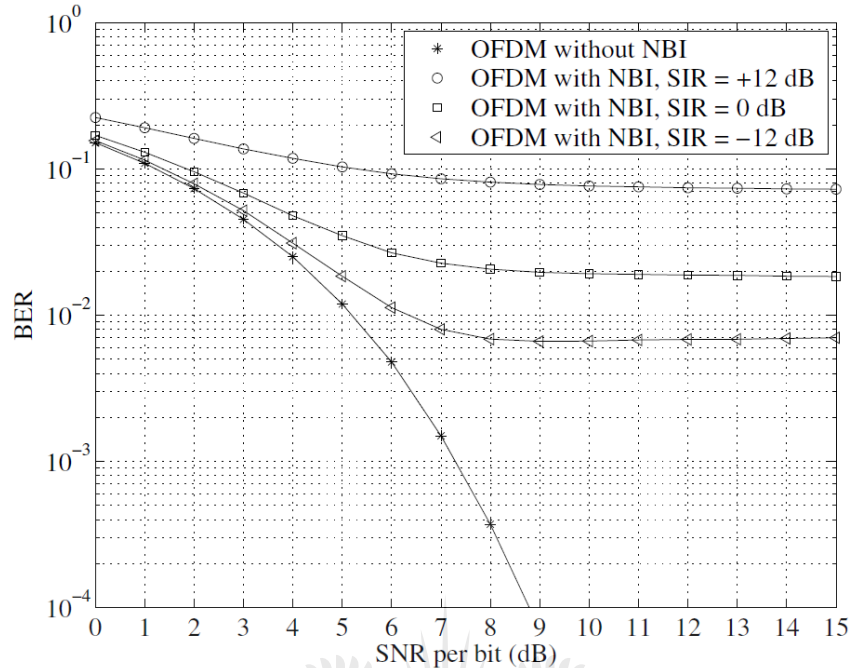
Figure 2.6: The error floor [48] of ODFM in the presence of NBI.

2.8 Related work

2.8.1 Mitigation techniques

In this section mitigation for NBI is investigated and various techniques may be used to estimate, cancel or suppress NBI such as cyclic prefix based methods [48], Linear Minimum Mean-Square Error estimates (LMMSE) [43], predictive error filters [9], Hanning window estimation [50] and selective notch filtering. Batra highlighted an important drawback with most of the mitigation techniques which is a result of applying notch filtering on the affected subcarriers. The data on those carriers can not be recovered and results in an irreducible error floor as seen in Figure 2.6 [9].

The cyclic prefix based algorithm relies on the redundant data introduced when adding guard intervals to the OFDM system. When estimating the NBI, the data bearing part of the carrier was removed which did yield some promising results [48]. LMMSE measures the

subcarriers at during states. This method has shown that spectral leakage caused by NBI can be suppressed to have a resultant power which is below the thermal noise of the system and therefore negligible [43]. Many mitigation methods are developed for specific implementations of OFDM in mind. Hanning window estimation relies on the symmetry available in the prefix of IEEE 802.11a systems and this technique did prove to be theoretically and practically effective [50].

Another method called frequency domain identification and cancellation was developed in order to prepare the OFDM system for future applications [51]. This method estimates the location of the NBI (or other impulse noise) by finding the maximum amplitude in the transmission spectrum. The NBI is then cancelled by subtracting the estimated NBI from the received signal. Combining this with a frequency domain suppression methods further improved the systems performance [40]. In the frequency domain NBI can be reduced after the Fast Fourier Transform (FFT) has been applied and the methods mainly involves subtracting the estimated interferer from the transmitted signal. The FFT is an extremely efficient algorithm of converting a signal to its representation in the frequency domain and it is easy implemented on integrated circuits and electronics. Applying frequency domain techniques and considering (2.31) gives a simple representation of the mitigation technique [52]

$$R'_{k,n} = R_{k,n} - \hat{I}_{k,n} \tag{2.33}$$

where $\hat{I}_{k,n}$ is the estimation of the interferer.

2.8.2 Spectral shaping techniques

In 1966 Gorog described how redundancy may be introduced in order to create codebooks with desired properties in their spectrum [53]. A certain type of spectral shaping code is called a spectral null code which has spectral nulls at selected frequencies. That is, the PSD at designed frequencies is zero. This is applied widely in the field of data storage, for example in magnetic and optical storage media. A notable application is the inclusion of pilot tones on magnetic storage devices and compact discs (CDs). A pilot tone will provide the

hardware with feedback on which physical part of a storage medium is currently being read, for example the current coordinates of a laser on a CD while it is rotating in the CD-ROM. The data on the CD is shaped using spectral null codes, and the pilot tones will coincide with the nulls in the stored data. This prevents pilot tones from corrupting the original data [8]. Gorog described the method for designing and constructing codebooks with codewords which have favourable spectral properties. Specifically, the construction of codebooks which will have spectral nulls at desired frequencies are called spectral null codes [53]. Spectral null codes has been researched extensively since then [8, 44, 54].

Ouahada *et al.* [44] proposed loading OFDM subcarriers with spectral null codes in an attempt to mitigate NBI. A PSD detector added to the receiver can detect missing nulls in the spectrum. Nulls goes missing when the channel corrupted the transmission. The affected carriers will then be substituted with a code from the spectral null codebook in an attempt to correct the error [44]. This concept is explained further by simulating how spectral null codes may be used in order to detect NBI present in the channel and how to cancel NBI.

2.8.3 Further investigations on spectral shaping and OFDM

The use of spectral shaping in the context of OFDM will be investigated further. Various questions such as the validity of using spectral shaping techniques in combination with OFDM, its impact on the OFDM system's performance in terms of the PAPR and BER performance and the effects that NBI has on this system, remains unanswered.

2.9 Overview

In this chapter the focus was on existing literature and fundamental theories which is relevant to the investigations in the rest of this document. Information theory was introduced in order to define the terminology used. The history of Information theory was briefly discussed and entropy introduced. Coding schemes, channel capacity and various other properties of the wireless channel including small and large scale fading, path and shadow loss, multipath

fading and delay spread was also introduced in this chapter. The BER is defined and will be used to assess the performance of the communication systems.

The spectral sensing in cognitive radio and power spectral density estimation using Welch's method was introduced. A brief look at related work in the NBI mitigation field and spectral shaping techniques was also presented. The sources and characteristics of NBI was investigated. The focus was on NBI in the OFDM system and how it might effect the system's performance. Finally, related work was mentioned and recommendations for improvement and areas requiring more research was made.

In the next chapter an optimised OFDM system is derived and the performance assessed.

Chapter 3

Optimised OFDM System

3.1   Introduction

From observations of developments in society, it is clear that the demand for access to mobile connectivity is on the increase. Modern day applications on mobile devices is dependant on high speed, high bandwidth Internet connections. The increasing amount of devices with access to the Internet motivates the development of more reliable and more efficient telecommunications systems [55]. Another problem is the availability of the usable radio spectrum which is already over crowded. Orthogonal Frequency Division Multiplexing (OFDM) is a popular modulation scheme which addresses both of the mentioned problems. It is inherently robust to noise present in a channel and the overlapping of orthogonal subcarriers makes it spectral efficient. Previously frequency division multiplexing (FDM) implementations required carrier to be non-overlapping. The overlapping carriers in OFDM lead to a spectral efficiency which can be up to twice as efficient when compared to other multicarrier modulation schemes [23, 24, 56].

OFDM has multiple orthogonal and overlapping subcarriers. A single subcarrier in the time domain may be expressed as a rectangular pulse with a duration T_u. In the frequency domain a single subcarrier is expressed by the $sinc^2$ function $\left(\frac{\sin(\pi f/\Delta f)}{\pi f/\Delta f}\right)^2$ [12, 57] as illustrated in Figure 3.1. This observation is important when constructing the system using the Fourier transform as discussed in Subsection 3.4.3.

The definition of orthogonal subcarriers x_{k_1} and x_{k_2} is

$$\int_{mT_u}^{(m+1)T_u} x_{k_1}(t)x_{k_2}^*(t)dt = 0 \qquad k_1 \neq k_2 \tag{3.1}$$

$x_k(t)$ is the modulated symbol on the kth subcarrier. k is the subcarrier count as defined in Figure 3.3. The orthogonality of subcarriers allows the peak of one subcarrier to coincide with a location where all the other subcarriers are zero, as seen in the spectrum in Figure 3.2 [57]. Should orthogonality be lost, inter carrier interference (ICI) will be the result and a single carrier at the receiver can not be extracted as easily [41, 58, 59].
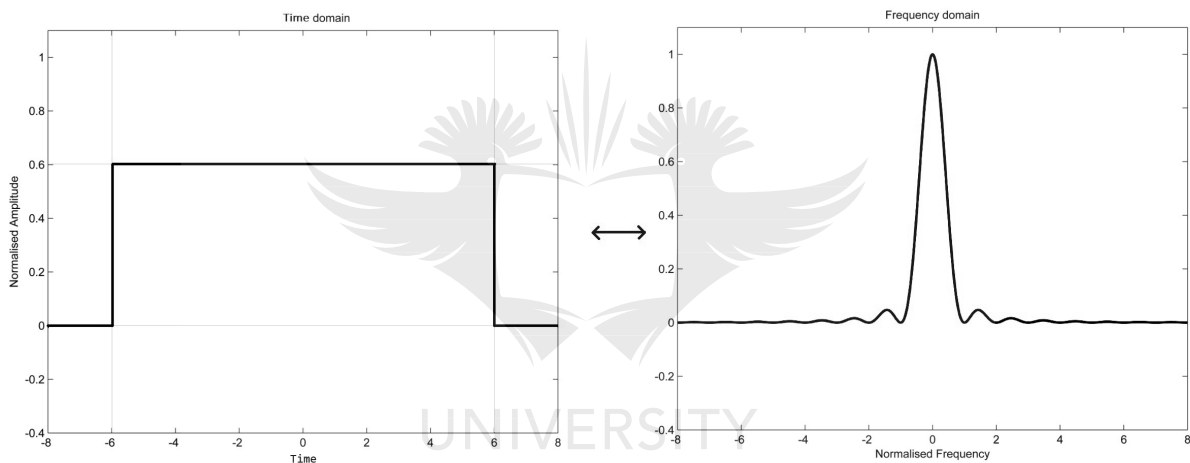
Figure 3.1: Constructing a single OFDM carrier [57]

A number N_c subcarriers can be modulated with any modulation scheme and the OFDM symbols are transmitted in parallel. Figure 3.3 shows how symbols are transmitted in parallel in the frequency domain [57]. This chapter introduces the theory behind OFDM and the implementation of an OFDM system [12]. The results of the simulation is analysed and an optimised set of parameters, yielding the best performance and simplest algorithm is derived.

3.2 Current implementations

OFDM dates back to the 1960's where it was developed for military applications requiring high data throughout rates. An upgrade to then Wireless LAN (WLAN) standard (IEEE
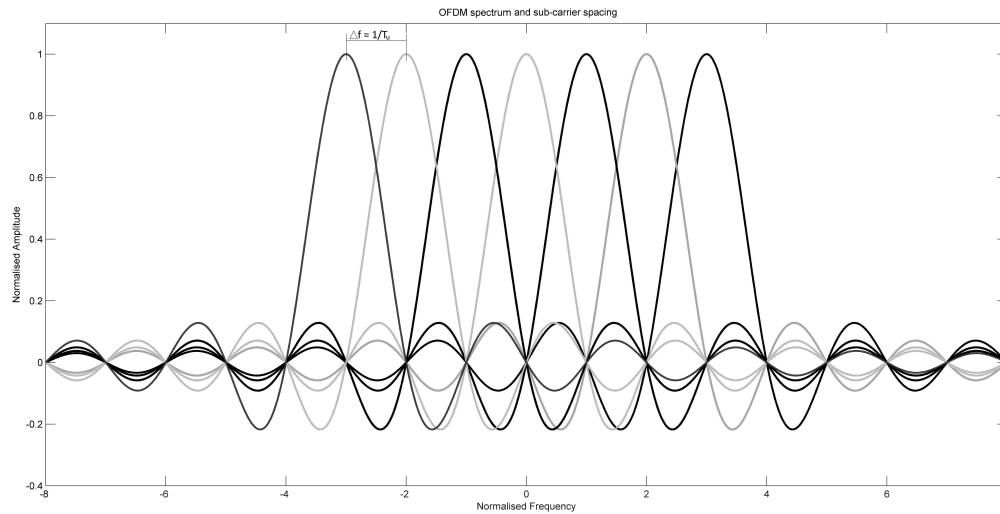
Figure 3.2: Spectrum for OFDM transmission with N_C subcarriers spaced at $\Delta f = 1/T_u$ and bandwidth $B = N_C \cdot \Delta f$
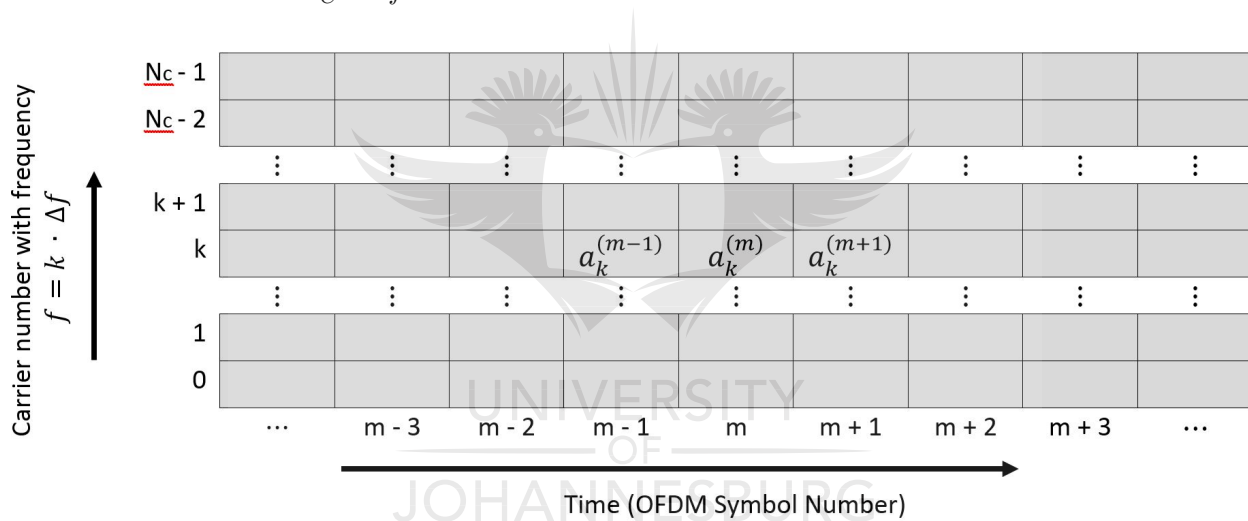
Figure 3.3: OFDM transmission of symbols m, across N_c subcarriers

802.11b) using OFDM (IEEE 802.11a and IEEE802.11g) showed improved throughput rates. Since the initial use of OFDM in WLAN, developments such as Multiple-Input Multiple-Output OFDM (MIMO-OFDM) further increased the performance of wireless standards such as IEEE802.11n and IEEE802.11ac. Some other techniques such as Code Division Multiple Access (CDMA) was first introduced during the third generation of mobile networks (3G) but it was surpassed quickly by its successors including the third generation partnership project (3GPP LTE), 4G and LTE. Other usages includes asymmetric digital subscriber lines (ADSL) and Digital Audio Broadcasting (DAB) (EN300401 2001a) and Digital Video

Broadcasting (DVB - T, DVT - H) [17, 60]. The system parameters for each application varies and factors such as the broadcast range and the quality of the channel is taken into account. Further improvements on performance is made when error correctional codes are applied, which is common practice in the mentioned applications [12].

Consider the latest in Wi-Fi technology, IEEE 802.11ac which makes use of Multiple User MIMO (MU-MIMO) and up to 256-QAM [61]. Table 3.1 shows how OFDM has become more popular in recent iterations of Wi-Fi evolution. Note how the implementations making use of OFDM shows data rates greater than 100Mb/s This trend is not limited to the use of Wi-Fi but to numerous other wireless and wired systems.

TABLE 3.1: Comparison of IEEE 802.11x Standards [61]

Feature \ IEEE Standard	802.11b	802.11bg/a	802.11n	802.11ac
Data rate (Mb/s)	11	54	100+	500+
Frequency band (GHz)	2.4	2.4/5	2.4 and 5	5
Channel width (MHz)	20	20/20	20 and 40 (optional)	20,40,80,160 and 80+80
Antenna technology	SISO	SISO	MIMO	MU-MIMO
Transmitter method	DSSS	DSSS and OFDM	OFDM	OFDM
Number of streams	1	1	4	8
Beamforming-capable	No	No	Yes	Yes
Date ratified by IEEE	1999	2003	2009	2014

3.3 OFDM simulation parameters

Section 2.3 describes how the wireless channel may be modelled. The wireless channel in conjunction with the properties of OFDM mentioned in this section, will define the implementation of the OFDM simulation. In order to aid discussion, the OFDM block diagram is presented in Figure 3.4 [5, 12, 57, 62]

The OFDM simulation consists of three main components namely the transmitter, channel and receiver. The transmitter will take the input data, modulate it and perform the IFFT. The IFFT will convert the signal's frequency components to the time domain by making use
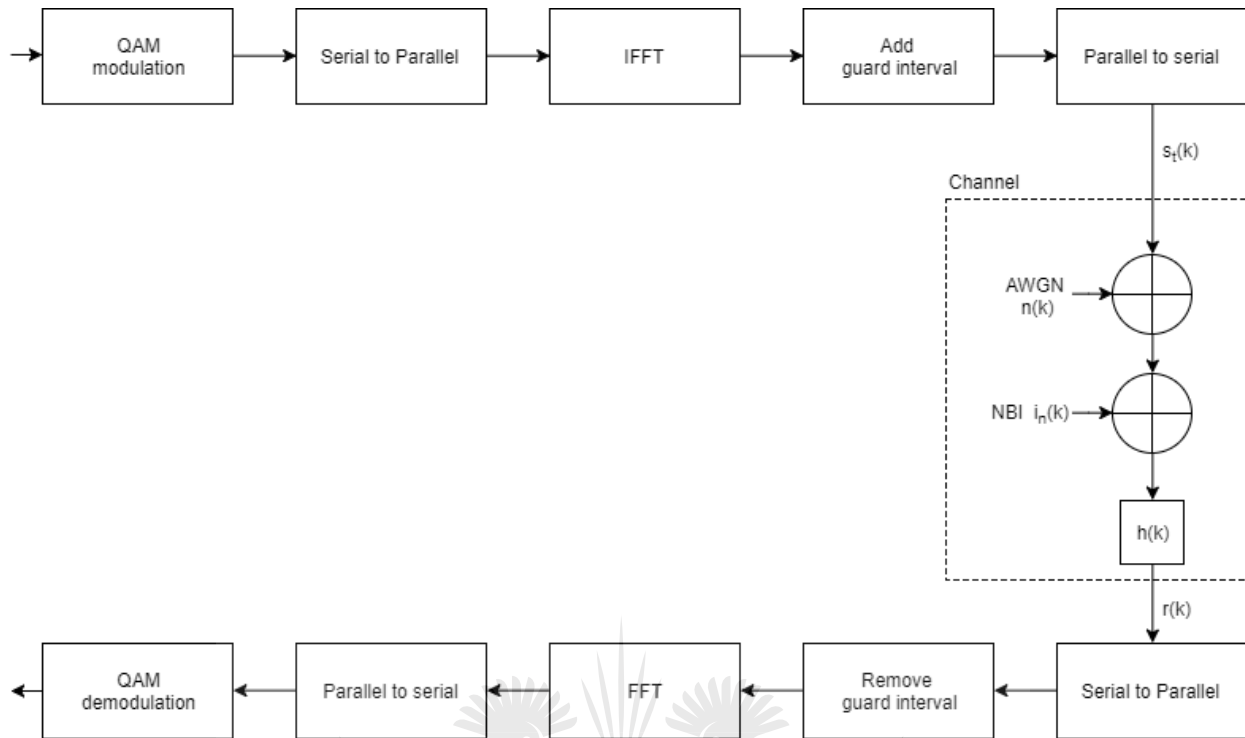
Figure 3.4: OFDM simulation block diagram

of the inverse of the efficient FFT algorithm. The channel is represented by a model describing a wireless environment which was defined in Section 2.3 and it includes Rayleigh fading, AWGN and NBI. The transmitter will perform the FFT and yield an output. The basic design for the OFDM system remains the same for both wired and wireless applications. The receiver will demodulate the transmitted data and analyse the PSD. Performance metrics such as the bit error rate (BER) is used to draw conclusions on the performance of the system as a whole.

3.3.1   Input

A codebook with spectral null codes is constructed and codewords from it is selected as the system's input.

3.3.2   Modulation

In digital communication systems, the binary input bits must be mapped to an electromagnetic wave representations to allow it to be physically transmitted over the channel. This process is called digital modulation or simply modulation. The electromagnetic wave referred to as the carrier, is typically a sinusoidal wave with an amplitude a, frequency f and phase φ [12, 24, 63].

Single carrier modulation

Single Carrier Modulation (SCM) requires a single carrier to be modulated. In the simplest implementations, one of the properties of the sinusoid is modulated based on the binary data. These modulations are amplitude-, frequency- and phase shift keying (ASK, FSK and PSK) [24]. In the case of ASK a varying amplitude will represent a 1 or 0 as seen in Figure 3.5. This concept may also be extended to make use of codewords to represent more than one bit of data at a time. In Figure 3.5 on the right hand side it can be observed how a change in phase represents different codewords. ASK and PSK symbols can be represented on the phasor plane, clearly showing the amplitude and phase with a constant frequency. This representation is called a constellation graph and it helps to easily identify different codewords. Consider the constellation examples in Figure 3.5 for ASK and PSK [24]

Consider a constellation with 2 symbols (BPSK) (Figure 3.5) on the left hand side. Binary-PSK is a flavour of phase shift keying with two states. Each symbol represents 0 or 1 respectively, namely 1 bit of data. When the constellation has 4 symbols, each may represent 2 bits of data, namely 00, 01, 10, 11. In general for a constellation with M symbols, the number of bits b represented by each symbol is [12, 23]

$$b = \log_2(M) \tag{3.2}$$

Constellations can also be constructed by adjusting both the amplitude and phase. This is referred to as quadrature amplitude modulation (QAM). This technique of modulation relies on two out of phase carriers whose amplitudes will be modulated. The development
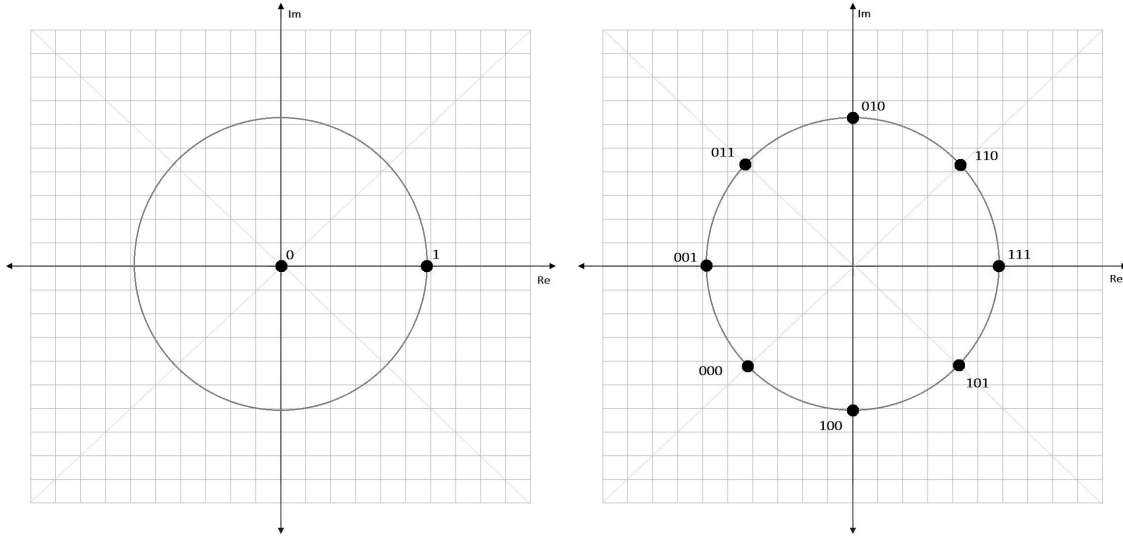
Figure 3.5: Binary Amplitude Shift Keying (Binary ASK) and 8 Phase Shift Keying (8-PSK) constellations

of QAM was a natural advancement as more computational power became available for the use in communications. An example of 32-QAM is shown in Figure 3.6. Note the use of Grey coding and $b = 5$ according to (3.2).

The error rate can be minimised by making use of Grey codes. The constellations mentioned above, makes use of Grey coding where adjacent symbols will only differ by 1 bit at most. It follows that a single symbol error will only result in 1 bit error, if it is assumed that only adjacent symbols will interfere [12, 23, 25]. Proakis described how the choice of M modulation symbols effects the upper bound probability of receiving a symbol error P_e as [64]

$$P_e \leq 1 - \left[1 - 2Q \left(\sqrt{ \frac{3}{(M-1)} \frac{E_b}{N_0} } \right) \right]^2 \tag{3.3}$$

where M is the number of symbols, E_b/N_0 is the ratio of bit energy to noise energy or SNR per bit. And $Q(\cdot)$ is the Gaussian PDF as illustrated in Figure C.1 [65].

$$Q(x) = \frac{1}{\sqrt{2\pi}} \int_x^\infty e^{t^2/2} dt \tag{3.4}$$

This shows that the upper bound for the error probability increases as more constellation
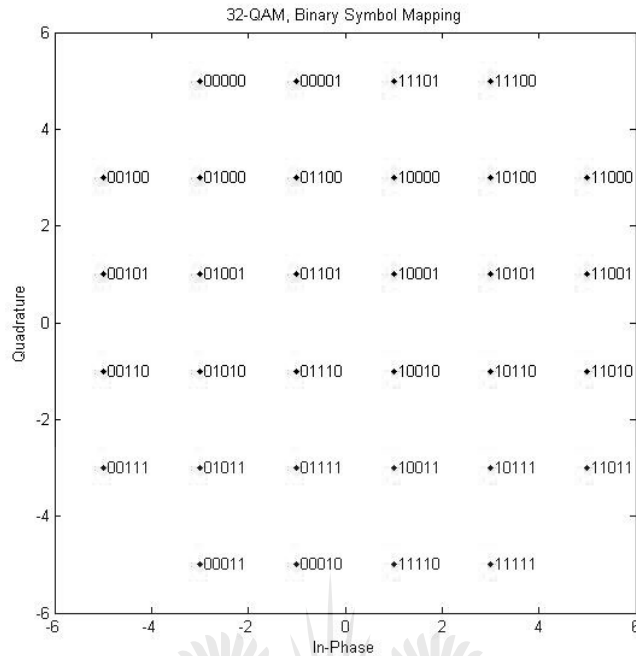
Figure 3.6: 32 Quadrature Amplitude Modulation (QAM)

symbols M are used.

3.4   Modelling interference and channel quality

A wireless environment will be used during the simulations since it is a more common use of the technology. Section 2.3 described the characteristics of the wireless environment and equation (2.15) is used as the transfer function. The Rayleigh distribution gives an adequate model for the channel. In addition, AWGN and NBI (see Section 2.7) is also present in the channel.

Various factors will play a role in the performance of the OFDM system. These includes phenomena such as inter-symbol and inter-carrier interference, small and large scale fading, multipath propagation, narrowband signal interference and Peak to Average Power Ratio (PAPR).

3.4.1 Multi carrier modulation

Each carrier in a multicarrier system has a selected frequency spaced a distance Δf from its adjacent subcarriers. Each carrier is modulated independently. A transmitter sums the modulated signals and transmits it. Modulation techniques such as PSK, ASK or Quadrature amplitude modulation (QAM) may be applied. QAM is often used in combination with OFDM and it modulates both the carrier's amplitude and phase, preserving the frequency. In the case of OFDM, the transmitted signal in discrete form is given by [24, 57]

$$x_n = x(nT_s) = \sum_{k=0}^{N_C-1} a_k e^{(j2\pi nk/N_C)} \tag{3.5}$$

where T_s is the sampling interval, n is the sample number $n = 0, 1, \ldots, \infty$, a_k is a complex number in the QAM constellation and k is the subcarrier number, $k = 0, 1, \ldots, N_C - 1$.

An arbitrary modulation scheme may be used, but generally this choice depends on the throughput and other performance requirements of the system [66].

3.4.2 Serial to parallel conversion

The serial to parallel (S/P) and its counter namely parallel to serial block (P/S) serves an important role in the OFDM system. The serial data bits is mapped onto N_c parallel subcarriers after which the IFFT can be performed. This is then transmitted serially through the channel. To facilitate the FFT operation at the demodulator, a parallel representation of bits is required and S/P is performed. Finally the FFT output can be converted back to a serial representation (P/S) which will be the received data [5].

3.4.3 Inverse fast Fourier transform and fast Fourier transform

In order for the receiver to distinguish between the received baseband signals, the frequency thereof needs to be analysed. The carriers arriving at the receiver are orthogonal, separated by a frequency Δf. Consider the trivial application of the Fourier transform on a rectangular signal $f(t)$ with a duration $T = T_u$

$$f(t) = \begin{cases} A, & \text{if } |t| \leq T \\ 0, & \text{if } |t| > T \end{cases} \tag{3.6}$$

Taking the Fourier transform yields

$$\begin{aligned} F(\omega) &= \int_{-\infty}^{\infty} f(t)e^{-j\omega t}dt \\ &= \int_{-T}^{T} Ae^{-j\omega t}dt \\ &= \left[-\frac{1}{j\omega}Ae^{-j\omega t}\right]_{-T}^{T} \\ &= -\frac{2A}{\omega}\left[\frac{e^{j\omega T} - e^{-j\omega T}}{2j}\right] \end{aligned}$$

$$F(\omega) = -\frac{2A}{\omega}sin(\omega T) \tag{3.7}$$

The construction of OFDM subcarriers from a rectangular pulse in the time domain is clear. This result is illustrated in Figure 3.1. Equation (3.5) bears a similarity to the inverse discrete Fourier transform (IDFT) of size N. This suggests that the modulated OFDM symbol a_k can be obtained by taking the inverse fast Fourier transform (IFFT) of the input [5,57]. The IFFT is an efficient and fast way to calculate the IDFT and the implementation of the IFFT (and its counter FFT) made the use of OFDM in practice feasible. The efficiency is increased further by selecting N in the form of 2^m with $m = 1, 2, \ldots$. The IFFT eliminates the complexity involved in conventional FDM modulators, where each carrier requires a separate modulator. Further, the signal at the receiver can be modelled as the discrete Fourier transform (DFT), meaning that the subcarrier at the receiver can be extracted by taking the fast Fourier transform [5]. The IFFT and FFT is a fast way to map or extract symbols. The orthogonality of subcarriers ensures that the subcarriers at the receiver does not interfere.

In conclusion, the symbol transmitted is the result of applying the IFFT. Figure 3.7 illustrates how the IDFT greatly simplifies the modulation process and removes the requirement for a modulator per subcarrier [67]
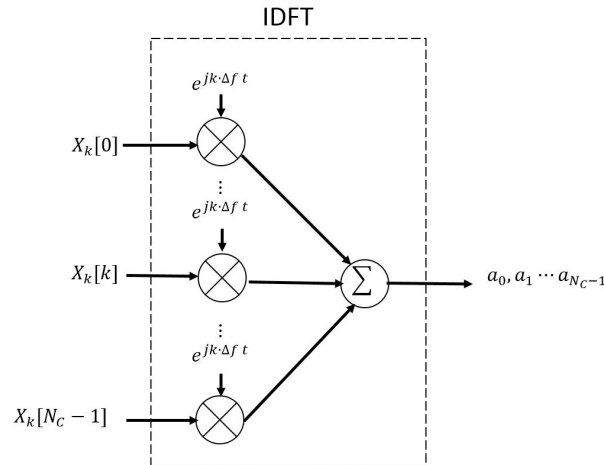
Figure 3.7: IDFT used to reduce the complexity of the OFDM modulation process

3.4.4 Guard intervals

Time dispersion, or delay spread, is caused by multipath effects as described in section 2.3. The delayed symbol overlaps with the boundaries of a preceding or succeeding symbols. This effect is known as Inter Symbol Interference (ISI) and a loss of orthogonality follows as a result. The effects thereof may be reduced by making the symbol duration T large relative to the channel delay spread [62]. In order to ensure OFDM is robust against time dispersion, a guard interval is used in order to increase the symbol duration [68]. Typically in practice the cyclic prefix (CP) is used but other variations of a guard interval exists. They are described in this section.

Cyclic prefix

The CP is applied to the output of the IFFT block. N_{CP} bits are duplicated from the end of the symbol with a length N, and placed at the start as in Figure 3.8 [12, 59]. The total length of the symbol becomes $N = N + N_{\mathrm{CP}}$. The symbol duration is $T = T_u + T_{\mathrm{CP}}$ The demodulator utilises a fraction of the signal power equivalent to $T_u/(T_u + T_{\mathrm{CP}})$, resulting in a reduction of power. The redundant CP bits introduced is removed at the receiver side. The chosen length of the cyclic prefix depends largely on the system in question and the expected duration of the time dispersion [57]. Adding a cyclic prefix reduces the usable power at the demodulator. It can be equated to a loss in SNR defined by [59]

$$\left(\frac{S}{N}\right)_{\text{loss, CP}} = -10\log_{10}\left(1 - \frac{T_{\text{CP}}}{T}\right) \tag{3.8}$$

The choice of CP length now becomes a trade-off between a reduction in ISI vs. SNR. The use of the CP is shown in Figure 3.8 [12]:
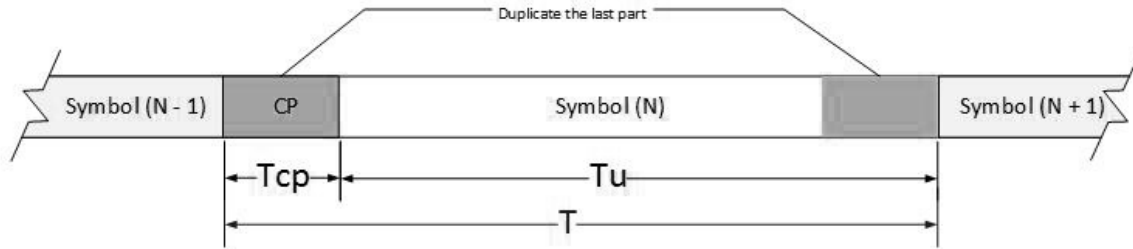
Figure 3.8: Cyclic prefix for a single carrier

Zero padding

Zero padding aims to improve the loss in power experienced in CP applications. A guard interval of length N_{ZP} symbols is appended at the end of each symbol and no signal is transmitted during this interval. This however leads to an noise enhancement [68].

Cyclic suffix

The cyclic suffix increases the symbol duration by T_{CS}. This is achieved by duplicating N_{CS} bits from the start of a symbol and placing it at the end.

3.4.5 **Subcarriers**

Instead of using a single sinusoid as a carrier, OFDM utilises multiple orthogonal sinusoids referred to as subcarriers. This is another degree of freedom in the OFDM system is the number of subcarriers N_c and the subcarrier spacing Δf. Choosing subcarrier spacing to be as small as possible results in an increased T_u and increased SNR performance according to (3.8). This however increases the sensitivity to frequency errors such as the Doppler spread. As a result orthogonality between subcarriers is lost and ICI occurs, degrading the system

performance [12, 57].

The choice of the number of subcarriers depends primarily on the available bandwidth in the application and the required level of quality of the transmission. Recall that OFDM has an increased spectral efficiency, making it an ideal candidate for modern day applications where the available spectrum is limited. The total bandwidth B required is [57]

$$B = N_c \cdot \Delta f \tag{3.9}$$

3.4.6 Inter symbol and inter carrier interference

Inter Symbol Interference (ISI) is caused by delayed symbols overlapping with the boundaries of a preceding or succeeding symbols at the receiver. The effect of this may be mitigated by making use of guard intervals during transmission. Inter carrier interference happens when a subcarrier interferes with one or more of its neighbours. The effect of this is that a single carrier at the receiver can not be extracted as easily and a decrease in system permanence follows.

3.4.7 Multipath propagation and fading

The channel characteristics was defined in Section 2.3. Multipath propagation and fading (large and small scale) disrupts the systems performance and special consideration needs to be given to these to ensure that the simulation is accurate.

3.4.8 Narrowband signal interference

As mentioned in Section 2.7, NBI is a type of impulse interference with a spectrum much smaller than the transmitted signal. It occurs when two different systems is operating in the same frequency range. NBI is particularly disruptive on OFDM systems due to the close spacing of subcarriers and spectral leakage.

3.4.9 Peak to average power ratio

Peak to average power ratio gives a factor of the peaks of a signal in relation to the effective power thereof. PAPR is a metric used to characterise the signal and it can be used to tune the digital modulator to minimise clipping and power usage [69]. In order to determine the PAPR the average signal power as well as the peak signal power is required. A high PAPR requires more powerful demodulators and power to operate the circuit. PAPR and the reduction thereof is discussed in Chapter 4.

3.5 Simulation results

Previously, the performance of OFDM in a wireless environment was investigated by making use of a simulation implemented in MATLAB [12]. The simulation is constructed according to the design in Figure 3.4 [12]. More specifically the parameters of interest included the cyclic prefix length (N_{CP}), the modulation scheme used (M-ary) and the number of subcarriers (N_C). Figures 3.9, 3.11 and 3.13 shows the averaged results from the simulations. At this point no action was taken to reduce PAPR.

The extent of these results are limited. Each of the system properties were evaluated independently. For example the performance of the CP was investigated by changing the CP length whilst keeping the other system parameters (modulation M and subcarrier count N_c) constant. Further no attempt was made to reduce PAPR and no error correctional techniques was applied. The performance of OFDM is investigated by finding the most optimal set of parameters.

3.5.1 Impact of cyclic prefix length

Figures 3.9 and 3.10 show the BER and constellation results when varying the length of the cyclic prefix used. $16-$QAM was used on $N_c = 1024$. Observe that increasing the CP length caused the performance to decrease. The use of a guard interval is required in order to avoid ISI. The length of the CP needs to be chosen carefully since a longer CP leads to a
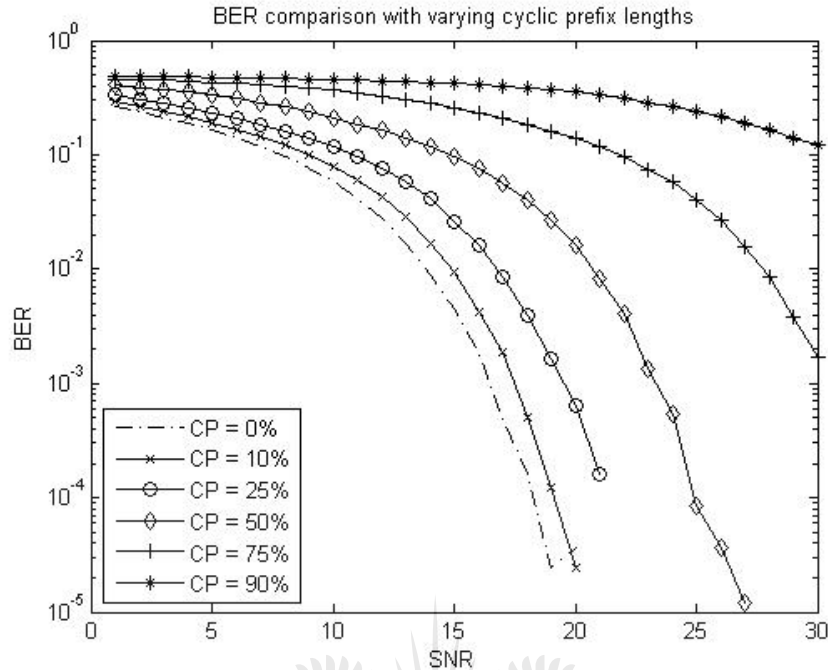
Figure 3.9: Results for different cyclic prefix lengths (CP in %), with $M = 16$ and $N_c = 1024$

decrease in system performance. From Figure 3.10 it can be seen that a long CP will cause the input data to become distorted which hinders the system's performance. This decrease in performance is described by an loss in SNR attributed to the CP added and its length as in (3.8) [59]

$$\left(\frac{S}{N}\right)_{\text{loss, CP}} = -10\log_{10}\left(1 - \frac{T_{\text{CP}}}{T}\right) \tag{3.10}$$

By observing Figure 3.9 it can be seen that a CP length $\leq 25\%$ is optimal. CP is useful in order to reduce ISI and it makes the system more robust and flexible in the presence of multipath propagation and other phenomena in the wireless channel. A typical choice for CP length in modern applications such as Wi-Fi IEEE 802.11ac is 20%.

3.5.2   Impact of modulation scheme

Figures 3.11 and 3.12 show the BER and constellation results when varying the modulation scheme used. The cyclic prefix remains constant at 25% and $N_c = 1024$. The general ob-
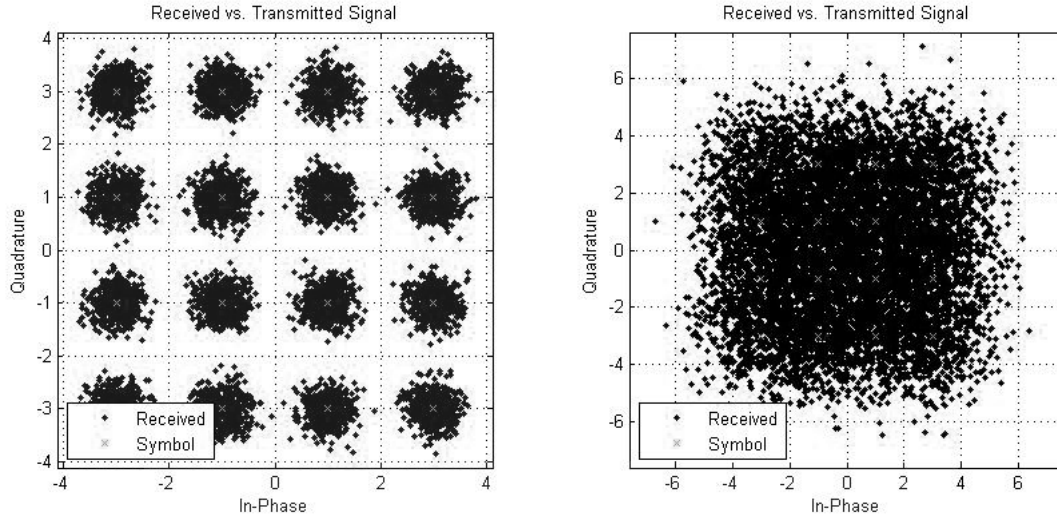
Figure 3.10: Cyclic prefix length for CP = 10% and CP = 75% respectively

servation here is that a hight modulation order degrades the system performance. Equation (3.3) describes how the choice of the modulation schemes affects the probability of obtaining an error. Consider Example 3.1 showing how a larger M will cause the likelihood of obtaining an error to be increased.

Example 3.1 [12]   Consider an arbitrary input with $E_b \backslash N_0 = 1$, using (3.3) we have

For $M = 2$:

$$P_e \leq 1 - \left[1 - 2Q \left(\sqrt{\frac{3}{(2-1)}(1)} \right) \right]^2$$

$$\Rightarrow 1 - \left[1 - 2Q\left(1.732\right) \right]^2$$

$$\Rightarrow 1 - \left[1 - 2(0.044565) \right]^2$$

$$\text{for M} = 2 : \quad P_e \leq 0.1703$$

$$\text{similary for M} = 8 : \quad P_e \leq 0.7654$$

$\square$
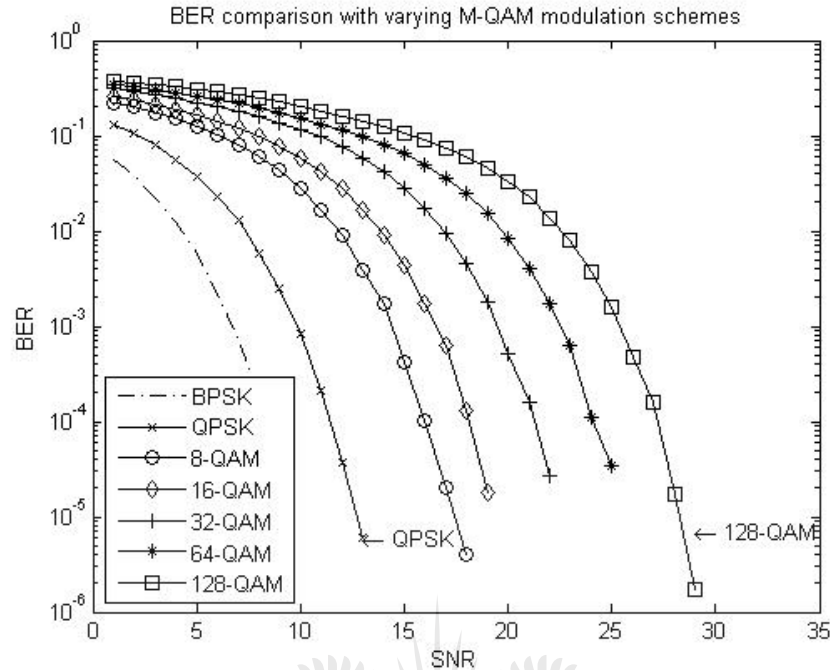
Figure 3.11: Results for modulation schemes (M-QAM) with $CP = 25\%$ and $N_c = 1024$

3.5.3   Impact of chosen number of subcarriers

Figures 3.13 and 3.14 show the BER and constellation results when varying the number of subcarriers which depends primarily on the available bandwidth described by (3.9).

It was observed that the amount of subcarriers does not have any significant impact on the BER of the system. This is because it was assumed that there was no limitations in the bandwidth B and therefore Δf was kept constant for all simulations. The performance of the system is more dependant on the spacing of the subcarriers than the number of carriers chosen. If Δf becomes small, or the carriers are spaced very closely together, then a decrease in system performance will be observed since ICI will degrade the system performance. The use of subcarriers makes the system more robust in the wireless environment and it makes efficient use of the available spectrum.
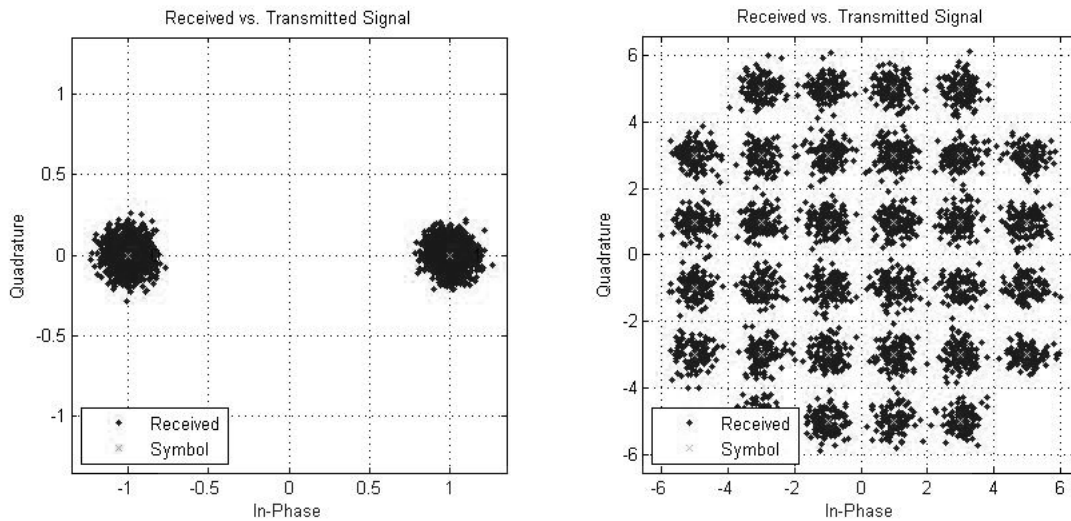
Figure 3.12: Constellation for M being BPSK and $M = 32$-QAM respectively

3.6 Overview

In this chapter an in-depth design of the OFDM system and its parameters was presented. A brief look at the history of OFDM was presented along with modern day applications making use of it. There are a few degrees of freedom when implementing an OFDM design and it differs greatly from application to application.

The OFDM block diagram illustrated the steps involved in OFDM communications. This included the QAM modulation schemes, IFFT, guard intervals and the effect of the channel on the transmitted signal. An experimental setup was defined where the effects of the various system parameters may be investigated. The parameters of interest were the modulation scheme, cyclic prefix length and the number of subcarriers used.

The channel and physical effects within the OFDM system was introduced and elaborated. The parameters of interest was thoroughly explained. Some of the most relevant physical effects present in the channel was reiterated. The importance of NBI in the OFDM environment in particular was suggested and the next chapters will discuss it in more detail. The concept of peak to average power ratio (PAPR) was also introduced here.
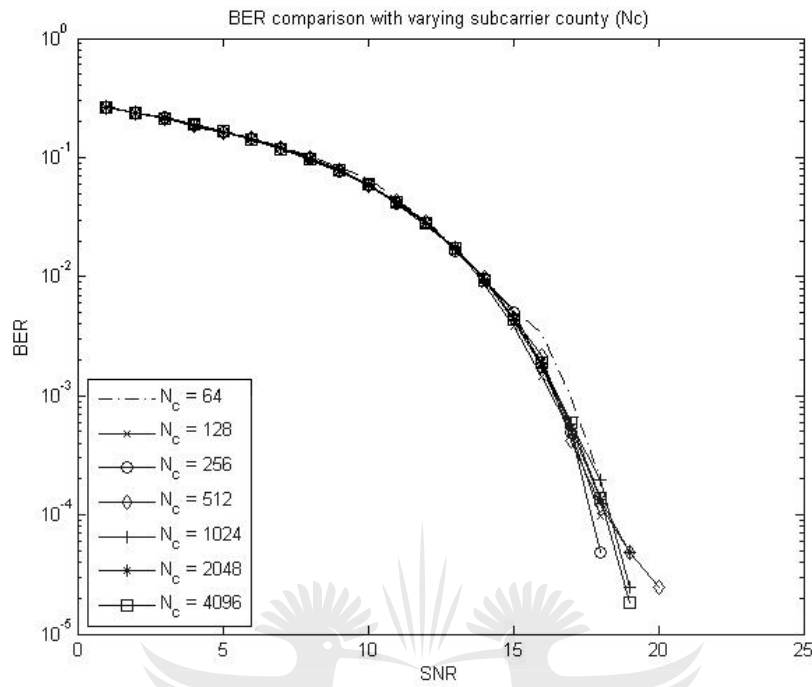
Figure 3.13: Results for varying subcarrier counts (N_c) with $M = 16$ and $CP = 25\%$
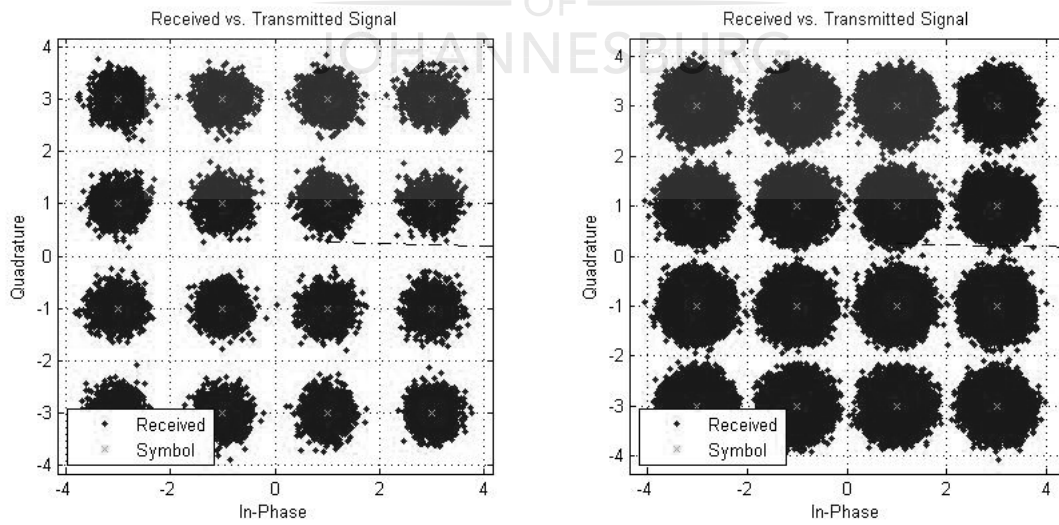
Figure 3.14: Constellation for $N_c = 64$ and $N_c = 2048$ respectively

The simulation results, conclusions and the analysis thereof was presented. In summary an increase in cyclic prefix length resulted in a decrease in system performance. This does not mean that the CP should be omitted completely, but careful consideration should be taken into account when choosing the CP length. Further an increased modulation scheme tends to decrease the system performance since it becomes difficult to make distinctions between small variations in the amplitude or quadrature. The number of subcarriers had little impact on the system performance. This was due to the fact that the bandwidth was assumed to be unlimited and increasing the number of subcarriers resulted in a wider bandwidth but a constant Δf.

The next chapter deals with one of the major issues with OFDM called peak to average power ratio. PAPR in OFDM systems is unusually high and it forced the use of high powered demodulators, resulting in more expensive and inefficient circuits. The problem of PAPR is addressed in order to make OFDM more viable and affordable for the consumer, especially since modern devices has limited battery capacity.

Chapter 4

Peak to Average Power Ratio Characteristics in OFDM

4.1 Introduction

Peak to average power ratio gives a factor of the peaks of a signal in relation to the effective power thereof. It gives an indication of how high the peaks in a signal is when compared to its average value. In OFDM very high peaks is observed which is problematic. PAPR is a metric used to characterise the signal and it can be used to tune the digital modulator to minimise clipping [69]. Clipping occurs when the highest part of a peak is too high for the demodulator to handle. This part of the signal is simply discarded and cause the system performance to degrade. In order to determine the PAPR, the average signal power as well as the peak signal power has to be know. Consider the time average message power (or average power) of an arbitrary waveform,

$$P_m = \lim_{T_m \to \infty} \frac{1}{T_m} \int_{-T_m/2}^{T_m/2} |x(t)|^2 dt \tag{4.1}$$

where $x(t)$ is the waveform and T_m is the time interval over which the average is calculated. Define $x(t)_{max}$ as the maximum value of the waveform over the same time interval. The PAPR is then defined as [70]

$$\mathrm{PAPR}_m = \frac{|x(t)_{\max}|^2}{P_m} \tag{4.2}$$

Example 4.1 Let $x(t) = \sin(2\pi f t)$. From Figure 4.1 we have $x(t)_{\max} = 1$ and $P_m = \frac{1}{2}$ from equation (4.1). The PAPR is given by (4.2) hence $\mathrm{PAPR}_m = \frac{1}{1/2} = 2$. Converting this to decibels gives $\mathrm{PAPR}_{\mathrm{m,dB}} = 10 \log_{10} 2 = 3.01 dB$. □

4.2 Complementary cumulative distribution function

The PAPR has to be calculated statistically because of the unpredictable and random nature of the signal $x(t)$. When tuning the modulator the clipping that occurs needs to be minimised since it will cause in band distortion and degrade the system performance. In order to determine the power level to set the modulator to, the probability of obtaining a signal power greater than some threshold (usually the average power) must be determined. The Complementary Cumulative Distribution Function (CCDF) can be used for this purpose [69, 71].

The CCDF is defined by

$$\mathrm{CCDF}(\epsilon) = P_r(\epsilon < \gamma) \tag{4.3}$$

The probability that the PAPR will exceed the threshold ϵ is defined by

$$F_{\epsilon \, \max(\epsilon)} = P_r(\epsilon > \gamma) = 1 - P_r(\epsilon < \gamma) = 1 - \mathrm{CCDF}(\epsilon) \tag{4.4}$$

The CCDF makes it easier to understand how the power of the system is distributed. A task which would normally be difficult. It gives a probability that the given input will have a power greater than that of the average for the entire system.

Example 4.2 Consider the simple sine wave signal in Example 4.1. Firstly choose an upper bound for γ, the PAPR exceeding the average. A reasonable assumption is to take $\gamma < 18dB$. Calculate the instantaneous power P as well as the PAPR of each sample. Ensure that all units are in decibels. Now evaluate each increment up to the upper bound and

calculate the probability that it exceeds the average power. We find the mean or average PAPR as $\epsilon = 0.500$ and we have $N = 1000$ samples in total. Refer to Table 4.1. The table can be read as follows; 50.2% of the input signal has a power equal to the average power of the signal, 41.8% of the input has a power which is $1dB$ above the average and 30.2% of the signal has a power which is $2dB$ above the average. Finally observe that none of the input signal's components has a power which is $4dB$ or more above the average signal power.

TABLE 4.1: CCDF calculation for $\sin(2\pi ft)$

γ to evaluate (dB)	Number of samples where $\epsilon < \gamma$	CCDF$(\epsilon) = P_r(\epsilon < \gamma)$
0	502	0.502
1	418	0.418
2	302	0.302
3	30	0.030
4	0	0.000
5	0	0.000
6	0	0.000
7	0	0.000
8	0	0.000
9	0	0.000
10	0	0.000
11	0	0.000
12	0	0.000
13	0	0.000
14	0	0.000
15	0	0.000
16	0	0.000
17	0	0.000
18	0	0.000

Sample $x(t) = \sin(2\pi ft)$ at $N = 1000$ samples and test for PAPR from $0\text{dB} - 18dB$. We find that 418 samples exceeds $1dB$ above the average PAPR, equivalently we write CCDF$(\epsilon) = P_r(\epsilon > \gamma) = P_r(\epsilon > 1) = 0.418$. Further 302 samples exceeds $2dB$ and so on. By evaluating the probability up to $18dB$, the CCDF can be constructed as in Figure 4.2. We observe that $P_r(\epsilon > 3)$ will always be approximately 0. Setting the modulator to a power of $3dB$ will ensure that no clipping will occur.

$\square$
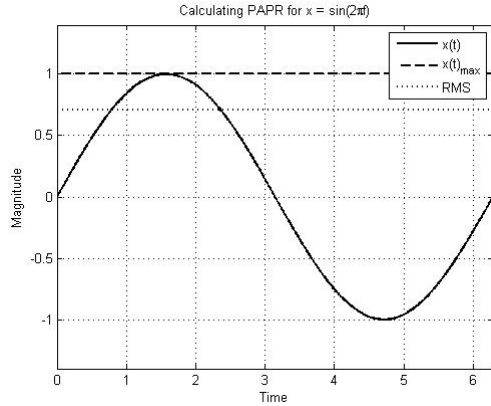
Figure 4.1: Peak to Average Power Ratio example on sin wave [72]
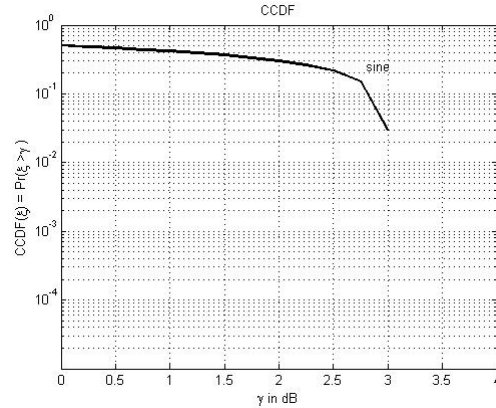
Figure 4.2: Complementary Cumulative Distribution Function for sin [69]

4.3   PAPR in OFDM systems

OFDM has a high PAPR which means that the circuit requires high powered amplifiers (HPA) with a wide operational range. If the circuit design is inadequate clipping and distortion may occur. The large peaks might exceed the saturation region of the HPA, causing distortion and clipping [73]. The draw back of using circuits with HPAs is the high power consumption and drop in efficiency. Especially since OFDM is widely used on hand held devices in wireless telecommunication environments. These devices requires optimal usage in order to preserve it's battery life. Having an huge HPA is undesirable because it will drain the phones battery a lot quicker than a smaller amplifier. The production of these HPAs is also expensive and can be a major contribution to the overall cost of implementing the circuit [70, 74].

Figure 4.3 shows the CCDF for a OFDM system with random data using $M = 32$ and $N_c = 1024$. We see that the event of PAPR exceeding ϵ is certain up to $4dB$. Thereafter after the probability of $\epsilon \geq \gamma$ decreases. At around $16dB$ the probability of $\epsilon \geq \gamma$ is almost zero. The HPA can then be configured to provide a linear operational region up to $16dB$ in order to minimise clipping. If the system caters for clipping which can occur, a smaller operational region may be selected which will reduce cost and power consumption of the circuit. In this system clipping will occur and needs to be handled appropriately in order

to avoid a degraded system performance. Comparing Figures 4.2 and 4.3 clearly shows how of OFDM has a significantly higher PAPR and requires higher powered amplifiers than that which would be required for a simple system. The result is increased power consumption and costs associated with the implementation of OFDM. In order to reduce these the PAPR of the OFDM can be reduced as discussed in the next section. The code for construction the PAPR for any given input signal is included in Appendix B in Listing B.7. No additional interpolation or massaging on the CCDF plots was done. The accuracy of these relies on the steps to evaluate the γ in which was set to $0.25dB$ yielding a fairly accurate representation for the CCDF going forward.
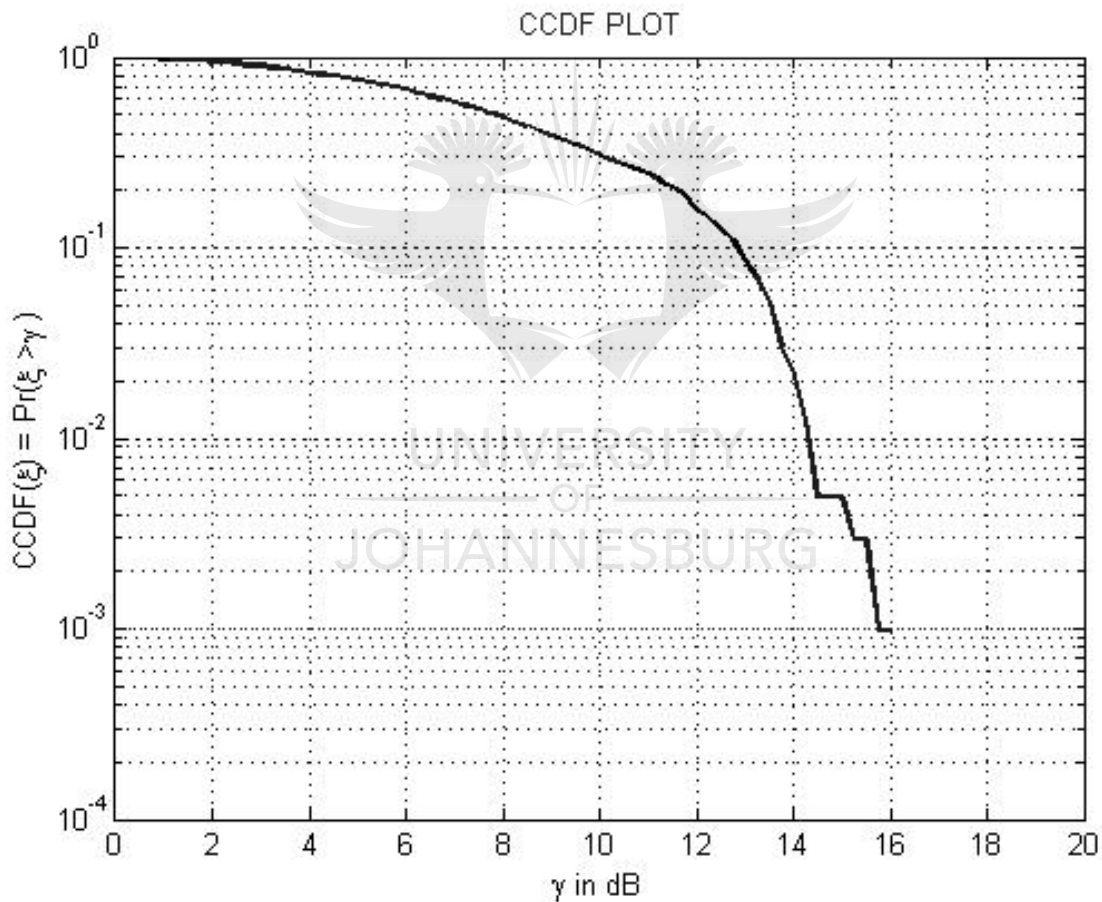
Figure 4.3: CCDF for OFDM with $M = 32$ and $N_c = 1024$

4.4 PAPR reduction techniques in OFDM systems

Numerous techniques has been developed in order to reduce the PAPR in OFDM systems such as Piecewise Exponential Companding (PEC), Luby Trasform (LT) codes, Selective Mapping (SLM), Partial Transmit Sequence (PTS), clipping and windowing [74–82].

4.4.1 Luby trasform codes

Luby transform (LT) codes, named after its inventor, is a type of fountain code. Fountain codes is used in cases where the message is transmitted in packets and a certain number of packets will convey the message in full. Each packet can either be transmitted without any errors, or discarded completely [83]. LT codes may be constructed based on the Robust Soliton Distribution (RSD) probability distribution for each information packet K. A parity check matrix as in Figure 4.4 is used to define the code. Let i be the number of columns, corresponding to the codeword length. V_i is a column in H. And let j is the number of rows relating to the encoded symbols C_j. Let the variable nodes be $V(i) = \{j : H_{ij} = 1\}$ and the check nodes $C(j) = \{i : H_{ij} = 1\}$ [84].

In order to construct the codes, initialise $j = 1$. For each element V_i generate a degree d from the RSD and randomly choose d distinct neighbours. Each C_j's value is the XOR of its neighbours. Repeat these steps until $j = L$ if L is defined, otherwise this process may be repeated infinitely [76, 84].

LT codes can be designed with a PAPR threshold in mind. Each codeword can be encoded to have a CCDF with a minimum value. The process remains similar to the above with only a few adjustments in order to create codes with a lower PAPR. Firstly, the source is divided into two groups, $G_1 = \{a_{i1}, a_{i2}, \cdots, a_{im}\}$ and $G_2 = \{a_1, a_2, \cdots, a_K\} - G_1$. The first group will have a PAPR $< \gamma$. Now calculate d as before and if $d = 1$ choose a symbol from G_1 and repeat the process. Otherwise if $d \neq 1$ choose d distinct random neighbours with the values being the XOR. Calculate the PAPR for each C_j and choose the one with smallest PAPR

$$
H = \begin{array}{c} \begin{array}{ccccccccc} V_1 & V_2 & V_3 & V_4 & V_5 & V_6 & V_7 & V_8 & V_9 \end{array} \\ \left[\begin{array}{ccccccccc} 0 & 0 & 1 & 1 & 0 & 0 & 0 & 1 & 0 \\ 1 & 0 & 0 & 0 & 1 & 0 & 0 & 0 & 1 \\ 0 & 1 & 0 & 0 & 0 & 1 & 1 & 0 & 0 \\ 0 & 0 & 1 & 0 & 1 & 0 & 1 & 0 & 0 \\ 1 & 0 & 0 & 0 & 0 & 1 & 0 & 1 & 0 \\ 0 & 1 & 0 & 1 & 0 & 0 & 0 & 0 & 1 \end{array} \right] \begin{array}{c} C_1 \\ C_2 \\ C_3 \\ C_4 \\ C_5 \\ C_6 \end{array} \end{array}
$$
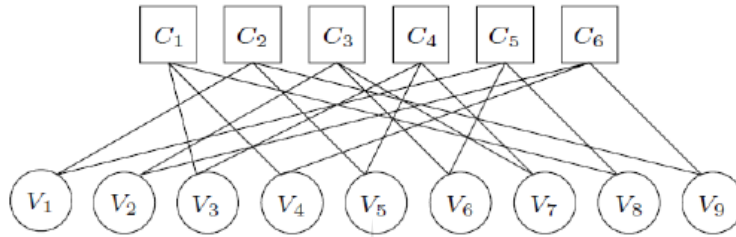
Figure 4.4: Parity check matrix and Tanner graph for constructing LT codes [76, 84, 85]

to be used. This method was proven to be effective in reducing the PAPR [76].

4.4.2 Selective mapping

Selective Mapping (SLM) does not cause distortion and the power requirements of the system remains unchanged. In principle, U alternative transmit sequences will be created based on the same data source. The sequence to transmit will be the one with the lowest PAPR. IF the input data is multiplied by some phase, the PAPR properties will differ after the IFFT was applied [73].

We have the input as $X = \{X_1, X_2, \cdots X_{U-1}\}$ and multiply it with $P = \{P_1^{(u)}, P_2^{(u)}, \cdots, P_N^{(u)}\}$ with $U = \{0, 1, \cdots, U-1\}$. After multiplying, the IFFT is applied. Each $X^{(u)}$ will have a different PAPR. Compare all independent sets and choose the one with the lowest PAPR value to transmit [73, 86].

Numerous PAPR reduction methods aimed at making SLM more effective has been developed such hybrid SLM algorithms [77]. The SLM algorithms can easily be implemented on hardware such as integrated circuits (ICs) and Field-Programmable Gate Arrays (FPGAs)

[87].

4.4.3 Partial transmit sequence

A Partial Transmit Sequence (PTS) divides the input data into different blocks, each multiplied by a different rotation. The technique was developed the with the reduction of PAPR and simplicity as a goal [88, 89]. This process is repeated until the optimal PAPR for each was calculated. The symbol with the lowest PAPR will be transmitted [90]. One drawback here is the complexity involved in implementing this system.

Figure 4.5 shows an simplified implementation of the PTS system [73, 77, 86]. The serial input is divided into blocks $X = \{X_1, X_2, \cdots, X_V\}$ in such a manner that the sum of all blocks will give the original input. Rotation factors is introduced and this system becomes similar to SLM with a restriction on the rotation vectors to be used (instead of $P^{(u)}$ in SLM) [86, 88].
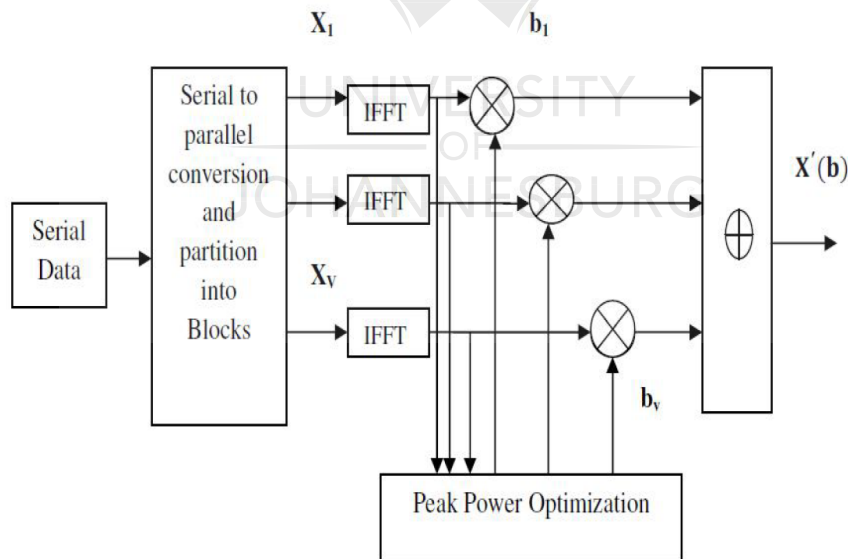
Figure 4.5: PAPR reduction using partial Transmit Sequence

Variations in the PTS technique does exist and it mainly revolves around the logic implemented in the optimisation block. Hee derived a new set of rotation vectors designed to

improve the performance of the system. The method is based on the optimisation method called a Gradient Decent Search (GDS). A set of phase vectors is chosen to start with and the GDS is applied in order to create an updated set of phase vectors within a certain radius r. Each set results in the a reduced PAPR. This method is iterative and continues until a set of vectors resulting in the largest reduction of PAPR is obtained. This can be repeated until no more improvement in PAPR is observed [78].

4.4.4 Clipping and peak windowing

Clipping and filtering is often considered to be one of the most practical and easiest PAPR reduction methods due to it's simplicity. It does however introduce some distortions, both in- and out-of band which can negatively affect the BER performance of the system and some of the spectral efficiency of the orthogonal carriers are reduced [90]. Figure 4.6 shows a simple setup for the clipping and filtering method [90,91]. This process is applied iteratively until the desired thresholds is achieved.
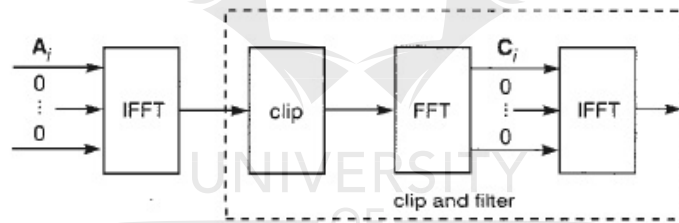
Figure 4.6: PAPR reduction using clipping and filtering technique

Peak windowing is another method which gives improved results when compared to clipping and filtering. Here a threshold level for the peak is set. This can typically be some fraction of the maximum peak value or some other chosen constant. If a peak exceeds the threshold the signal is multiplied with some windowing function. The improved performance comes from the fact that no hard-clipping is applied resulting in less distortion of the signal and an improved BER performance [90].

Clipping and peak windowing can be combined in order to keep the simplicity of the implementation without the BER performance degrading [92]. Figure 4.7 shows a proposed method achieving better performance than clipping on its own.
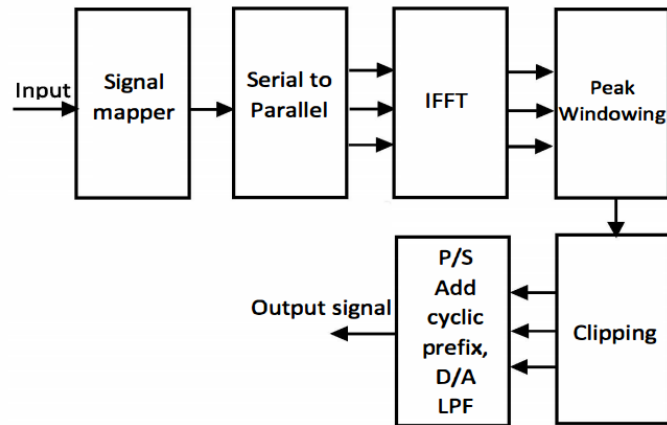
Figure 4.7: PAPR reduction using clipping and filtering technique in combination with Peak Windowing

4.4.5   Comparison of PAPR reduction techniques

Comparison studies of PAPR reduction techniques in OFDM found that peak insertion was one of the best performing methods in terms of the CCDF and BER performance of the system. However, the PAPR reduction technique relies on other factors such as the BER performance, complexity and power limitations in a given system. Figure 4.8 shows the results from a study on various PAPR techniques such as peak insertion and clipping [93]. The performance in terms of CCDF and BER is shown. The paper concluded that peak insertion perform best in term of the CCDF. The chosen method will also have an effect on the BER performance of the system and therefore choosing a PAPR reduction method is not trivial [76, 86, 93].
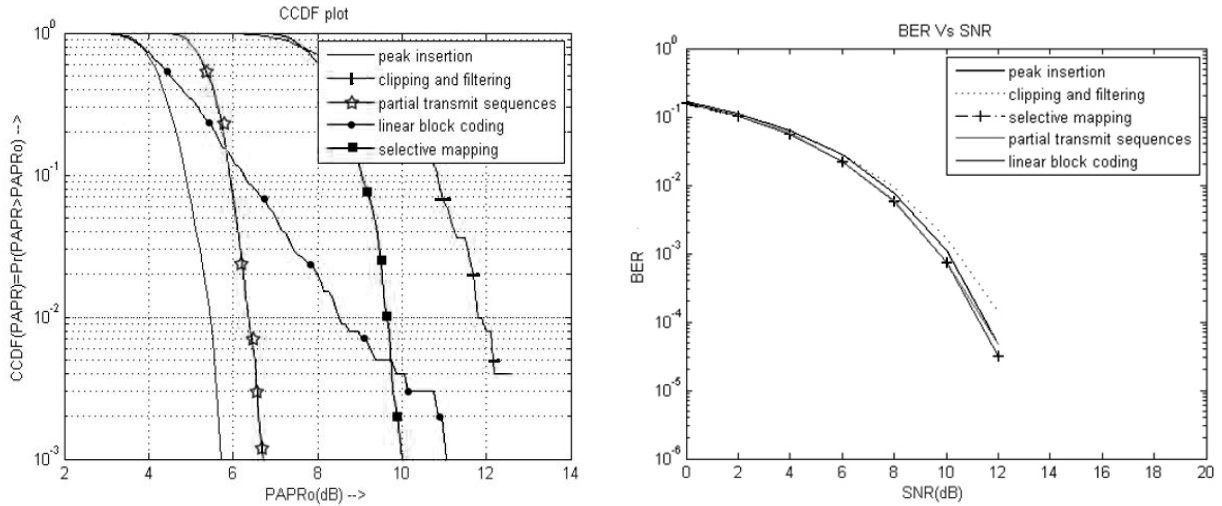
Figure 4.8: CCDF performance of various PAPR reduction techniques and BER performance of various PAPR reduction techniques

4.5 Simulation

4.5.1 Setup

The diagram presented earlier (in Figure 3.4) is modified to include the clipping and filtering method in order to produce results with acceptable PAPR levels. This OFDM system is near optimal and will be used for further investigation purposes in this document. Figure 4.9 shows the updated OFDM system. A clipping factor κ is defined as the factor of the average value of the input such that

$$\kappa = \tau \left(\frac{1}{K} \sum_{k=1}^{K} I_k(f_n) \right) \tag{4.5}$$

where κ is the clipping factor (or threshold where the input will be clipped at), $I_k(f_n)$ is the impulse at the receiver for the subcarrier with frequency f_n as defined in (2.28) and τ is a factor which may be chosen arbitrarily in this case. In general the design of the circuit and power usage constraints needs to be taken into account in order to design a suitable clipping threshold. The code in Appendix B, Listing B.2 shows how clipping was implemented for the simulation.
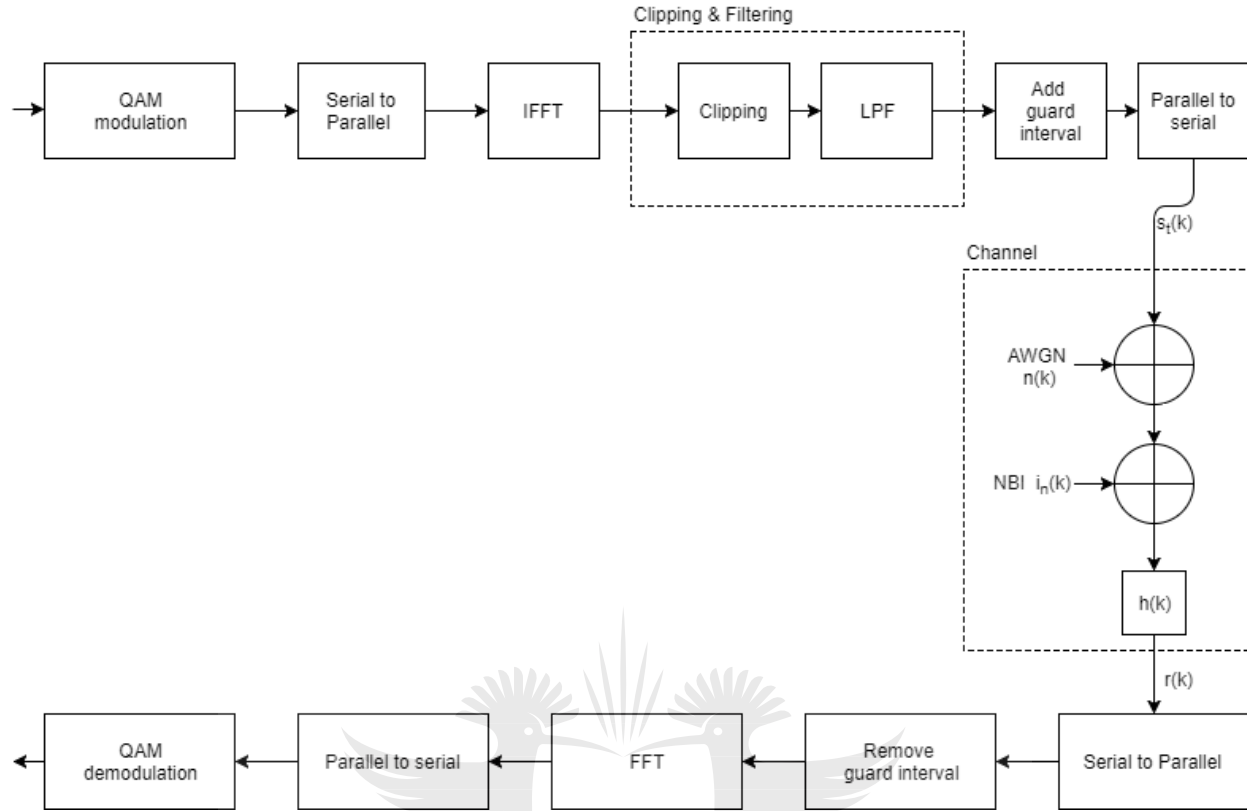
Figure 4.9: OFDM simulation block diagram with clipping and filtering applied as PAPR reduction technique

4.5.2 Results

The results obtained from simulations for the case where the clipping factor τ is adjusted and compared to a random input is shown in Figure 4.10. Figure 4.11 shows the same data but the results for random input without clipping is omitted in order to compare the effect of τ on the CCDF and BER without having to scale the axes and distorting the observations.

In Figure 4.10 from the CCDF on the left hand side (LHS) it is seen that any form of clipping will yield a better system performance. A reduction of approximately $4dB$ is observed when compared to the random input. This improved performance will result in more efficient and cheaper circuitry. The BER shown on the right hand side (RHS) shows poor performance for the clipped signal at $\tau = 1$ when compared to the BER of random data. The reason for this is because the system did not employ any error correctional techniques
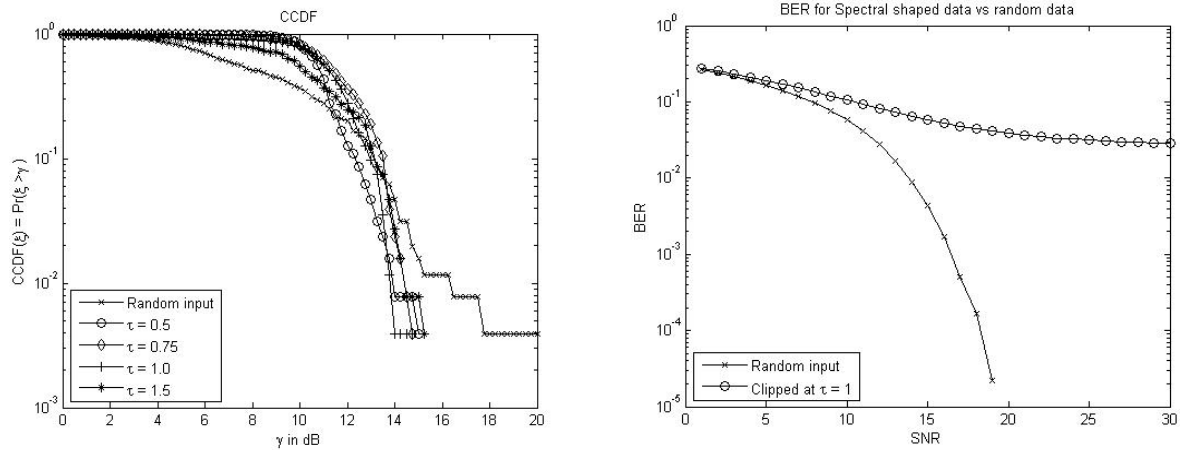
Figure 4.10: Comparison of PAPR and BER performance with random input vs clipped input ($\tau = 0.5$)

or attempt to recover lost data. The clipping threshold with $\tau = 1$ is set at the average power of the transmission. This resulted in data being clipped along with the peaks of the impulse noise. The choice of τ is not trivial since it can have major performance implications as evident in these simulations.
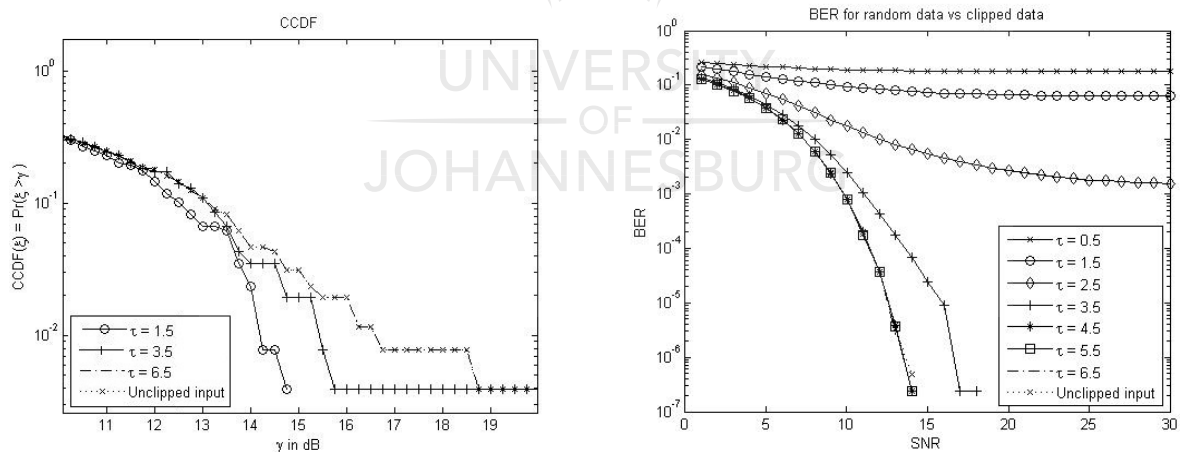
Figure 4.11: Comparison of PAPR and BER performance in terms of clipping threshold τ

Further investigations led to the usage of τ which is much greater than 1. Figure 4.11 on the RHS shows the performance of the system when using a wide range for the clipping factors. Note how at $\tau = 0.5$ to $\tau = 2.5$ the system did not yield much of a performance improvement in terms of BER. It did however give good CCDF performance. This is be-

cause a maximum amount of clipping was applied, voiding some of the useful data in the transmission. With $\tau = 3.5$ an acceptable PAPR performance is obtained, which is still well below that of an unclipped system and also an excellent BER performance. This shows that the highest peaks of the system is most probably above the value of $\tau \hat{P}(f_n)$ where is $\tau = 3.5$ and anything above and beyond the threshold is surely due to impulse noise. Everything below the threshold probably contains useful information. The clipping threshold should ideally lie between the average value and peak value of the system in such a way as to allow the important data of the system to be preserved.

Figure 4.12 represents the findings in an alternative fashion by making use of the constellation plots of the clipped signals. An increase in τ gives more accurate results during demodulation, leading to an improved BER performance of the system. From the CCDF it can be concluded that an acceptable value for τ is around 3.5 since it gives a good BER performance and an acceptable PAPR.

4.6 Overview

In this chapter the problem with OFDM name PAPR was introduced. It gives a factor of the peaks of a signal in relation to the effective power thereof. PAPR is a metric used to characterise the signal and it can be used to tune the digital modulator to minimise clipping. A high PAPR results in more expensive circuits and leads to more energy consumption which is a major concern with modern mobile devices with limited battery life.

The CCDF was defined in terms of fundamental concepts and sinusoids. It was applied in the context of OFDM systems and it was immediately clear that it was a problem.

Numerous methods exists to reduce the PAPR in OFDM systems. This topic is still researched actively today as OFDM is becoming more popular in wireless and PLC systems. Some of the PAPR reduction techniques was investigated including Luby Transform codes, SLM, PTS, Clipping and Windowing. These were compared in terms of the performance,

BER and complexity of implementation.

For the purpose of this research, clipping was chosen as the preferred method of PAPR reduction. This method is effective, efficient and relatively simple to implement. The simulation was constructed by modifying the OFDM block diagram from Chapter 3 to include the clipping and windowing phase. Results showed that a carefully designed clipping threshold can guarantee an acceptable PAPR and BER performance.

The next chapter will introduce the concept of Spectral Shaping and a specific method called spectral null codes.
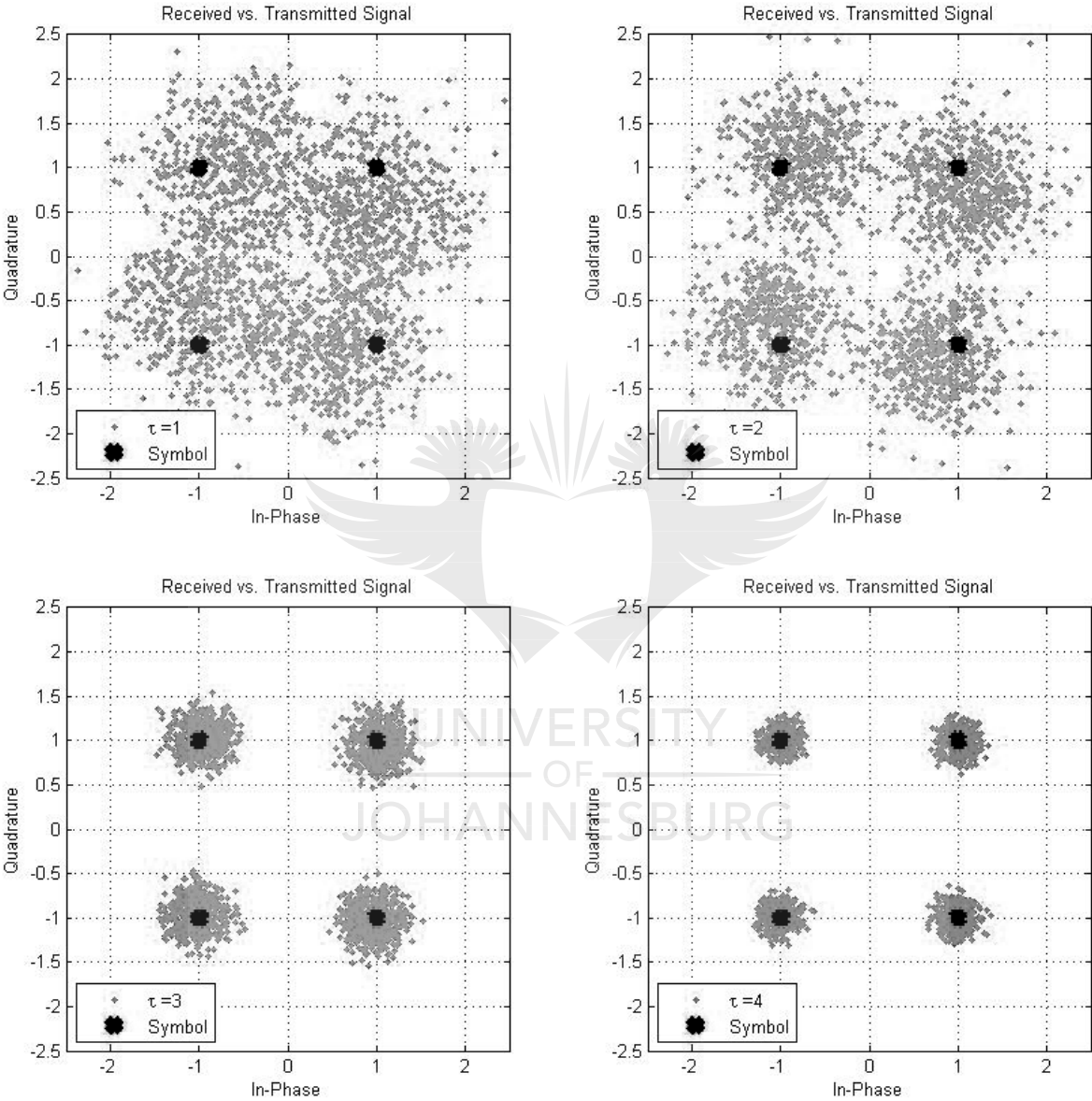
Figure 4.12: Comparison of constellation for $\tau = 1.0$, $\tau = 2.0$, $\tau = 3.0$ and $\tau = 4.0$ respectively

Chapter 5

Spectral Shaping Techniques and Spectral Null Codes

5.1   Introduction to spectral shaping

Coding is used in order to improve the reliability and the efficiency of the system in question. Immink [94] originally described how to use codes in digital recording systems such as CD and DVD. Channel coding makes reliable transmission possible in an effective manner, given the limited capacity of the channel. Reliability is defined as the probability of receiving incorrect data or a bit error [94]. Reed-Solomon codes is a type of block error correcting code that relies on redundant bits in order to recover from errors which may have occurred during transmission. The Reed-Solomon codes are also used with CD and DVD applications. It can be used to successfully recover from burst errors such as a fingerprint present on the surface on the medium [95]. Markov models is used in order to model burst errors introduced in the channel [96]. These errors span a small portion of the total spectrum for example the fingerprint on the CD or impulse noise interfering on the OFDM transmission.

Previously error correctional codes (ECC) has been used in conjunction with OFDM in order to reduce the effects of ICI which occurs when orthogonality between subcarriers is lost, resulting in a higher BER [97]. The study of coding techniques spans a broad range of topics and methodology. For this chapter the particular code of interest is known as spectral

null codes. By adding redundancy, the power spectral density (PSD) of the signal may be designed to meet certain criteria.

Gorog [53] proved the existence of redundant codes with certain properties in their spectrum. This differs from the traditional method where redundancy in codes was introduced for the purpose of error correctional purposes. Some error correctional codes provides redundancy in order to recover from bit errors as a result of noise in the channel, whereas spectral shaping codes makes use of redundancy in order to obtain desirable properties in the spectrum of the signal.

The system design during this chapter will be based on the spectral properties of the codewords. Historically spectral shaping codes had numerous applications in industry. An example of a spectral null code is the pilot frequencies on magnetic and optical storage systems [8, 53].

5.2 Spectral null codes

Spectral null codes are of interest to use because these are designed to have a zero power spectral density (PSD) at selected frequencies. The technique of creating spectral nulls at desired frequencies of the spectrum is called spectral shaping [8]. This chapter briefly describes the methodology for designing spectral null codes and constructing a codebook with a known power spectral density.

Spectral null codes are used widely in information theory and the storage of data. A classic example of its usage is to allow pilot tones to be included on magnetic disks. These tones guide the disk reader head as to where it is currently reading data from. It is a kind of coordinate system. This is commonly done by adding auxiliary or pilot tones. Data and pilot tones can occupy the same space by creating spectral nulls in the data to coincide with the location of the pilot tones [8, 53]. Spectral null codes may be used to prevent the data stored on the disk and the pilot tones from interfering. The data stored is encoded

that the PSD thereof is zero at the pilot tone frequencies [8]. Spectral null codes with nulls at low-frequencies have special applications as well. These codes are called dc-free codes [94].

Spectral null codes is a type DC-free code which is applicable in many data storage systems such as magnetic tapes and optical mediums. In the case of data storage, a positive charge can represent a *one* and a negative charge can represent a *zero* bit. DC-free codes are codes where the number of positive symbols is the same as the number of negative symbols or where the difference between the number positive and negative symbols is bounded by a finite number. In data storage applications a code where the number of positive and negative symbols are the same is desired and these types of codes are referred to as zero-disparity codes [98, 99].

It becomes important to have a code with minimal or no DC components. This is required in order to preserve the symbol shape when passing it through a high pass filter. Low frequency noise, such as a fingerprint on a CD, may be removed by passing the signal through a high pass filter [44]. Error correctional codes may be used in order to mitigate the effects of narrowband interference present in the channel. Many applications of data storage require DC-free codes in order to reduce DC-wander.

Knowing the spectral properties of a codebook allows the communications system to be designed according to the spectral properties, which allows for some interesting usages such as the use of auxiliary signals as described earlier. The PSD may also be used to make conclusions on the transfer function of the channel and other estimations. For the purpose of this document the effect of NBI on the PSD is investigated and this research may easily be extended to various other studies on the PSD and channel estimations.

5.2.1   Construction of spectral null codes

Consider a set S, referred to as a codebook of codewords. The vector y is an element within S. Let $y = (y_1, y_2, \ldots, y_n)$ with $y_i \in \{-1, +1\}$. A codebook of codewords with spectral nulls at desired frequencies may be constructed. Having spectral nulls, is the equivalent to

equating the power spectral density function to zero. Let $H(\omega)$ be the power spectral density function defined as [44, 53]

$$H(\omega) = \frac{1}{C_s M} \sum_{i=0}^{M-1} |\mathcal{Y}^i(\omega)|^2 \tag{5.1}$$

where C_s is the cardinality of the codebook and M the length of the codeword. $\mathcal{Y}$ is the Fourier transform of the codeword defined by,

$$\mathcal{Y} = \sum_{i=1}^{M} y_i e^{-ji\omega}, \qquad -\pi \leq \omega \leq \pi \tag{5.2}$$

Let S have a spectral null at $f = \frac{\omega}{2\pi} = \frac{1}{N}$, thus $\omega = \frac{2\pi}{N}$. From (5.1), observe that $H(\omega) = 0$ when $|\mathcal{Y}(\omega)| = 0$. Substituting for ω, it can then be noted that $\mathcal{Y}\left(\frac{2\pi}{N}\right) = 0$ is a sufficient condition for the sequence to have a spectral null at a specific frequency.

From (5.2) it can be obtained that [44, 53]

$$\sum_{i=1}^{M} y_i e^{-j2\pi i/N} = 0 \tag{5.3}$$

Let $M = Nz$, where N is an integer representing the number of spectral null groupings.

The amplitude of the vector i is denoted by

$$A_i = \sum_{r=0}^{z-1} y_{i+rN}, \qquad i = 1, 2, ..., N \tag{5.4}$$

A_i can take the value of

$$A_i \in \{\pm M/N \mp \alpha\} \tag{5.5}$$

where $\alpha \in \{0, 2, \ldots M/N\}$ if M/N is even, or $\alpha \in \{0, 2, \ldots (M/N - 1)\}$ if M/N is odd.

A spectral null code may be constructed by balancing the N vectors. N may be chosen as prime or non-prime. In order to construct a dc-free code, zero-disparity codewords can be selected. That is codes with an equal number of *1's* and *0's* [94].

The construction of spectral null codes is explained by means of examples in the next sections, depending on N.

If N is prime

If N is prime and considering (5.4), the following condition with respect to the amplitude A of the vectors must hold [53]:

$$A_1 = A_2 = \cdots = A_N \tag{5.6}$$

Equivalently, by substituting (5.4) and (5.6) results in:

$$y_1 + \cdots + y_{1+(M-N)} = y_2 + \cdots + y_{2+(M-N)} = y_N + \cdots + y_M \tag{5.7}$$

Now (5.4) can be rewritten as

$$A_i = \sum_m y_m, \qquad i = 1, 2, \ldots, N \tag{5.8}$$

with

$$m \in \{i, i+N, i+2N, \ldots, i+(M/N-1)N\}, \qquad 1 \leq i \leq N \tag{5.9}$$

The cardinality of the codebook is described by [53]

$$|C_b(M,N)| = \sum_{i=0}^{M/N} \binom{M/N}{i}^N \tag{5.10}$$

where $\binom{M/N}{i} = \frac{(M/N)!}{i!(M/N-i)!}$. $C_b(M,N)$ represents the entire codebook of codewords with know PSD properties. The cardinality is equal to the number of codewords in the codebook with spectral nulls at $f = \frac{1}{N}$. The location of spectral nulls can be defined based on the value of N as

$$f = \frac{1, 2, \ldots, (N-1)}{N}, \qquad \text{where } N \text{ is prime} \tag{5.11}$$

The following example demonstrates how a codebook of spectral null codes may be constructed if N is prime:

Example 5.1   Let $M = 4$ and $N = 2$. Therefore $z = M/N = 2$. The codewords will have a spectral null at $f = \frac{1}{2}$ of the normalised frequency according to (5.11).

Recall that $i = 1, 2, \ldots, N$. From (5.4) and (5.8) we have

$$A_1 = \sum_{r=0}^{1} y_{1+rN} = y_1 + y_3 \tag{5.12}$$

$$A_2 = \sum_{r=0}^{1} y_{2+rN} = y_2 + y_4 \tag{5.13}$$

Property (5.6) must hold since N is prime, so

$$A_1 = A_2 \tag{5.14}$$
$$y_1 + y_3 = y_2 + y_4 \tag{5.15}$$

And $y_i \in \{-1, 1\}$, for simplification, replace -1 with 0.

TABLE 5.1: Codewords with $M = 4$

Entry	y_1	y_2	y_3	y_4	$A_1 = y_1 + y_3$	$A_2 = y_2 + y_4$
1	0	0	0	0	-2	-2
2	0	0	0	1	-2	0
3	0	0	1	0	0	-2
4	0	0	1	1	0	0
5	0	1	0	0	-2	0
6	0	1	0	1	-2	2
7	0	1	1	0	0	0
8	0	1	1	1	0	2
9	1	0	0	0	0	-2
10	1	0	0	1	0	0
11	1	0	1	0	2	-2
12	1	0	1	1	2	0
13	1	1	0	0	0	0
14	1	1	0	1	0	2
15	1	1	1	0	2	0
16	1	1	1	1	2	2

From Table 5.1 the codebook $C_b(4, 2)$ can be constructed by selecting entries which sat-

isfies (5.6). They are the entries where $A_1 = A_2$, hence entries $1, 4, 7, 10, 13, 16$ in Table 5.1 as indicated by the shaded area.

The codebook of codewords obtained is

$$C_b(4,2) = \begin{Bmatrix} 0 & 0 & 0 & 0 \\ 0 & 0 & 1 & 1 \\ 0 & 1 & 1 & 0 \\ 1 & 0 & 0 & 1 \\ 1 & 1 & 0 & 0 \\ 1 & 1 & 1 & 1 \end{Bmatrix} \tag{5.16}$$

Using (5.10) it is confirmed that the cardinality of the codebook is in fact 6 as expected. Furthermore, note how (5.5) describes the possible values for A_i obtained in table 5.1. Clearly $A_i \in \{-2, 0, 2\}$. This is not a dc-free code since the codebook did not exclude non-zero-disparity codewords such as $\{0, 0, 0, 0\}$ and $\{1, 1, 1, 1\}$. Figure 5.1 shows the PSD for this example. Note that this is not a dc-free code because the low frequency power is not zero. Further equation (5.11) confirms the observation that a spectral null occurs as $f = \frac{1}{2}$

A MATLAB application was developed in order to construct a codebook for any given inputs. Figure 5.1 shows the PSD for the codebook in (5.16). The PSD is estimated by making use of the `pwelsh` function in MATLAB [100]. Welsh's method of PSD estimation is described in Chapter 2.6 and Appendix B, Listings B.3 through B.6 shows the code used for this implementation.
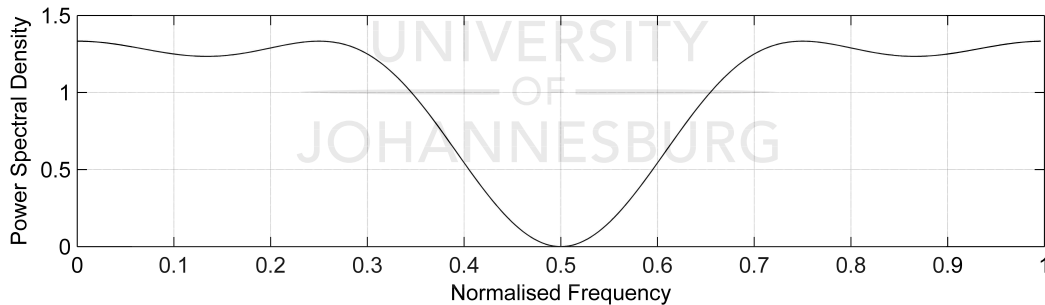
Figure 5.1: Power spectral density for the codebook $C_b(4,2)$ with $M = 4$ and $N = 2$

If N is not prime

If N is not prime, the following must hold to allow for spectral nulls to occur [53]:

$$A_u = A_{u+vc}$$
$$u = 1, 2, \ldots, c, \tag{5.17}$$
$$v = 1, 2, \ldots, d-1,$$

where c and d is found by taking all possible factors of N where $N = cd$ and $c \neq 1$ and $d \neq 1$. The codebook of spectral null codes may be found by taking the union of the solutions to (5.17).

Equations (5.4) and (5.5) are verified in the case where N is not prime. Consider the following example:

Example 5.2   Let $M = 12, N = 6$ and therefore $z = 2$. From (5.4) we have:

$$
\begin{aligned}
A_1 &= y_1 + y_7 \\
A_2 &= y_2 + y_8 \\
A_3 &= y_3 + y_9 \\
A_4 &= y_4 + y_{10} \\
A_5 &= y_5 + y_{11} \\
A_6 &= y_6 + y_{12}
\end{aligned}
$$

To satisfy (5.17), N is factorised to obtain

$$
\begin{aligned}
1 &\times 6 \\
2 &\times 3 \\
3 &\times 2 \\
6 &\times 1
\end{aligned}
$$

Since $c \neq 1$ and $d \neq 1$ we have $N = 2 \times 3$ and $N = 3 \times 2$.

For $N = 2 \times 3$, $c = 2$ and $d = 3$:

$$\begin{cases} u = & 1, 2 \\ v = & 1, 2 \end{cases} \quad \Rightarrow \quad \begin{cases} A_u = A_{u+vc} \\ A_u = A_{u+vc} \end{cases} \quad \text{thus} \quad \begin{cases} A_1 = A_3 \\ A_2 = A_4 \end{cases} \quad \text{and} \quad \begin{cases} A_1 = A_5 \\ A_2 = A_6 \end{cases} \tag{5.18}$$

For $N = 3 \times 2$, $c = 3$ and $d = 2$:

$$\begin{cases} u = 1, 2, 3 \\ v = 1 \end{cases} \quad \Rightarrow \quad \begin{cases} A_1 = & A_4 \\ A_2 = & A_5 \\ A_3 = & A_6 \end{cases} \tag{5.19}$$

The codebook is constructed by finding the codewords which satisfies the union of the above solutions,

$$\begin{cases} A_1 = A_3 \\ A_2 = A_4 \end{cases} \quad \cup \quad \begin{cases} A_1 = A_5 \\ A_2 = A_6 \end{cases} \quad \cup \quad \begin{cases} A_1 = & A_4 \\ A_2 = & A_5 \\ A_3 = & A_6 \end{cases} \tag{5.20}$$

Using (5.4), the above may be rewritten as

$$\begin{cases} y_1 + y_7 = y_3 + y_9 \\ y_2 + y_8 = y_4 + y_{10} \end{cases} \quad \cup \quad \begin{cases} y_1 + y_7 = y_5 + y_{11} \\ y_2 + y_8 = y_6 + y_{12} \end{cases} \quad \cup \quad \begin{cases} y_1 + y_7 = & y_4 + y_{10} \\ y_2 + y_8 = & y_5 + y_{11} \\ y_3 + y_9 = & y_6 + y_{12} \end{cases} \tag{5.21}$$

There is two elements in each grouping and by (5.5) $A_i \in \{-2, 0, 2\}$. Constructing the codebook from here is trivial as it found by simply searching for entries satisfying the above.

Equation (5.11) does not hold in the case where N is prime. This is observed from the plot of the PSD. Certain nulls disappeared due to the union. This observation is noted here but the study of the disappearing nulls due to the union can be a study on its own.
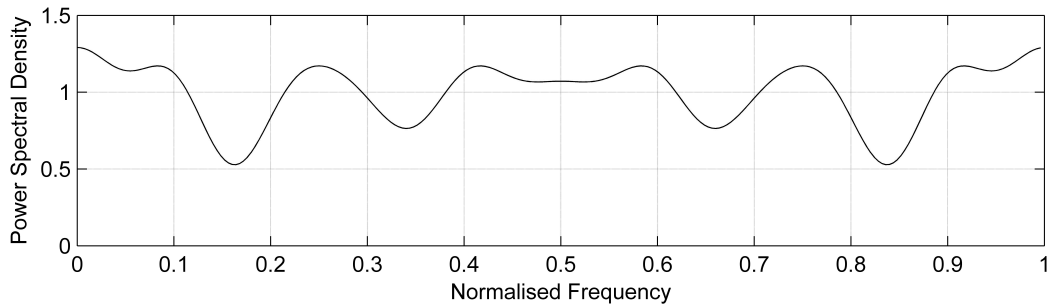
Figure 5.2: Power spectral density for the codebook $C_b(12,6)$ with $M = 12$ and $N = 6$, with non-zero-disparity codewords

If the search is narrowed further to include only zero-disparity codewords, the PSD is as shown in Figure 5.3, which is clearly a dc-free code characterised by the zero PSD at low frequencies. Observe that the spectral nulls does not have a PSD of exactly 0, but a significant drop in the power is observed at the designed frequencies. This is due to the total power of the transmission across the spectrum which must remain constant before and after applying the spectral shaping.
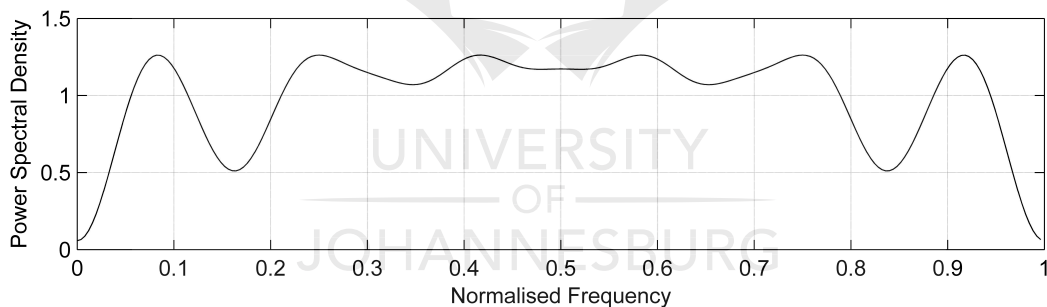
Figure 5.3: Power spectral density for the codebook $C_b(12,6)$ with $M = 12$ and $N = 6$, with zero-disparity codewords

$\square$

5.2.2   Using MATLAB to generate a codebook

The code for generating a codebook is included in Appendix B, Listings B.3 through B.6. A matrix is constructed defining the relationships which must hold according to (5.4). Each row of this matrix contains the indices of the amplitudes which should be equal. Next all binary combinations of codes with length M is created. This step was problematic during

experimentations since it took some computational power in order to calculate and store the results of `de2bi`. The system's available resources restricted the length of the spectral null codes to be 16. A check was built into the code in order to prevent the user from choosing codes larger than the system can handle. The alternative is a system crash and decreased performance.

The code will check if N is prime or non-prime in order to choose the next steps. If N is prime, the list of all codewords is iterated and those satisfying (5.8) is selected. If N is non-prime, u and v is calculated and all codes satisfying (5.17) is selected.

Finally choose zero-disparity codewords. The remaining codes in the matrix is the codebook $C_b(M, N)$ with the spectral properties as originally specified. These codes may be used in any transmission system as the input. The input data will be codded with these spectral shaped codes before transmission.

This method for generating codebooks with spectral null codes having the specified properties will be used throughout the rest of this document in order to generate the input of the simulations.

5.3 Overview

In this chapter the concept of spectral shaping was introduced and investigated. The use of these methods in industries such as data storage and audio recording was emphasised. The specific code of interest in this case is the spectral null code since it is already used widely in practice and implementations thereof is well documented. The spectral null code will have nulls at the desired frequencies allow the engineer to make use of auxiliary signals in the same spectrum as the primary signal. This can have interesting applications.

The construction of spectral null codes was explained from first principles. The design is based on the desired length of the codeword as well as the number of spectral null group-

ings. Depending on the chosen number of groupings (being prime or non-prime) a set of equations describing the properties of the codeword is derived. From there the construction of a codebook becomes trivial since a simple lookup can be used to find the codes satisfying the relevant equations. This method was demonstrated practically by means of example. A brief description of the MATLAB code used in order to create any codebook was presented in which some of the limitations of the code was raised such as the limited codeword length due to a limited amount of system resources and computing power.

The next chapter will attempt to combine spectral null codes with an OFDM transmission. The PSD will be investigated with the focus on NBI and how it affects the PSD of the spectral shaped system.

Chapter 6

Combined Spectral Null Codes and OFDM

6.1 Introduction

Previously OFDM (Chapter 3), the problem with PAPR (Chapter 4) and spectral shaping techniques (Chapter 5) was introduced. The optimised implementation of an OFDM system was derived with assistance from a simulation. The effects of NBI was investigated and incorporated into the simulation. Finally the use and construction of spectral shaping techniques was presented. This chapter introduces a new method which can be used detect narrowband signals in an OFDM system by making use of spectral null codes. In short, OFDM carriers will be loaded with spectral null codes, giving the system known spectral properties. Investigations into how the presence of narrowband signals can be detected is conducted. Finally the aim is to further improve the system performance by selectively switching carriers affected by NBI off.

The PSD of an OFDM system where all subcarriers are loaded with codewords having spectral nulls at a selected frequency f_n is investigated. For the purpose of this investigation the standard OFDM system is modified slightly to accommodate the usage of spectral shaped data. The key differences is the usage of a codebook in order to select symbols to be mapped onto the parallel subcarriers. Source code is modified to index spectral null coded words

which can be mapped directly onto the available subcarriers.

6.2   Detecting nulls within the OFDM spectrum

The PSD is used to visually show the energy per frequency. Studies has shown that the modulation scheme chosen effects the performance of the system, where a higher order of modulation typically has more power at the same frequency [101].

Spectral analysis is the investigation and close examination of the signal in the frequency domain [102]. Section 2.6 introduced the method named after P.D. Welch which is commonly used in order to estimate the PSD of a signal. His method relies on the Fourier transform which gives describes the frequency components of the signal. The Fourier transform can be computed efficiently by making use of the FFT. Dedicated ICs used on modern computers can easily perform this function. Spectral analysis can be applied to any given signal. In this section a brief introduction to some of the methods used in order to evaluate the spectrum is given.

6.2.1   Long-term average spectrum

The Long-term average spectrum (LTAS) is applied when the average spectrum of any given signal is of interest. It allows for white noise to be cancelled and the emphasised peaks and patterns of the system can be analysed [102].

$$LTAS = \frac{1}{J} \sum_{l=0}^{L-1} X_l^d \tag{6.1}$$

Where L is defined in Section 2.6 as the number of segments (or frames), $l = 0 \cdots L - 1$, the index and X_l^d is the lth segment which has a magnitude and phase. The application of LTAS results in a loss of some of the information contained in the signal [102]. For the purpose of this chapter, this loss is not a concern since the investigation is about detecting spectral nulls and not some average component such as white noise. This method has a similarity to Welsh's technique. LTAS is often used in the analysis of audio signals in order

to identify the fundamental frequency and harmonics [102].

6.2.2 Visualising the spectrum

The spectrum estimate using any of the methods discussed previously may be represented on a linear scale or a logarithmic magnitude scale. The log scale makes it easy to notice small variations and fluctuations in the signal whilst the linear scale is effective at visualising the prominent peaks and harmonics. Figure 6.1 shows the visual difference between the selection of the scale for a signal with predominantly low frequency components [102]. Note that both graphs shows the same data, just on a different scale. For this application the linear scale is sufficient.
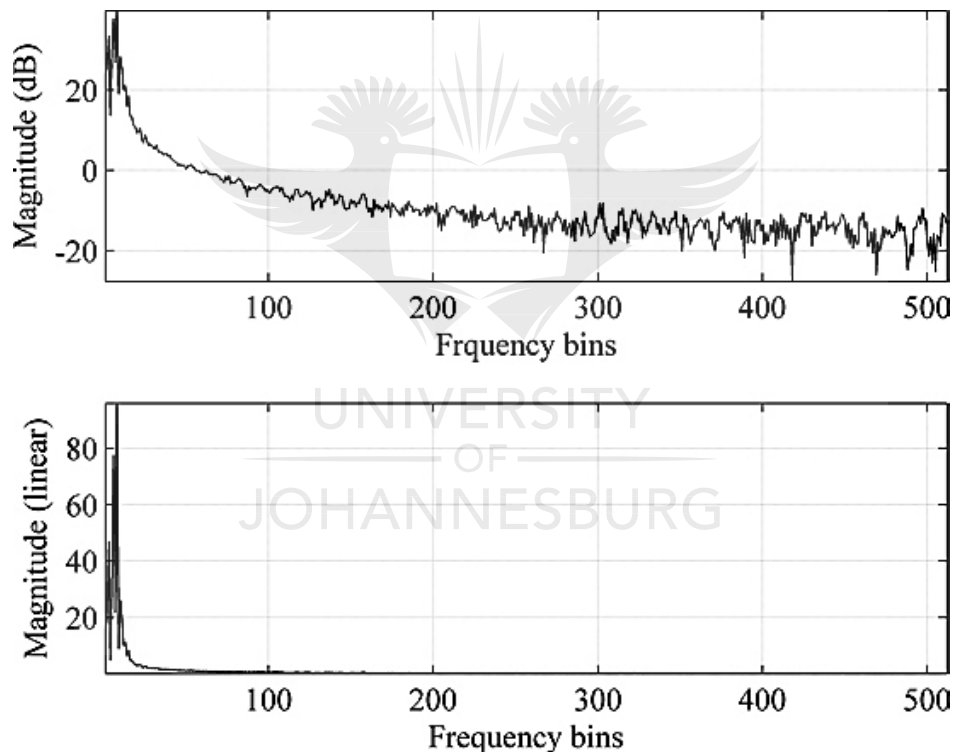
Figure 6.1: Log vs. Linear magnitude plot for a sound signal with low frequency components (bass guitar)

6.2.3 Detecting and computing peaks and valleys

When observing Figure 6.1, it is obvious that this signal is composed of a low frequency peak and an outline of the spectrum is easily drawn visually based on the magnitude of the

frequency components. This is called the spectral envelope [102]. Achieving the same by making use of computation is a bit more difficult. A peak or a valley is defined as the point where the slope of the spectrum changes from positive to negative or vice versa. Detecting a peak or a valley is the same operation applied to an inverse of the data set. For large data sets, simply marking all the points where the gradient changed from positive to negative might not necessarily give useful results. Consider Figure 6.2 where peaks and valleys was identified simply by detecting a change in the gradient of the graph. Even a slight change in the gradient caused the algorithm to detect a peak. A more reasonable definition of the spectrum envelope may be defined by applying some threshold limiting the number of peaks included in the final definition. This can be to only include peaks with a magnitude being 75% or some fraction of the highest peak. Or only using the x highest peaks. Or looking at the distance magnitude between two subsequent peaks. Various filtering techniques may also be used to achieve this [102]. For this application a threshold is applied to the peaks.
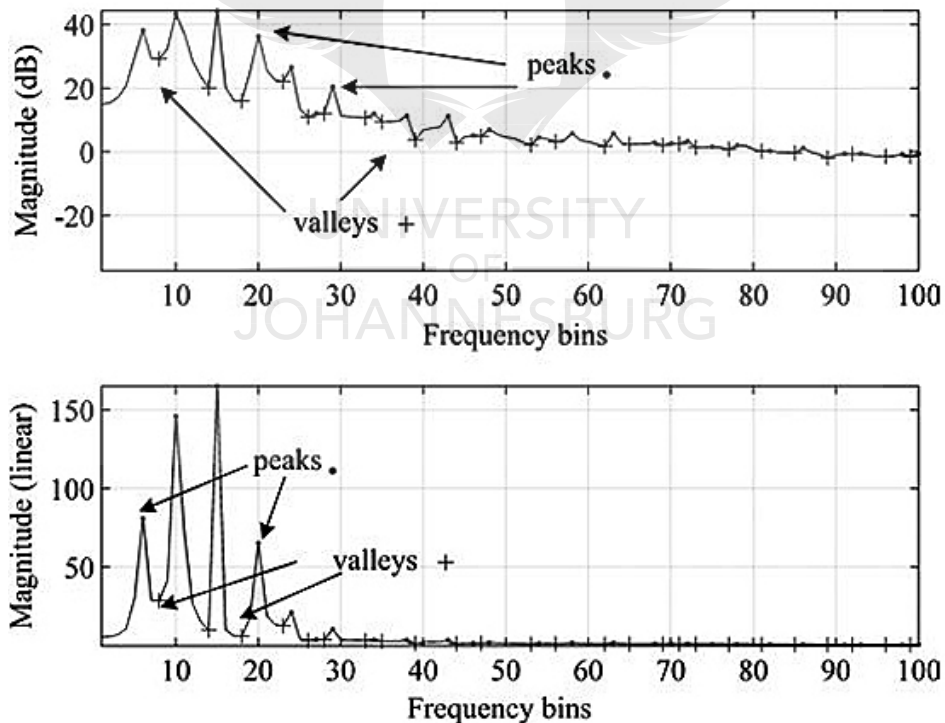
Figure 6.2: Peaks and valleys identified simply by detecting a change in the gradient of the graph

6.3 Loading OFDM carriers with Spectral Null Codes

Refer to Section 2.5 on Cognitive Radio and methods used to sense the spectrum in use. One such method was introduced and is known as waveform based sensing. This method relies on the fact that a predetermined sequence of bits will be transmitted at some point and the shape of the wave will be known and it may be used to detect the spectrum. This may be used to achieve synchronisation by correlating the received sequence with the predetermined sequence [34]. Equations (2.20) and (2.22) describe the sensing error floor (SEF) which describes the rate of true detection (not a false positive) related to the number of bits N_B used. It follows that a longer sequence will lead to an improved performance of the waveform based detection algorithm [34, 37]. For this section spectral null codes is used as the predetermined and known sequence. At the receiver, rather than correlating a sequence of bits, the spectrum will be analysed. Synchronisation will be achieved when a known sequence is detected. The properties of the transmitted signal such as the modulation was used in order to build a simple detector [32].

Previously, NBI was cancelled by making use of filters at the demodulator. Refer to Section 2.8.1 on mitigation techniques. Note that NBI effects only a few subcarriers due to its nature as mentioned in previous chapters. The most important conclusion made on NBI was that the energy introduced by impulse noise, greatly exceeds that of the signal [41, 54] and the usage of guard intervals does not mitigate NBI altogether and some more complex methods such as interference cancellation or Nyquist windowing is required. NBI causes a saturation of the demodulator at the specific frequency of the carrier affected. This means that the received bits on a carrier hit by NBI will be unrecoverable [54]. The OFDM system introduced in Figure 3.4 must be expanded to provide for NBI detection and mitigation at the receiver side.

Ouahada *et al.* [54] previously described how the presence of narrowband interference (NBI) can be detected by adding a power spectral density (PSD) detector to the OFDM demodulator. NBI can be identified by looking for extreme peaks in the power spectrum

density. Ouahada *et al.* further proposed loading spectral null codes with nulls at f_n onto the subcarrier with the same frequency. If this carrier is hit with NBI, the effects thereof might be mitigated. In order to achieve this, an OFDM multiplexer was added to the system to preserve the codewords when loading them onto the carriers [54]. A proposed method for cancelling NBI was to load carriers with spectral null codes and assuming NBI by finding for sequences being always on (all 1's at the receiver). The corrupted symbols are then replaced by a codeword from the codebook of spectral null codes by referencing a lookup table. This method is not an error correcting and replacing corrupted bits from the lookup table is only done to eliminate the saturated bits affected by NBI, with a codeword with the same desirable spectral properties [54]. It did not correct any errors.

The detector will be designed according to the chosen codebook with codewords producing nulls at know frequencies. The objective of this chapter is to combine OFDM with spectral null codes and to detect the presence of the expected nulls. It will then continue to investigate the effect of spectral nulls on the PSD.

6.3.1   Simulation setup

The OFDM system is modified in order to accommodate spectral shaped inputs and PSD detectors was used to analyse the spectrum directly before and after transmission. Refer to Figure 6.3 showing the block diagram including the peak detector from Section 6.2, the spectral null code generator from designed in Chapter 5 and the PAPR reduction technique from Chapter 4. This is the most complete block diagram and the simulations was implemented according to it.

Consider the codebook from earlier examples as in (5.16). For this example, the carriers are serially loaded with codewords from the codebook. The codebook has a cardinality $|C_b(M, N)| = 6$ from (5.10). Let the codebook of codewords be defined as
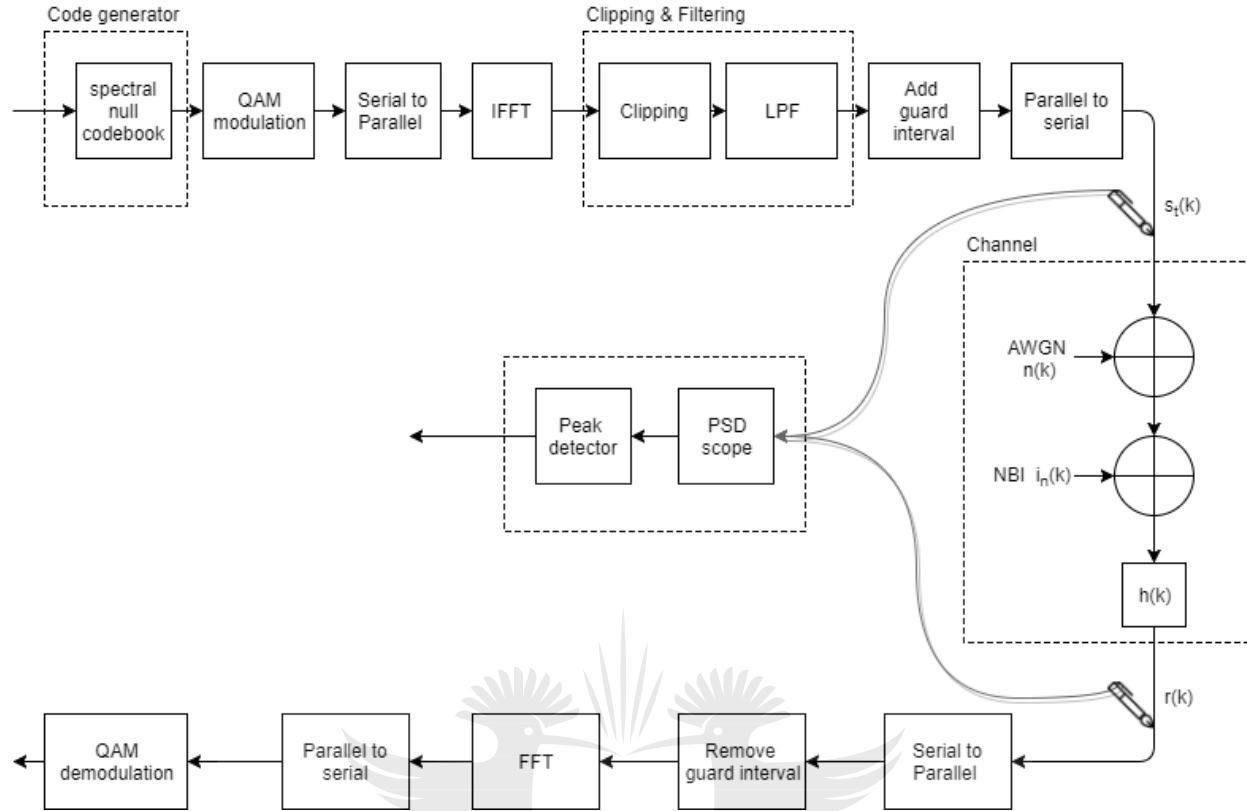
Figure 6.3: OFDM block diagram including the generator at the input creating codebooks of spectral null codes, PAPR mitigation by means of clipping and filtering and PSD scopes and peak detectors added to both the transmitted $s_t(k)$ and received $r(k)$ signals

$$
\begin{aligned}
C_{w1} &= \{0,0,0,0\} \\
C_{w2} &= \{0,0,1,1\} \\
C_{w3} &= \{0,1,1,0\} \\
C_{w4} &= \{1,0,0,1\} \\
C_{w5} &= \{1,1,0,0\} \\
C_{w6} &= \{1,1,1,1\}
\end{aligned}
$$

For the intents and purpose of the simulation, an OFDM system with 1024 subcarriers was implemented. Each carrier is serially loaded with a random codeword from the codebook, each with an equal probability as shown in Figure 6.4.

The PSD of modulated data was inspected before passing it into the wireless channel

and results are shown in Figures 6.5 and 6.6 for random and shaped inputs respectively. The addition of a PSD scope to the block diagram enabled this measurements.
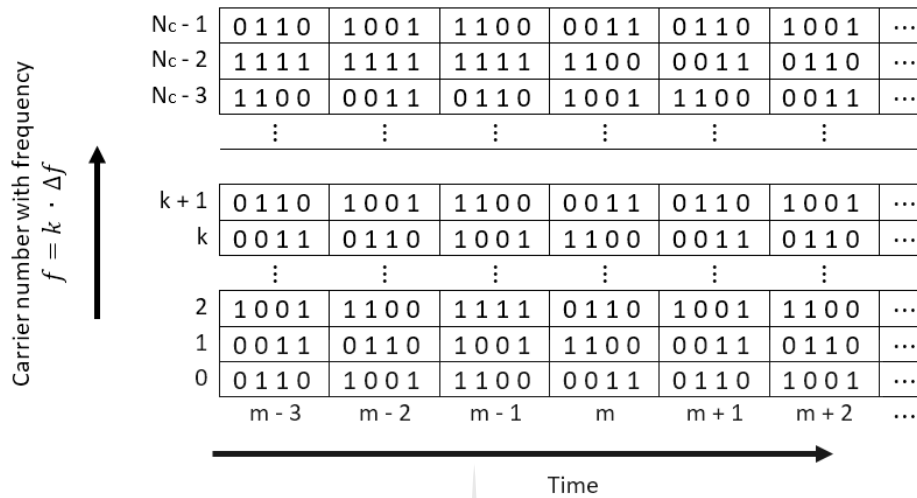
Figure 6.4: Loading OFDM carriers with spectral null codes from the codebook. $N_c = 1024$ for this example

6.4   Simulation

It has been shown how the spectral shaped data will influence the power spectra of the OFDM transmission in Figure 6.6. Clearly there is a null at the intended frequency of $f = \frac{1}{n}$. This observation holds for any number of spectral null groupings N. Figure 6.7 shows the PSD for the system a codebook designed to have two spectral nulls. The spectral shaping techniques is therefore relevant to OFDM systems as well. The next chapter will discuss possible implementations.

6.4.1   Performance

Let's consider the performance of the OFDM system when the carriers are loaded with spectral null codes. Figure 6.8a shows that the BER performance of the OFDM system remained largely the same after spectral null codes were used. Hence no performance implications is expected when making use of shaped inputs instead of some random input. Figure 6.8b further strengthens this point since the constellation plot was as expected.
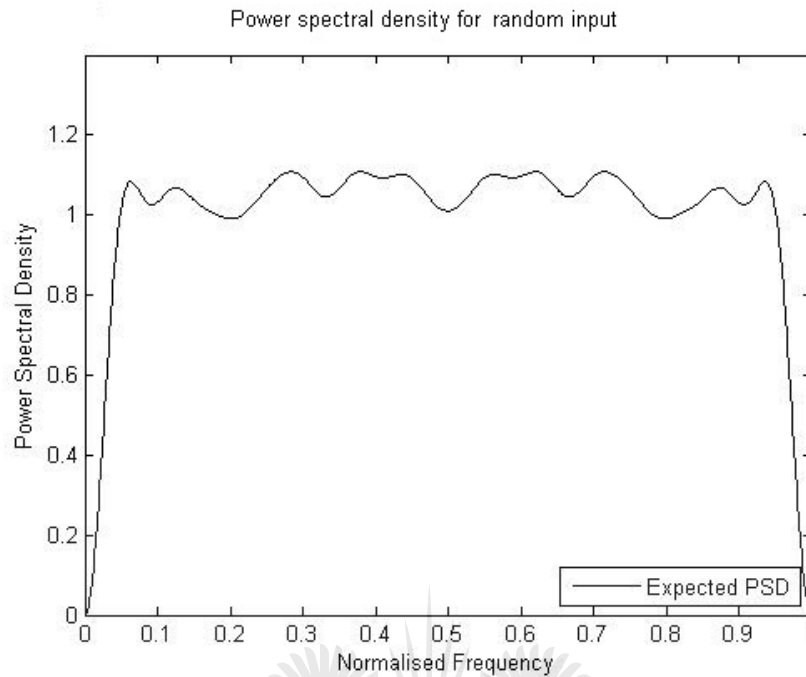
Figure 6.5: PSD for the OFDM simulation by making use of Welsh's method for random data used as the input
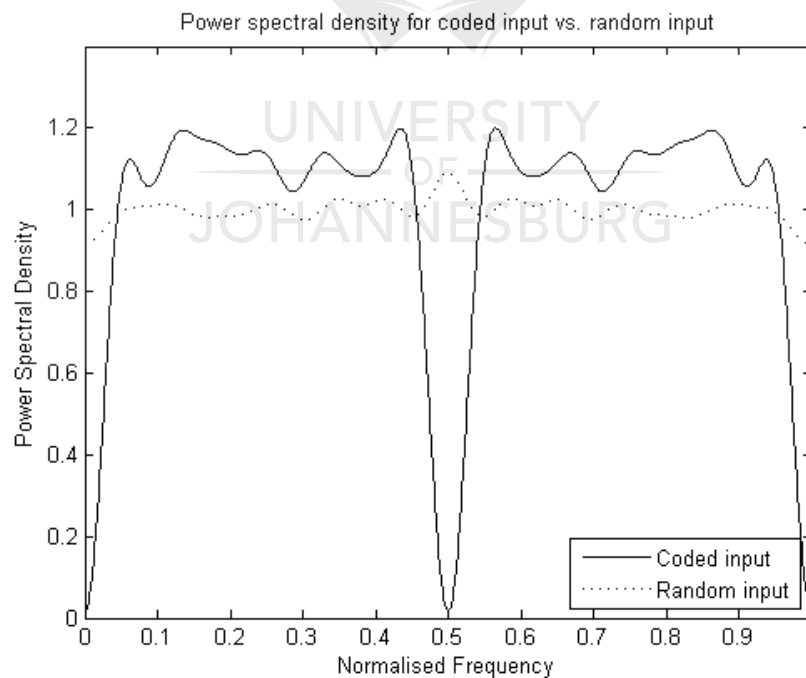
Figure 6.6: PSD for the OFDM simulation by making use of Welsh's method for spectral shaped data used as the input compared to the PSD of random input data. Codebook $C_b(4, 2)$ was used. One null is observed as expected from the designed null code.
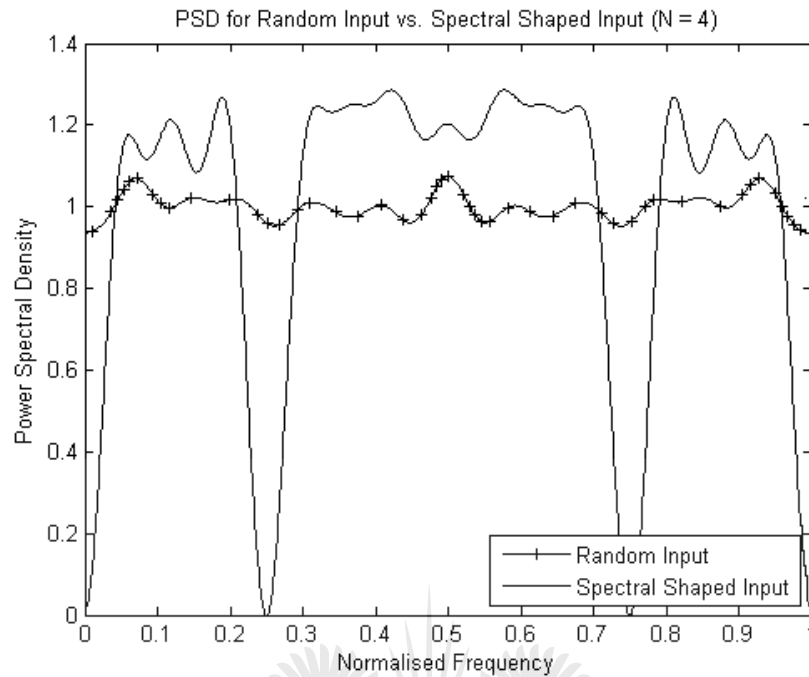
Figure 6.7: PSD for the OFDM simulation by making use of Welsh's method for spectral shaped data used as the input compared to the PSD of random input data. Codebook $C_b(4,4)$ was used. One null is observed as expected from the designed null code.
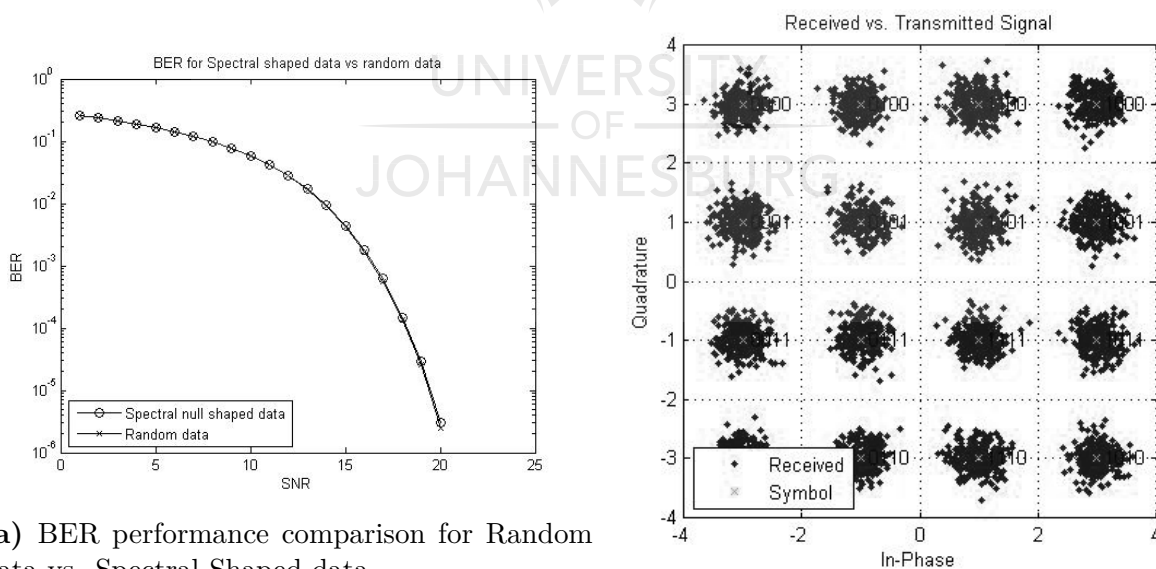
(a) BER performance comparison for Random data vs. Spectral Shaped data

(b) Constellation for shaped data

Figure 6.8: BER and constellation plots for OFDM with spectral shaping techniques applied. The performance of both systems are equivalent and it can be derived that the spectral null codes has no major impact on the system performance.

6.5   Estimating channel integrity

Consider an OFDM signal, encoded with spectral null codes of length N. Any noise present in the channel, be it Gaussian noise, NBI or Rayleigh fading, will corrupt some of the transmission. This problem is common in any communication system. This section propose the use of spectral null codes in order to determine the channel quality or the integrity of the transmitted data. This is done specifically in the case of an OFDM system and it is used to determine how NBI is detected in a multicarrier system.

Fundamentally the peaks and valleys of the signal is analysed and properties which indicates the presence of noise is identified. Detecting a peak is an exercise performed on the input signal where a change in gradient from positive to negative occurs. When the gradient changes from negative to positive it results in a valley being created. Alternatively detecting a valley is the same operation as taking the inverse of the signal and detecting the peaks. For this reason the terms peak and valleys will be used interchangeably in this section.

The channel quality estimation is performed by detecting the peaks of the system and comparing it to the expected peaks. Recall that the design of the spectral null code ensures that the values of the expected peaks is known. The idea here is to show that the loss of a spectral null can be detected and is indicative of noise and corruption in the channel. This can be extended further by calculating the magnitude of the difference between the expected peak and received peak. This magnitude may be correlated to the extent of the corruption. Figure 6.9a and 6.9b shows this correlation. So the distance between the expected zero and the actual value of the null at f_n gives an indication on how the system performs. The spectral null is less salient when the SNR is low (associated with a high BER and degraded system performance). For better performing channels the spectral null becomes more prominent. The more prominent the spectral null, the better the performance will be.

(a) PSD for different SNR with $C_b(4, 2)$

(b) PSD for different SNR with $C_b(4, 2)$ (subplot)
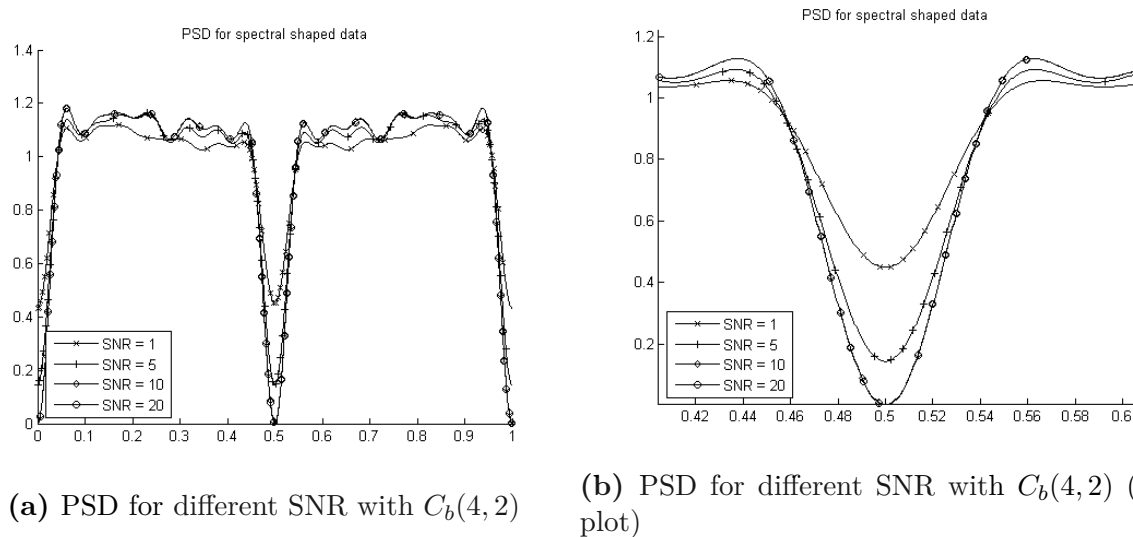
Figure 6.9: PSD for different SNR with $C_b(4, 2)$

6.6 Overview

In this chapter the focus was on loading OFDM with spectral shaped data such as the spectral null code. This was achieved by constructing a codebook C_b and only selecting codes from there to map onto the subcarriers. Detecting the spectral nulls is similar to detecting the peaks or valleys of a function. The algorithm looks for a change in the gradient from positive to negative to determine that a point is a peak. Applying the same logic on the inverse of the function yields the locations of the valleys. A linear magnitude scale will provide a good view on the peaks of the PSD. This method will detect the presence of spectral nulls. The null was designed to occur at a specific frequency and any deviation or missing null gives an indication of the quality and integrity of the channel.

The simulation was set up to include the principles from previous chapters with the addition of a PSD scope and peak detector at the transmitter and at the receiver. This made it possible to determine the effect the channel has on the PSD and the peaks of the transmission.

Simulations showed that spectral null codes used on OFDM subcarriers still results in a shaped frequency. Further the use of spectral null codes did not impact the system per-

formance in terms of its BER. From there observations was made on how the SNR of our transmission impacted the shape of the spectrum and the channel quality was estimated.

The next chapter extends the observations made in this chapter by introducing NBI in the channel. It incorporates all the elements and techniques discussed thus far in this document.

Chapter 7

Optimised orthogonal frequency-division multiplexing based communication systems for wireless environments

7.1 Introduction

In this chapter the methods discussed in previous chapters are combined into a comprehensive OFDM simulation. It will include the generation of spectral null codes, reducing the PAPR by means of clipping and filtering, PSD scopes and peak detectors at the transmitter and receiver and a channel modelling the wireless environment including NBI. Results for numerous simulations are presented and analysed. The performance impact spectral shaping might have on the system is investigated as well as the effects of NBI on the OFDM transmission. The focus here is how the PSD is shaped by various of the systems' properties. The BER performance of the system is also kept in mind during these simulations. Results are compared when using random input data versus spectral shaped data.

The objective here is to understand the following

1. How the spectral shaping affects the system performance

2. How the NBI in the channel affects the system performance and its PSD

3. Can the spectral null codes mitigate NBI

4. Possible applications of spectral shaping used with OFDM

7.2 Simulation implementation

Figure 6.3 shows the complete setup used for the simulation. The focus here is more on the effect of NBI $(i_n(k))$ in the wireless channel. The OFDM signal will be coded with spectral null codes from the code generator. Some PAPR reduction method was applied to make the simulation more realistic. A simple clipping and filtering method was chosen. PSD scopes along with a digital peak detector algorithm was added to the transmitter $s_t(k)$ as well as the receiver $r(k)$. This creates a good opportunity to analyse the effect of the channel (including the added NBI) on the signal. The simulation was implemented in full by making use of MATLAB. See Appendix B for the relevant source code of the simulation.

As a reference for the rest of this chapter, Figure 7.1 shows the PSD output of the simulation at the receiver where random input data was used and without any NBI present in the channel. This is the basic simulation and no alterations to the OFDM system was made. Unless otherwise stated, the channel will have AWGN with SNR $= 20dB$. The number of carriers is $N_c = 2048$ and $M = 16$ modulation scheme is used. The input is spectral null codes with a zero-disparity from the codebook $C_b(16, 2)$ or $C_b(16, 4)$ which is loaded onto the subcarriers. Since the focus is with the effects of the channel on our signal, all results shows the scope at the receiver.

7.3 Spectral shaping

Figures 7.2 and 7.3 show the PSD for OFDM systems where spectral shaped codewords, as well as non-coded bits (random data) are used. The shaped codewords is selected at random
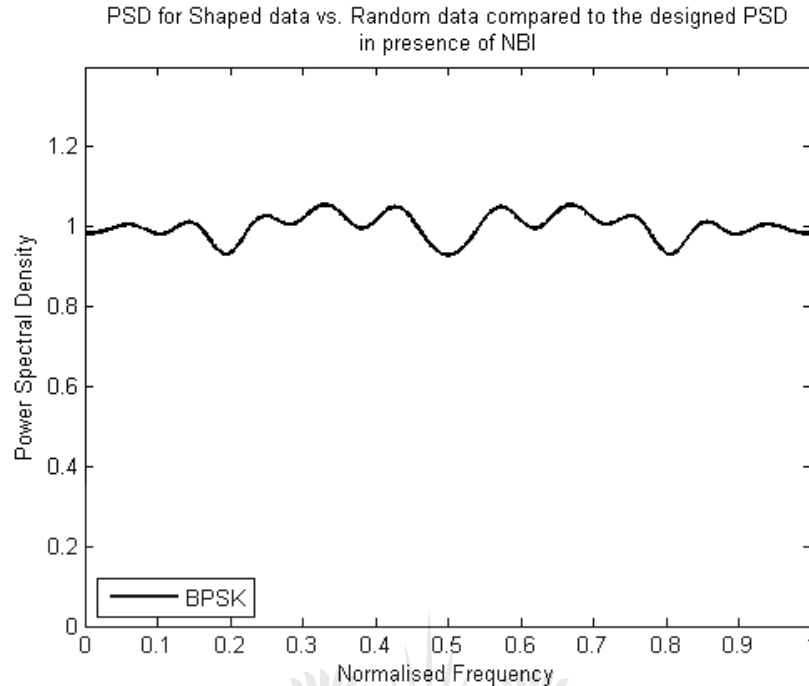
Figure 7.1: PSD for the basic simulation where random data instead of shaped data was used as the input and no NBI was present in the channel

from the codebook $C_b(16, 2)$ and $C_b(16, 4)$ respectively. In the case of $C_b(16, 2)$ the codes are designed to have a null at $f = \frac{1}{2}$ of the normalised frequency, satisfying (5.11). This is clear when observing the null PSD for the coded input. The random input has a PSD which remains more or less constant throughout the bandwidth which is as expected. The same is observed in Figure 7.3 where the PSD for codebook $C_b(16, 4)$ with nulls at $f = \frac{1}{4}$ and $f = \frac{3}{4}$ is shown.

Using the spectral null codes and loading them onto OFDM subcarriers resulted in a PSD with nulls at desired frequencies. Both of these cases has AWGN present in the channel, which did not affect the PSD shape in any significant way. This design and the knowledge of the system's spectral properties has some interesting applications. The results are similar to other methods of spectral shaping such as FIR-filtering [6] and notch filtering [103]. The Finite Impulse Response (FIR) filter is a digital filter where discrete time samples is convoluted with the coefficients of the filter in order to obtain an output with only frequencies in desired ranges. The notch filter allows all frequencies to pass except those in a certain
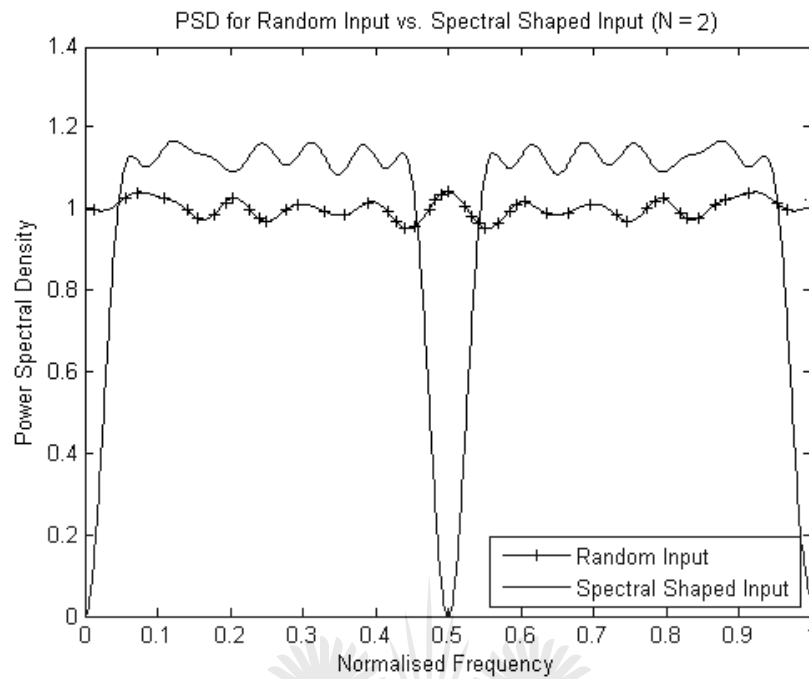
Figure 7.2: PSD for random input vs. shaped input
(N = 2)
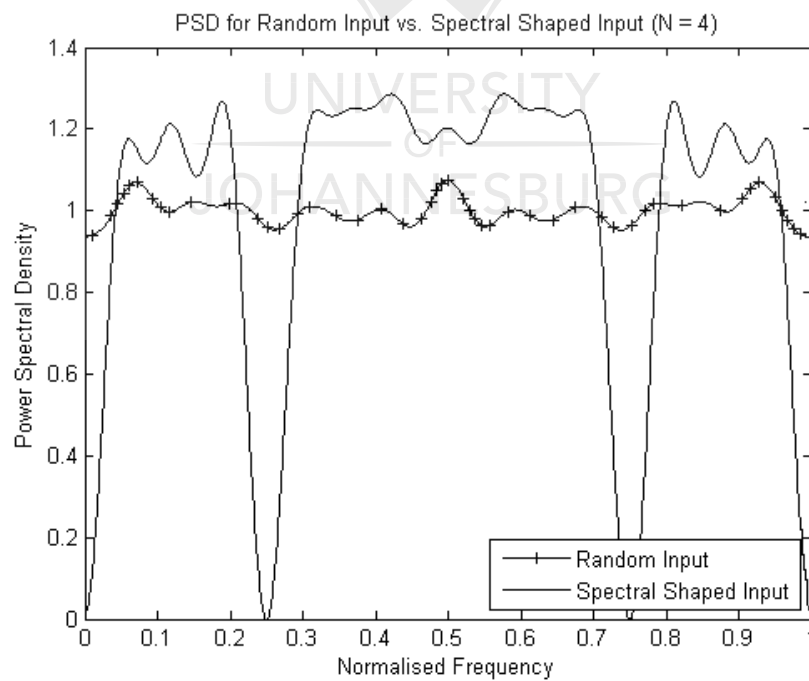
Figure 7.3: PSD for random input vs. shaped input
(N = 4)

narrow exclusions band.

Figure 7.4 and 7.5 shows that the use of spectral null codes does not impact the BER and CCDF. Both shaped data and random data loaded onto the subcarriers shows identical results. We can then infer that the use of spectral shaping techniques will not have any negative impact on the system's performance in terms of the bit error rate or CCDF.
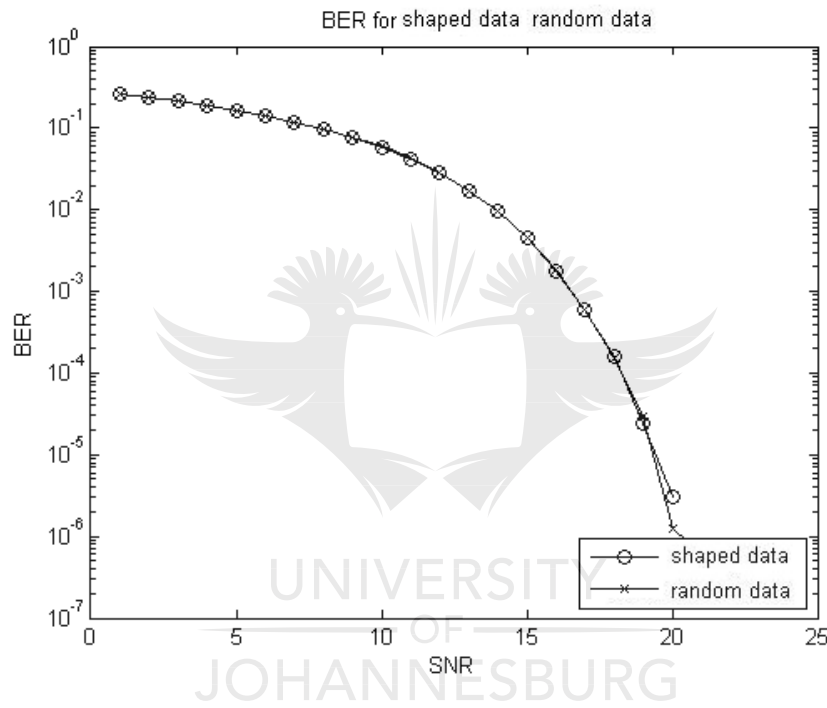
Figure 7.4: BER performance of ODFM systems with Shaped data vs. Random data.

This section shows that the use of spectral shaping techniques in OFDM systems is feasible and it has no negative impact on the system performance.

7.4   Introducing NBI

NBI present in the channel can have a devastating impact on the system performance. If no mitigation technique is applied it becomes impossible to recover the transmitted signal. Figure 7.6 shows how NBI degraded the BER system performance. The results from the simulation agrees with the results found by other studies as in Figure 2.6 [47, 48].
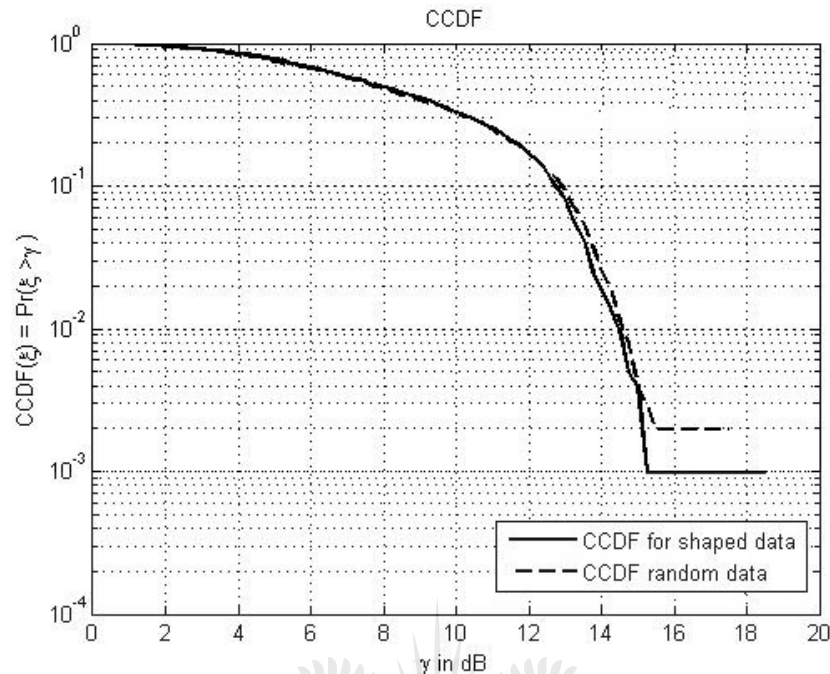
Figure 7.5: CCDF performance of ODFM systems with Shaped data vs. Random data

From the previous section is has been shown that the OFDM power spectrum may be shaped by loading specially designed spectral null codes onto the subcarriers. Consider Figures 7.7 and 7.8 showing the PSD for random data and the effect of NBI on it compared to the case where no NBI was present. The NBI was modelled by (2.32) with an amplitude being an order of magnitude greater than that of the OFDM signal. The impact of the NBI is clearly visible at distinct frequencies where it interacts. Observe the increased power at those frequencies. This pattern of increased peaks appearing in the PSD can be used to determine if NBI or any other narrowband signal is present in the channel since its magnitude is greater than the expected value of the signal. The same peak detection algorithm can be used to detect both the peaks caused by narrowband signals as well as the valleys due to the spectral null codes.
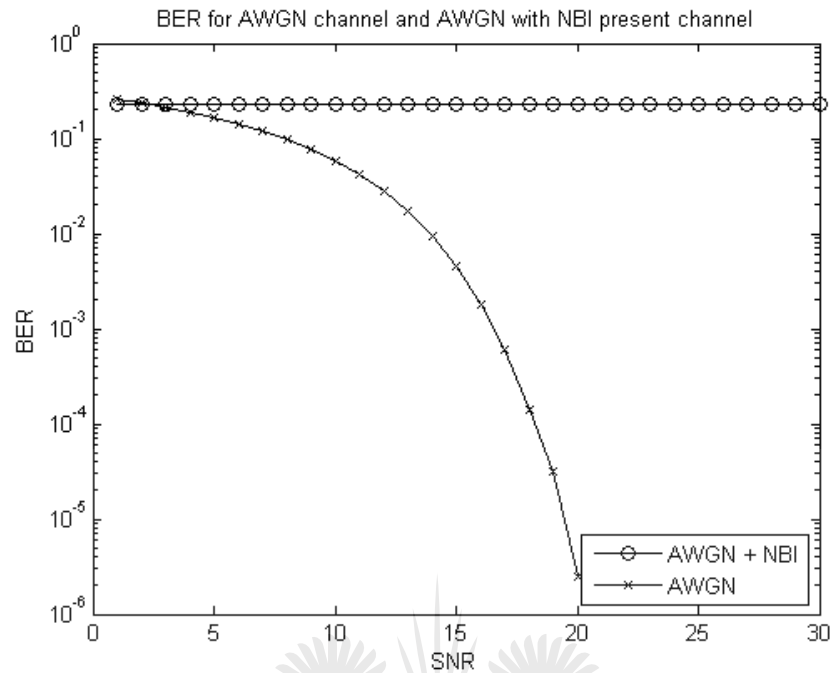
Figure 7.6: The BER of OFDM system in the presence of NBI compared to the case where no NBI is present
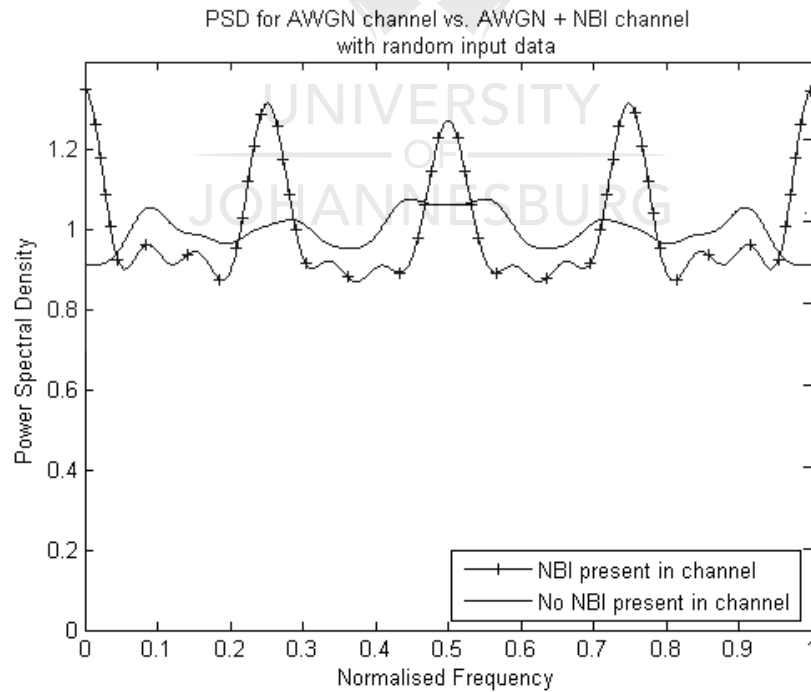
Figure 7.7: The effect of NBI on unshaped PSD compared to the PSD of random data in the absence of NBI
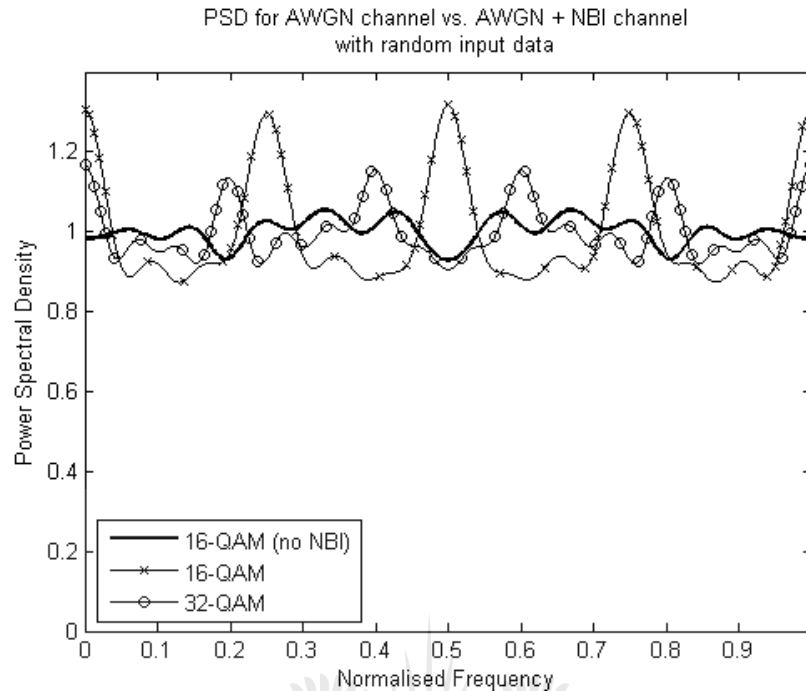
Figure 7.8: The effect of NBI on unshaped PSD and BER of OFDM system in the presence of NBI (showing results for different modulation schemes)

7.5   Spectral Null Codes to Mitigate NBI

The narrowband signal corrupted a small number of subcarriers. It is assumed that the bits become corrupted in such a manner that they do not adhere to any of the requirements for being a spectral null code. For those subcarriers, the PSD will tend more towards that of random data, diminishing the spectral properties which was designed. Figure 7.9 and 7.10 shows the results of adding NBI to the channel. These are compared to the designed PSD shape with spectral nulls. In the case where random input data was used, the NBI caused peaks in the PSD. And with shaped data the NBI malformed the expected spectral null shape since the spectral nulls disappeared and the PSD resembles that of random data in an AWGN channel. Figure 7.11 shows that similar observations can be made for codebooks with a different number of null groupings ($N = 4$) in Figure 7.11.

The close spacing of subcarriers makes the system susceptible to NBI. Since the power of NBI can be an order of magnitude higher than that of the signal, an increase in signal power
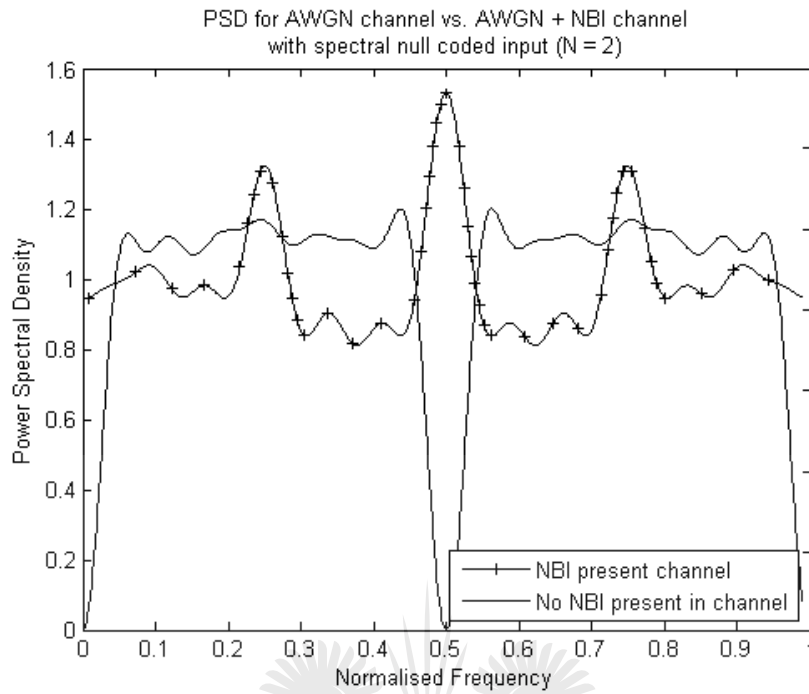
Figure 7.9: Spectral null coded data compared to the PSD of random data when NBI is present
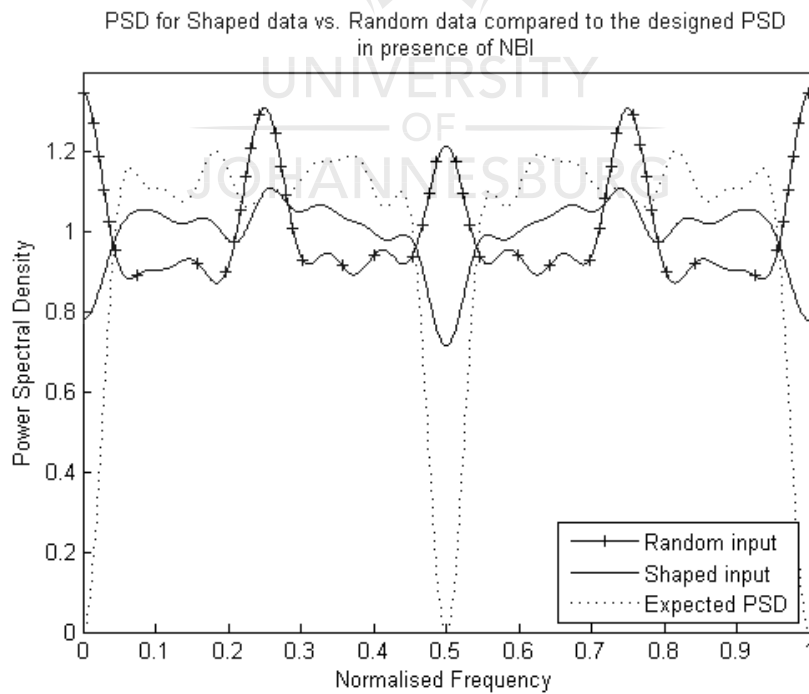
Figure 7.10: Spectral null coded data affected by NBI compared to expected PSD
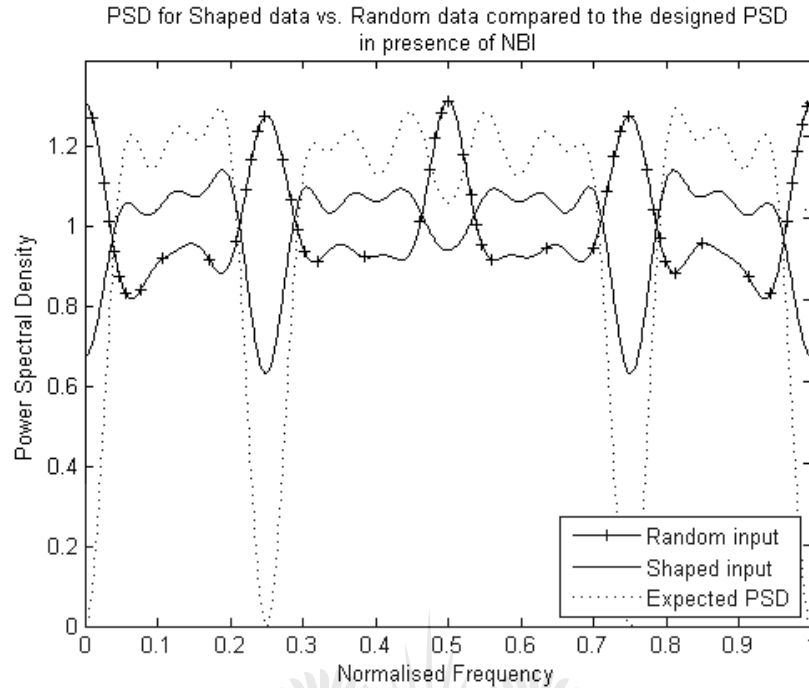
Figure 7.11: PSD for shaped data with NBI compared to expected PSD ($N = 4$)

does not improve performance. The use of spectral null codes, even when the NBI coincides with the null frequency, did not improve the system performance. Figure 7.12 shows that the spectral shaping did not mitigate any of the errors caused by NBI in the channel.

Without mitigation or error correctional techniques the performance of the system is degraded by NBI. Spectral coding therefore does not cancel NBI but rather serves as a sensor for the quality of the channel. Spectral nulls are expected as per the design. When a null disappears it can be concluded that some noise was present.

The PSD designed is the one observed when there is no NBI present in the channel. Observe that the addition of narrowband signals in the channel affects the shape of the PSD. The system does not conform to the designed spectral shape since the PSD at $f = \frac{1}{2} \neq 0$ in Figure 7.11. Similarly it was observed that spectral nulls also disappeared as a result of NBI in the case where $N = 4$ (Figure A.10).
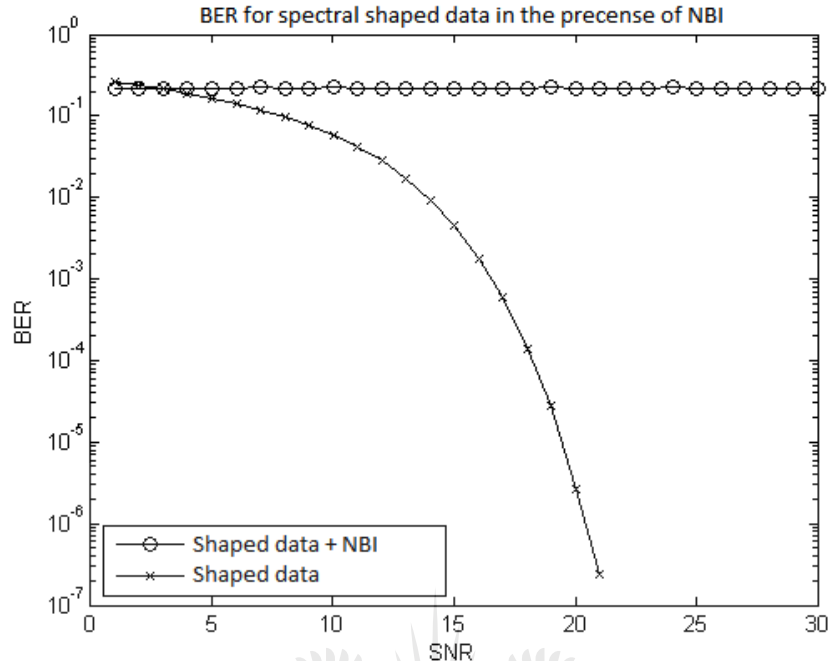
Figure 7.12: BER performance for shaped data with NBI compared to shaped data without NBI

7.6 Overview

In this chapter the results from the completed simulation was presented. A concise description of the simulation was presented since the important components were designed and discussed in full during previous chapters.

The simulation shown that the use of spectral null codes on OFDM carriers did not affect the system performance negatively in terms of the BER as well as the CCDF performance. The spectrum was shaped according to the designs proving that OFDM can be shaped by making use of conventional spectral shaping techniques.

Further NBI or any narrowband signal or impulse noise may be identified by the peaks it creates in the spectrum. These have a magnitude far greater than the system average and it's unlikely that it will occur by chance if it's not caused by the noise.

Finally observations was made in the case where NBI was present and the OFDM sub-carriers was loaded with spectral null codes. Simulations has shown that the NBI will distort the shape of the designed PSD. Therefore spectral shaping will not be able to improve the system performance in terms of the BER. An alternative application for using spectral nulls can be for a sensor of the channel. Any errors happening in the channel will cause the spectrum to deviate from the expected shape. The degree of this deviation can give an estimate of the channel quality.

The effect of narrowband signals on the shape of the PSD is observed. The spectral null is less prominent in the presence of narrowband signals and the spectrum tends more towards that of a random input. Using these observations, the channel quality can be determined and narrowband signals which might be present in the channel can be detected. However, applying spectral shaping does not yield a better performance in terms of the BER. The carriers loaded with spectral null codes still contained useful bits which became corrupted. The benefit of using spectral shaping techniques lies in the desired spectral shape which can be used to draw conclusions on the quality of the channel. The disappearance or diminishing of the spectral null where a null is expected, is indicative of narrowband signals present in the channel. These results holds for both wired and wireless channels.

Future work will be focused on improving the channel quality estimation by correlating the designed PSD to the received PSD. Better algorithms for more reliable detection of narrowband signals, specifically by loading only selected carriers with spectral null codes can also be investigated. The possibility of automatically cancelling narrow band interference when detected will also be investigated further.

A summary of the findings up until this point will be presented in the next chapter along with planned future work and branches of study.

Chapter 8

Conclusion

8.1 Introduction and overview

Previous chapters introduced some of the problems experienced with modern wireless communications and motivated how new methodologies needs to be researched to ensure that future generations will have sufficient access to the Internet and other means of communications. A good candidate for modern communications, primarily wireless but also wired and optical mediums, is OFDM. It is a method making optimal use of the already crowded radio frequency spectrum by using multiple and overlapping orthogonal subcarriers. The research is focused on designing novel methods of using OFDM in order to make it more sustainable for future use.

This chapter presents a brief overview on the findings during the course of research including optimisations to the system, mitigating of some of the fundamental problems with OFDM and employing conventional techniques in new ways in combination with OFDM. The investigation was conducted primarily by making use of simulations based on mathematical models of the wireless environments. The theory and observations here are also relevant in other mediums.

8.2   Restatement of research objectives

Section 1.3 initially stated the research objectives. Modern society has an increasing demand for access to wireless mobile communications. This is due to the technology becoming cheaper and more accessible and also due to the increasing population. Existing technologies may be improved upon making it more efficient and reliable. One such method is called OFDM which already shows promising prospects for usage in the next generations of communication systems. OFDM was investigated and determined if the current implementation may be improved in order to make it more sustainable and relevant for future use.

The research is focused on optimising the parameters of the OFDM system including the number of subcarriers, the modulation scheme used and the optimal length of the cyclic prefix. A fundamental problem with OFDM called a high PAPR will also be addressed. Finally a novel method of using conventional spectral shaping techniques will be developed and tested in an OFDM system. The system needs to be more robust against narrowband interference and other impulse noise which is a common occurrence in the wireless environment and notoriously difficult to avoid or recover from. It was determined if the spectral shaping can help to mitigate the effects of narrowband interference on the system and possible applications of this technique was explored.

Investigations will also focus on detecting the presence of narrowband disturbances in the channel and the cancellation thereof by employing spectral shaping methods and analysing the received spectrum.

8.3   Achievement of objectives

The primary objectives was to optimise the OFDM system, reduce its PAPR as well as shaping the OFDM spectrum.

The conventional OFDM system was modified at the transmitter as well as the receiver in order to detect NBI which may be present in the channel. This has been achieved by adapting the multiplexer to load carriers with spectral null codes and adding a power spectral density detector at the modulator and demodulator. The results have shown that the spectrum of OFDM can be shaped by employing conventional techniques. The disappearance of spectral null indicates some corruption occurred. Further the system was created to be more robust and applicable in modern applications by addressing the problem of the high peak to average power ratio. This was done by clipping the input at a certain threshold. This reduces costs and energy consumption. The most optimal properties was investigated and implemented in this simulation.

More specifically, the design and implementation of the OFDM system was discussed in Chapter 3. The system performance was investigated in terms of the number of subcarriers, the modulation scheme used as well as the length of the CP. For each of the parameters results were compare to one another and recommendations was made for choosing an optimal implementation. The knowledge of how these parameters impacts the system allows for quicker designs when implementing new systems. The major factor is usually the constraints of the environment in which the system operates.

Chapter 4 investigated the fundamental problem where OFDM systems has a high PAPR because of how the subcarriers are constructed. If a circuit design is inadequate clipping and distortion may occur. A high PAPR requires high powered amplifiers with a wide operational ranges in order to decode the signal without clipping. These are usually expensive and high powered making it problematic for future use. Various methods for reducing PAPR was investigated and clipping and filtering was chosen to be applied in the simulation. The PAPR was reduced by 4dB and this technique was applied in the simulations.

In Chapter 6 the simulations has shown that it is possible to shape the PSD of an OFDM system by loading the carrier with spectral null codes. By doing this the system performance was not affected in a significant way when comparing both the BER and CCDF performance.

Adding AWGN to the system did have an impact on the shape of the designed spectrum. This is an indication that the spectrum can act as a sensor for the quality of the channel.

Finally the effects of NBI on the OFDM system was investigated. As expected it degraded the system performance significantly. It also produced peaks in the PSD with a magnitude far greater than the average of the signal. A peak detection algorithm looking for a change in gradient of the spectrum can easily detect the locations of the interference. The next step was to create spectral null codes coinciding with the frequency of the interference. The results showed that the NBI and spectral null acted to *cancel* each other, but this was only as far as the PSD was concerned. The spectral null codes still carried useful data which the NBI corrupted. Spectral shaping will not improve the BER performance of the system in the presence of NBI. It is more useful as a sensor for the channel.

8.4 Shortcomings

One of the objective of this research was to investigate how spectral shaping applied in the context of OFDM can be used to mitigate the degrading effects NBI has on the system. The initial assumption that this would be the case was incorrect. Even though spectral shaping did cancel the impact of NBI on the PSD, it did little to cancel the corruption caused by NBI. What this has shown is that the spectral null codes still contains useful data which will be corrupted by noise present in the channel. This opened the possibility that spectral shaping might be more useful when it is employed as a sensor for the channel quality rather than a mitigation technique. This is an avenue which can be investigated in future work.

8.5 Future work

Figure 8.1 shows the planned course for future work and investigations related to OFDM combined with spectral shaping techniques. Future work will be focused on making use of the spectral shaping and its properties in order to make estimations on the quality of the channel and noise present at certain frequencies. The idea is to develop a mathematical ex-
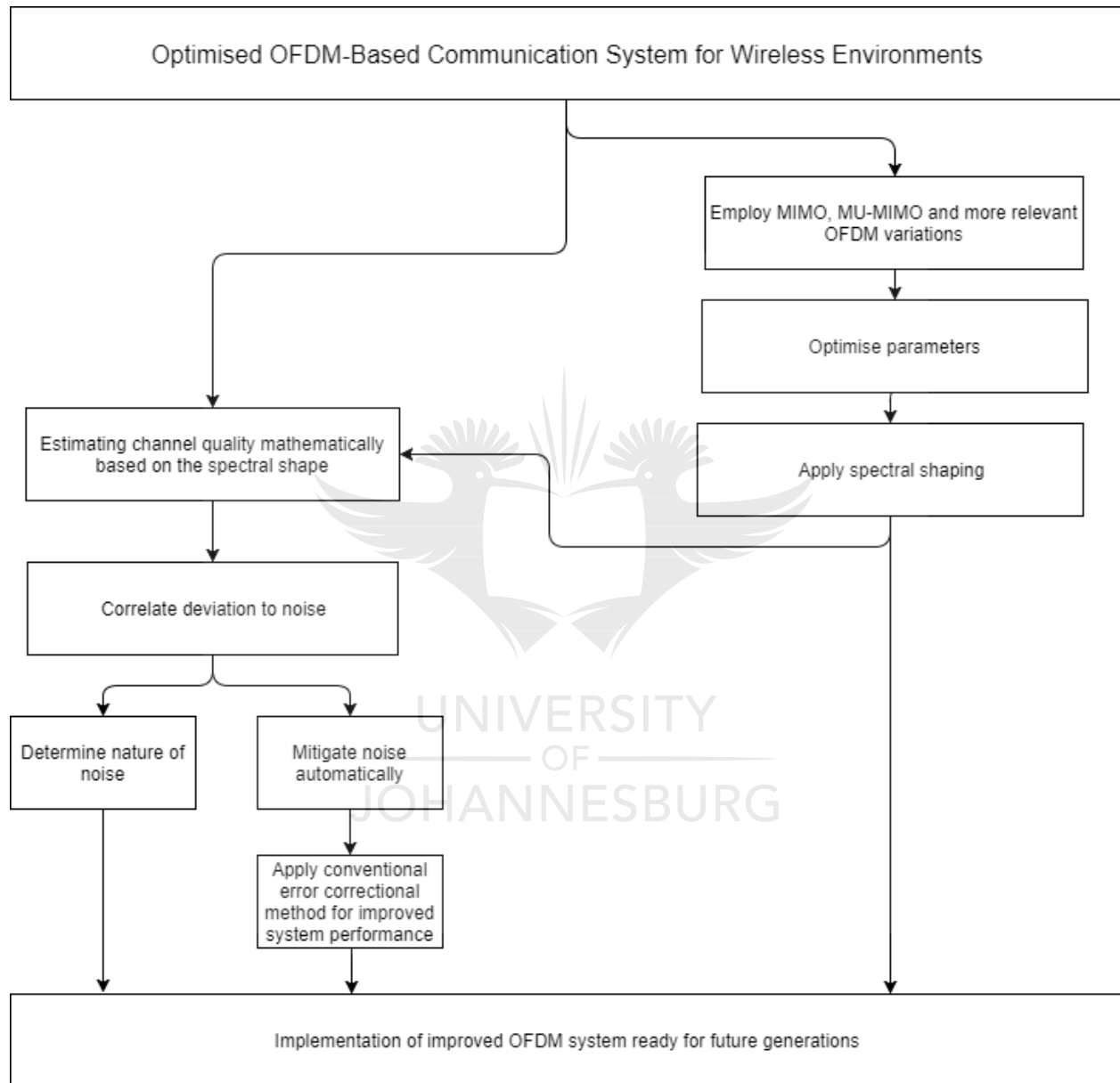
Figure 8.1: Future work related to the study of OFDM combined with spectral shaping techniques

pression which can properly and accurately describe the deviation in the spectral shape and correlate its cause too the noise present in the channel. When it is certain that noise caused the spectral shape to deviate from its designed shape, methods can be employed which will cancel the NBI at certain frequencies. This might be in the form of automatically switching carriers off which has been hit with NBI. If the channel sensing is done continuously and carrier effected by noise is dynamically switched off, it may greatly improve the overall performance of the system.

OFDM has many applications in PLC channels and Visible light communication (VLC) channels [104]. The new optimised OFDM parameters and the usage of spectral null codes can be extended and applied in those channels as well.

Furthermore, the OFDM system can be extended to model a modern MIMO system which is more relevant for new technologies. The arguments for OFDM will extend to the MIMO and MU-MIMO implementations and a function for the effect of noise on this system will be derived as well. Finally a new system will be presented which will be even more relevant, robust and sustainable. It will intelligently estimate the performance and noise present in the channel and by making use of that metric the noise can be adaptively cancelled by employing error correctional techniques.

8.6 Overview

An increasing demand for broadband wireless access motivates the development of more reliable and efficient techniques to be used in the next generation of communication systems, beyond the 4th generation of mobile communications and Long Term Evolution. Orthogonal Frequency Division Multiplexing allows data to be transmitted efficiently and reliably by using multiple orthogonal subcarriers. It provides robustness against noise and corruption in the channel. The channel can be either wired or wireless depending on the particular application. Due to the close spacing of subcarriers, OFDM is susceptible to corruption caused by various narrowband signals such as Narrowband Interference (NBI). OFDM has a

high peak to average power ratio (PAPR). Circuits typically require high powered amplifiers with a wide operational range. If the circuit design is inadequate clipping and distortion may occur. This adds to the cost and power consumption of the system. In order to improve battery life an efficient implementation of OFDM was investigated and proposals for various methods which may be used in order to reduce PAPR is made.

Spectral shaping shapes the Power Spectral Density function in order to have certain properties. Spectral shaping might improve the effectiveness of OFDM and make it sustainable in the long run for applications beyond the 4th generation of mobile communications and LTE. Spectral null codes is used and loaded onto OFDM subcarriers. Introducing narrowband signals in the channel degrades the system's performance and also eliminates the designed spectral properties. From this observation it can be inferred that some noise is present in the channel. Previously, carriers hit by NBI or other narrowband noise had to be switched off manually. It was found that combining OFDM with spectral shaping allows the presence of Narrowband signals in the channel to be detected and conclusions can be drawn over the channel quality. This did not improve the system in terms of bit error rate performance but it did give an indication of noise being present in the channel.

Appendix A

Simulation results

This appendix provides some additional simulation results which was not presented in the earlier chapters.
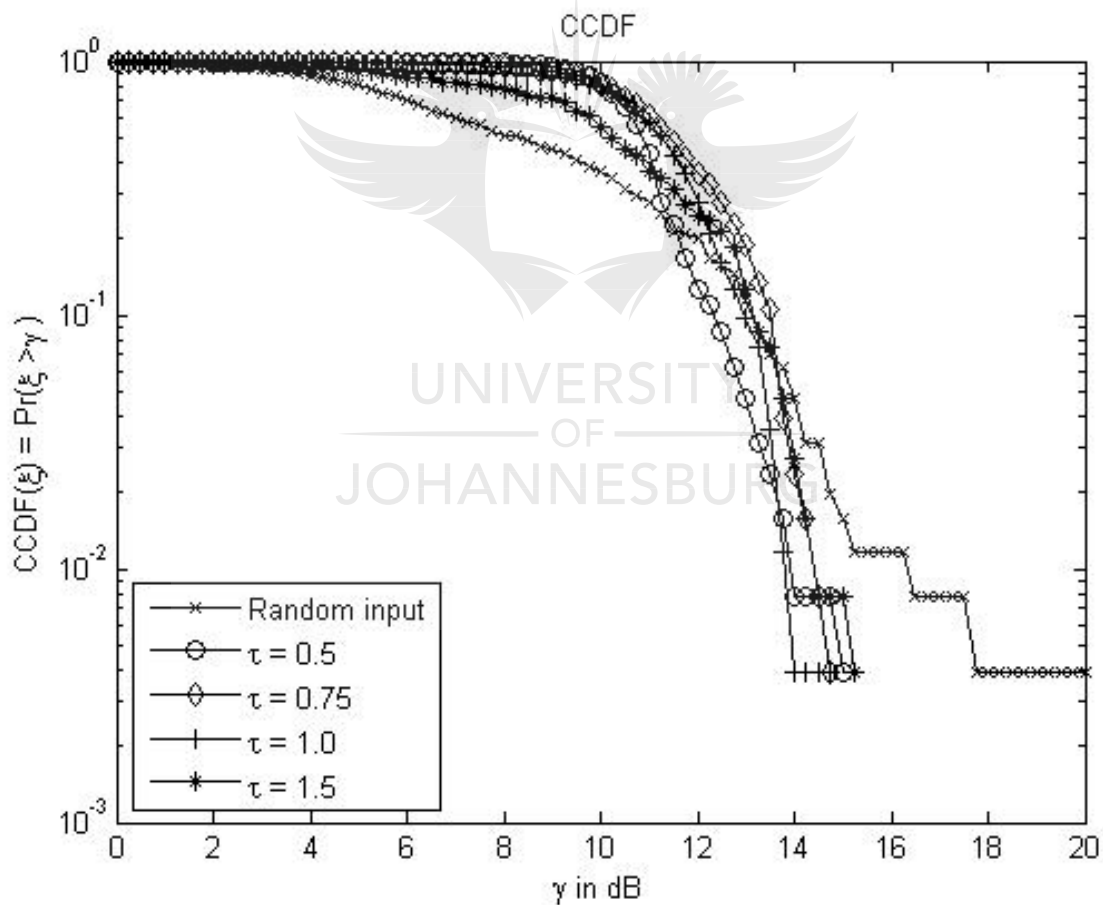
Figure A.1: Comparison of PAPR and BER performance with random input vs clipped input ($\tau = 0.5$)

In Figure A.1 the CCDF shows that any form of clipping will yield a better system perfor-
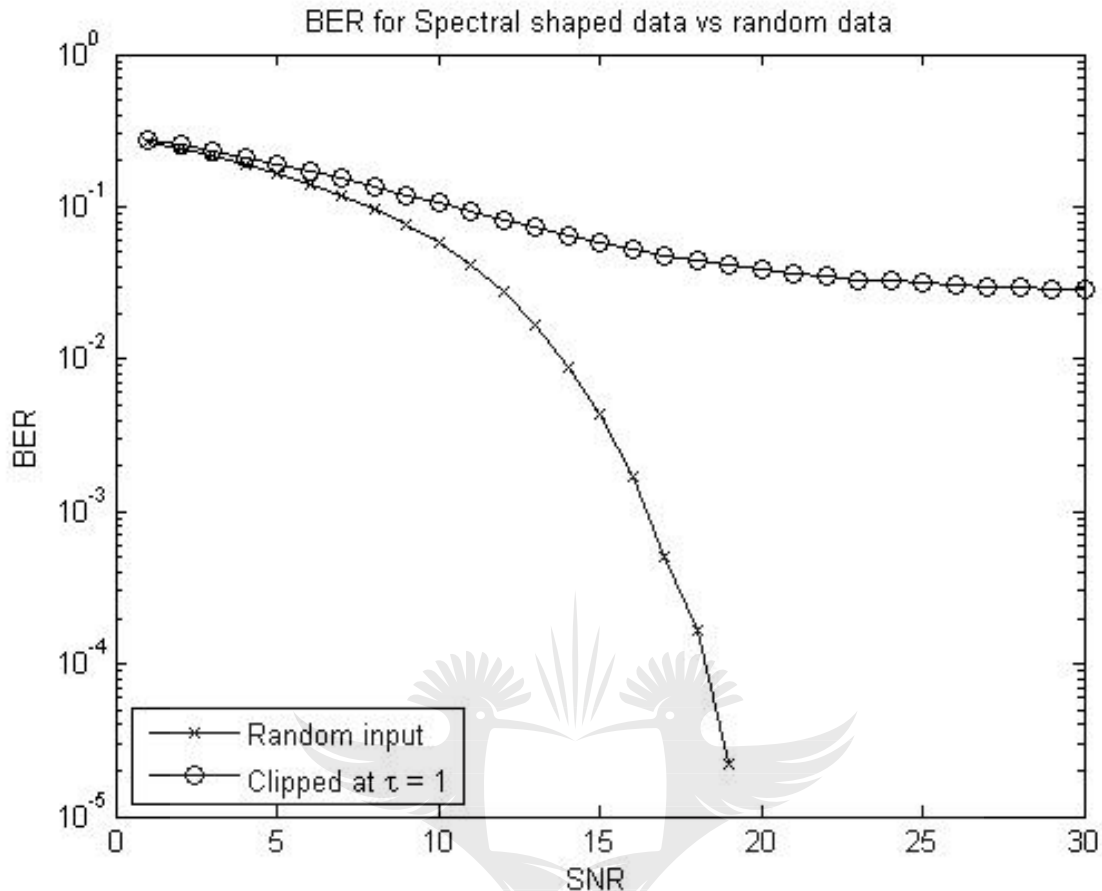
Figure A.2: Comparison of PAPR and BER performance with random input vs clipped input ($\tau = 0.5$)

mance. This is a reduction of approximately $4dB$. This improved performance will result in more efficient and cheaper circuitry. The BER in Figure and A.2 shows poor performance for the clipped signal at $\tau = 1$ when compared to the BER of random data. The reason for this is because the system did not employ any error correctional techniques or attempt to recover lost data. The clipping threshold with $\tau = 1$ is set at the average power of the transmission. This resulted in data being clipped along with the peaks of the impulse noise. The choice of τ is not trivial since it can have major performance implications as evident in these simulations.

Figure A.3 shows the performance of the system when using a wide range for the clipping factor. Note how at $\tau = 0.1$ the system did not yield much of a performance improvement. This is because a minimal amount of clipping was applied. For $\tau = 0.5$ we can still see
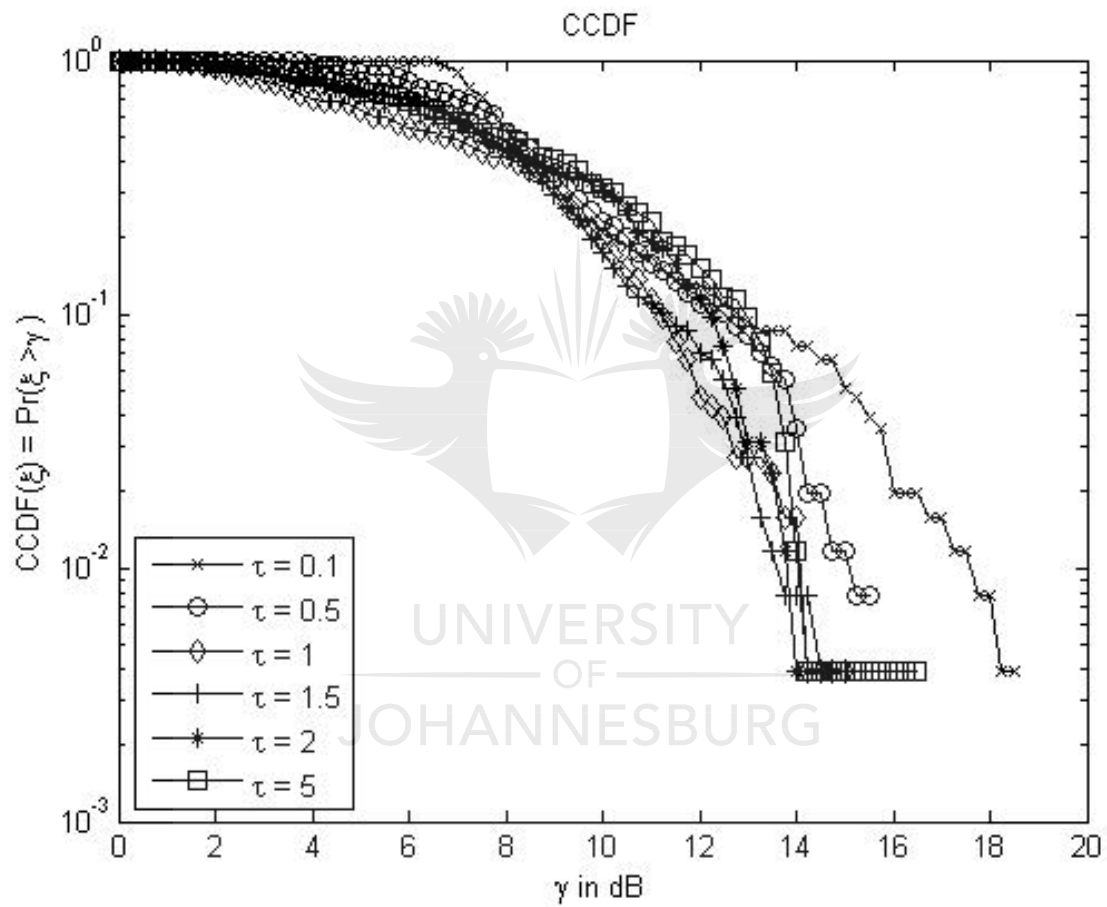
Figure A.3: Comparison of PAPR and BER performance in terms of clipping threshold τ
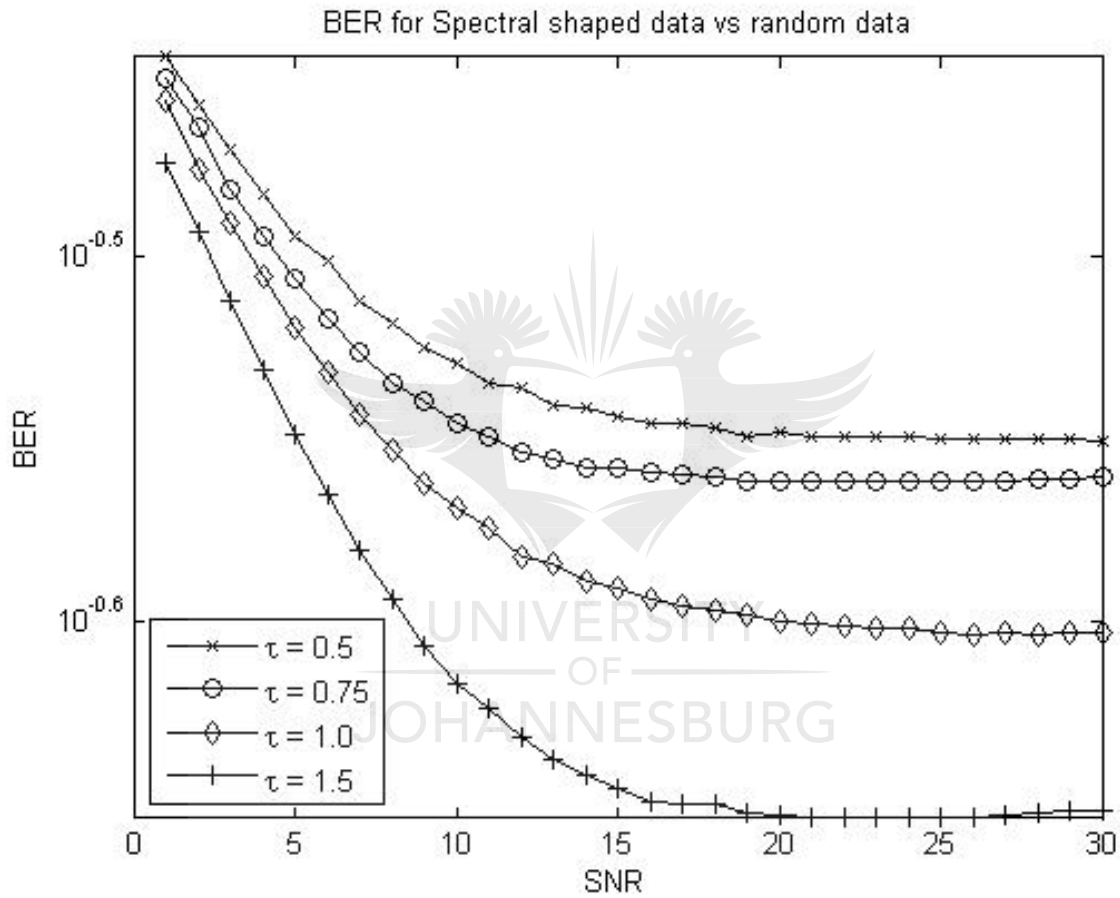
Figure A.4: Comparison of PAPR and BER performance in terms of clipping threshold τ

a slight deviation in the system performance. For $\tau = 2$ to 5 we see little change in the performance of the system as τ increases. This shows that the highest peaks of the system is most probably below the value of $\tau \hat{P}(f_n)$. The BER for this setup was compared in terms of τ (see Figure A.4). Although this is sill poor performance, a general trend is visible, where an improved system performance is observed when the clipping factor is increased. The reason for this is straight forward, a large clipping threshold will clip less values from the peaks. If no data carrier is clipped, the systems performance can be very similar to that of random data. The clipping threshold should ideally lie between the average value and peak value of the system.
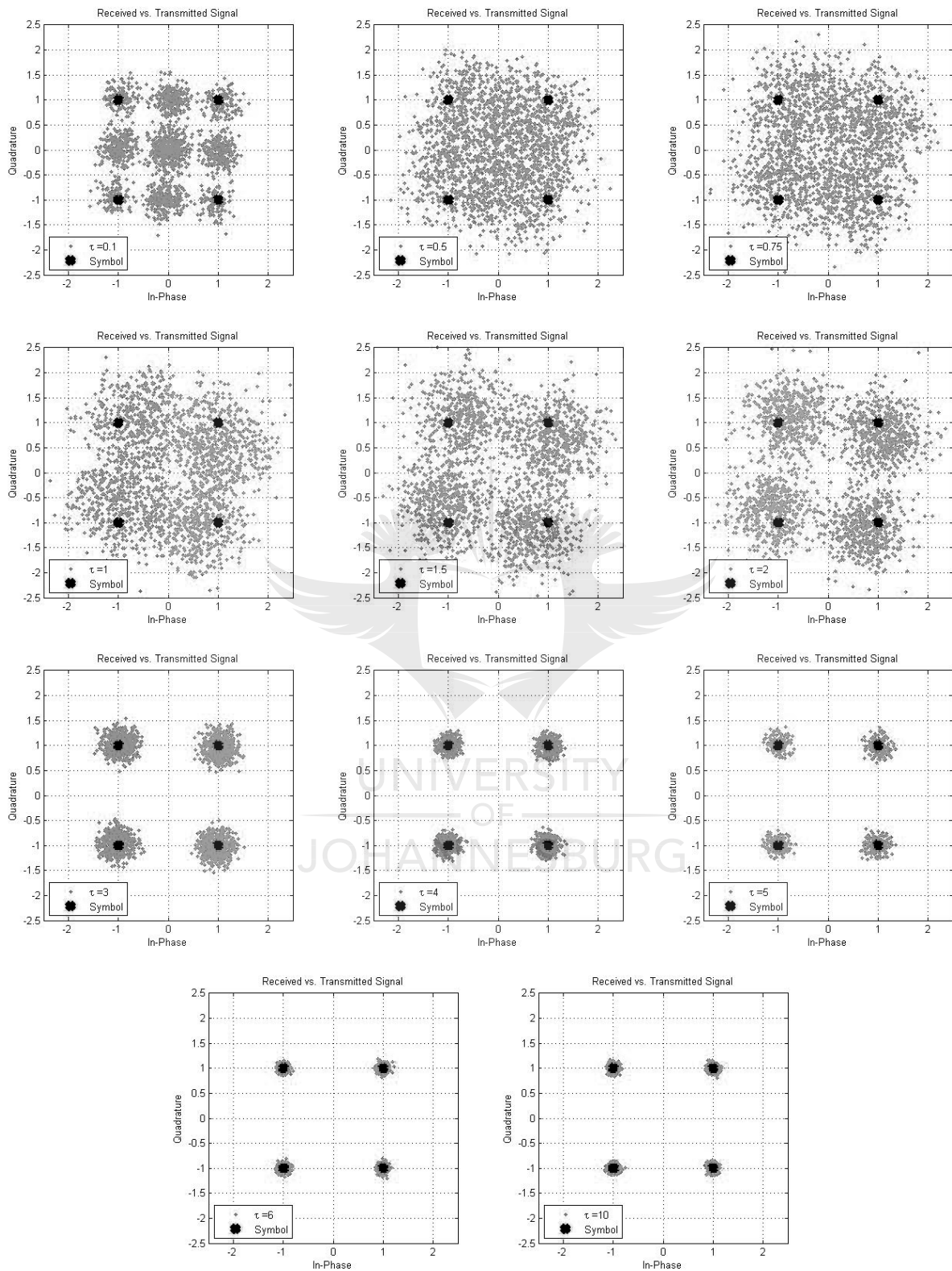
Figure A.5: Comparison of constellation for $\tau = 0.1$ through $\tau = 10.0$ respectively
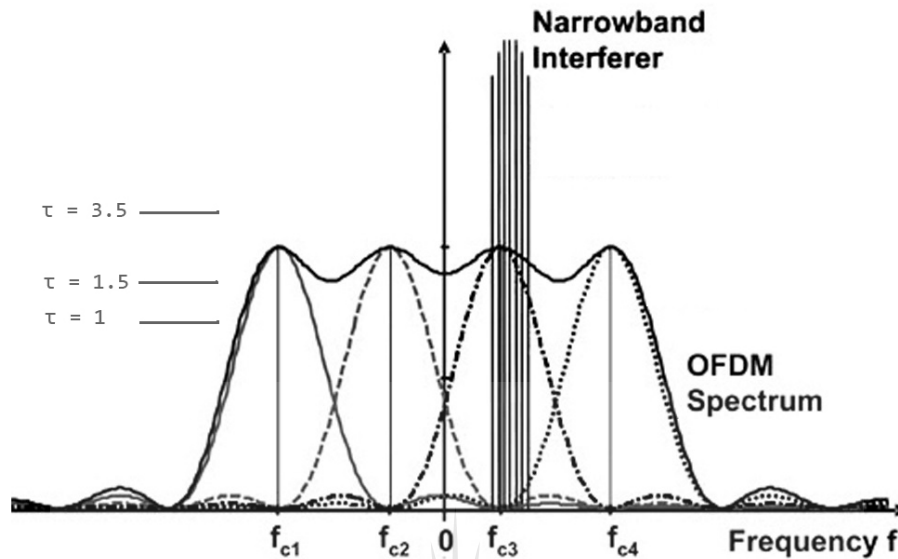
Figure A.6: Choosing a clipping ratio τ for effective PAPR reduction. Clipping will disregard any signal above τ. Clearly when $\tau = 1$ a large portion of useful data is discarded, greatly decreasing system performance. $\tau = 3.5$ on the other hand only discards some noise and keeps the OFDM data intact, yielding a good PAPR performance.
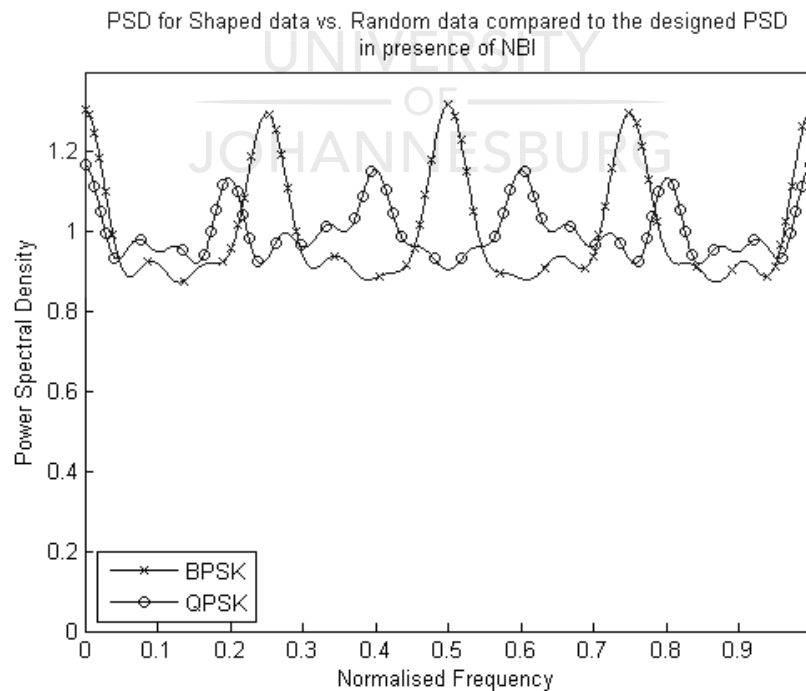
Figure A.7: PSD for shaped data with NBI compared to expected PSD ($N = 8$)
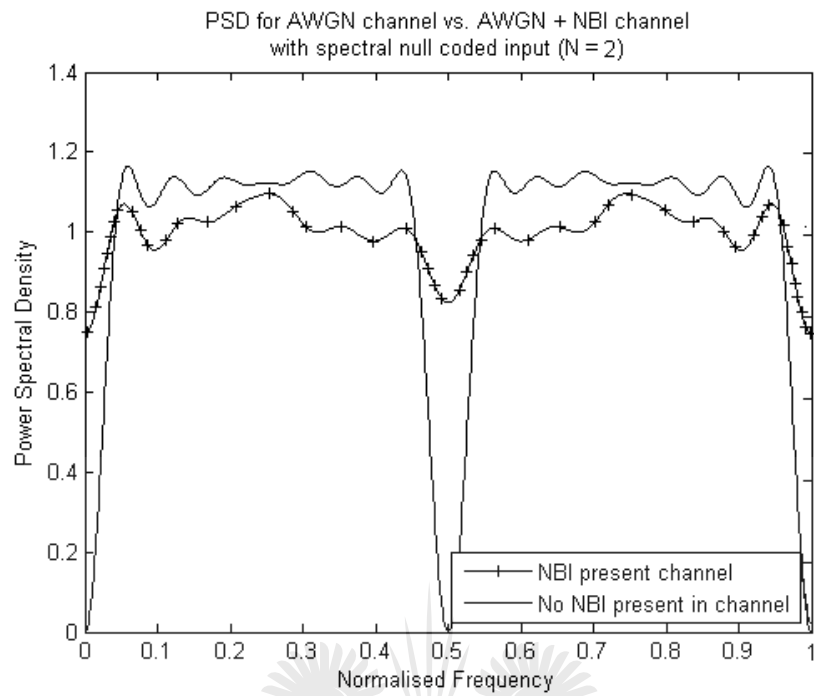
Figure A.8: PSD for spectral null coded input in AWGN vs. AWGN + NBI channel ($N = 2$)
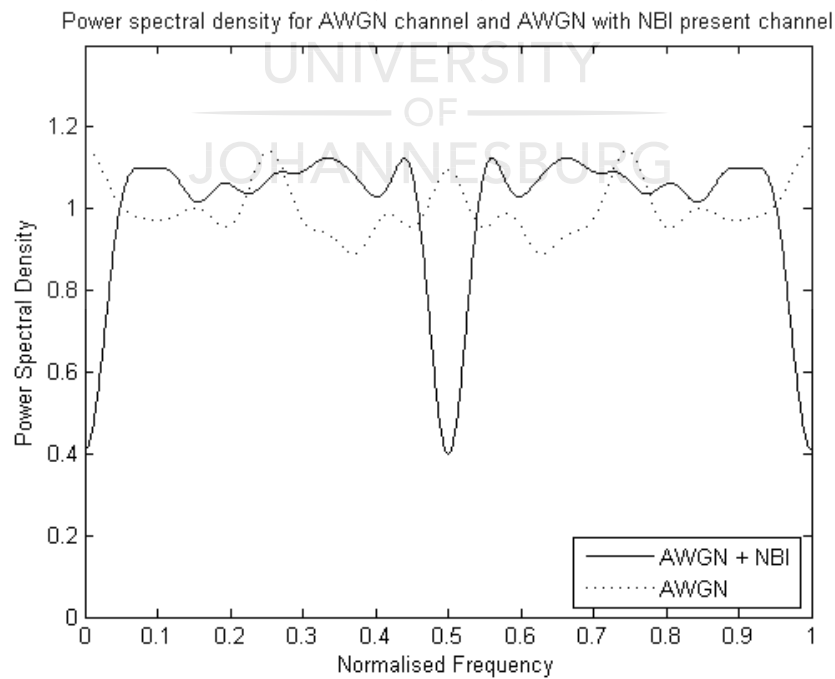
Figure A.9: PSD for shaped data with NBI compared to expected PSD ($N = 8$)
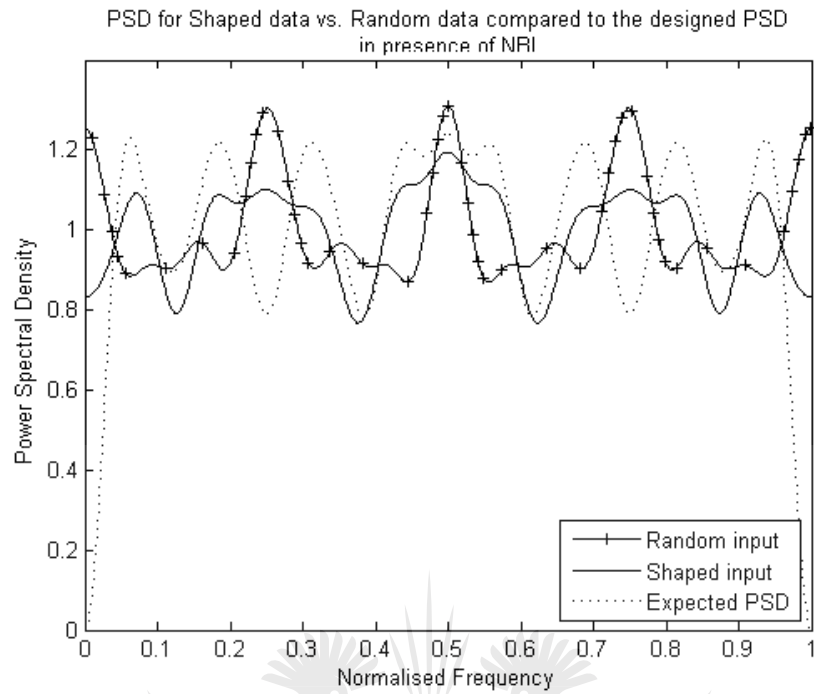
Figure A.10: PSD for shaped data with NBI compared to expected PSD ($N = 8$)
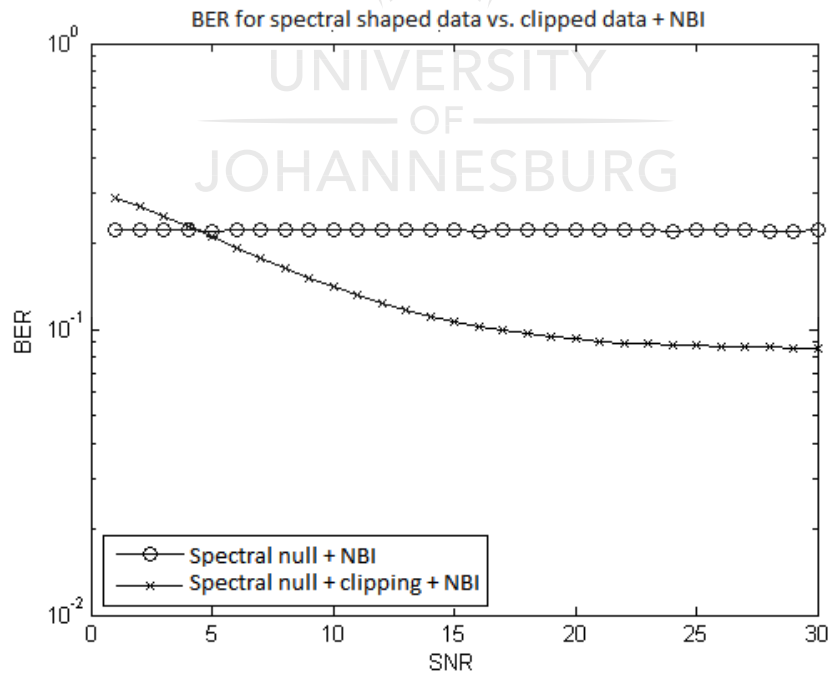
Figure A.11: BER for shaped and clipped data in the presence of NBI

Appendix B

Simulation source code

Relevant source code for the simulation application is provided in this appendix. For a full set of source code please contact the author. The code is kept in an online version control system.

Listing B.1: Main function code coordinating all the steps according to the block diagrams

```
1  % FILE:  OfdmSystem.m
2  % AUTH:  Martin  Trollip  -  201174479
3  % DATE:  2017/02/27
4  % DESC:  Main  simulation  file
5  %% Setup  and  clear  workspace
6      tic ;
7
8      clf ;
9      clc ;
10     clear  all ;
11     close  all ;
12
13 %% Initialise  variables
14     snr_to_plot = 20;
15     nbi = 1;
16
17     M = 16;
```

```
18        cyclic_prefix_perc = 0.25;
19        subcarrier_count_Nc = 1024; %Must be a log2(M) factor here () (rows)
20        codelength_n = 16;
21        snr_range=1:30;
22        number_iterations = 1000;
23        num_nulls = 16;
24
25  %% Generate Input
26
27  %   We modify the source to generate parallel signal which can be mapped ...
        directly
28  %    onto the available sub carriers. (Instead of making use of a serial ...
        input,
29  %   assume that step is trivial enough). We shall choose random codewords ...
        to
30  %   place on a selected carrier (ie 8 bits per carrier).   Then we repeat
31  %   those bits and analyse the results.   The following will be tested:
32  %        - All carriers has symbols out of the codebook
33  %        - Only put symbols from the codebook on random channels
34  %        - Put symbol from the codebook on one carrier only
35  %        - Purely random data
36  %        - Loading symbols on time vs frequency domain
37  %        - Demonstrate that it works for more zeros
38  %        - Method of detecting NBI in a channel (synched receiver and
39  %        transmitter?
40  %
41  %    serial_input = generate_serialInput(num_nulls,codelength_n);
42
43        parallel_input = ...
              generate_parallelInput(num_nulls,codelength_n,subcarrier_count_Nc);
44        random_input = ...
              parallel_input;%generate_randomInput(codelength_n,subcarrier_count_Nc);
45  %      parallel_input = random_input;
46  %% Transmitter Tx
47        to_transmit = transmitter(parallel_input, M, subcarrier_count_Nc);
48        random_to_transmit = clip(transmitter(random_input, M, ...
```

```
                subcarrier_count_Nc),2.5);
49        expected = to_transmit;
50        plot_CCDF(to_transmit, random_to_transmit);
51
52  %TODO add zero padding
53        ber = zeros(length(snr_range),number_iterations);
54        random_ber = zeros(length(snr_range),number_iterations);
55        outputs = zeros(subcarrier_count_Nc, codelength_n,max(snr_range));
56        random_outputs = zeros(subcarrier_count_Nc, codelength_n, ...
                length(snr_range));
57        for snr = snr_range
58            display(snr);
59            for itr = 1:number_iterations
60                %% Channel
61                    transmitted = channel(to_transmit, snr,1);
62                    random_transmitted = channel(random_to_transmit, snr,1);
63                    expected_transmitted = channel(expected, snr,0);
64                %% Receiver
65                    output = receiver(transmitted,M,subcarrier_count_Nc);
66                    random_output = ...
                        receiver(random_transmitted,M,subcarrier_count_Nc);
67                    expected_output = ...
                        receiver(expected_transmitted,M,subcarrier_count_Nc);
68                %% BER Analysis
69                    ber(snr,itr) = calculate_ber(parallel_input, output);
70                    random_ber(snr,itr) = calculate_ber(random_input, ...
                        random_output);
71
72                    mean = (outputs(:,:,snr) + output)/2;
73                    outputs(:,:,snr) =  mean;
74            end
75
76            if (snr == snr_to_plot)
77                plot_(random_output,output,expected_output);
78            end
79        end
```

```
80
81  %% Analysis
82      plot_ber(snr_range, ber, random_ber);
83
84  %% Finalise
85      toc;
```

Listing B.2: Code for clipping the input and reducing PAPR

```matlab
1  % FILE: clip.m
2  % AUTH: Martin Trollip
3  % DATE: 2017/04/26
4  % DESC: Clip the input at a clipping ratio \tau
5  function [clipped] = clip(input, tau)
6      in_real = real(input);
7      x_mag = abs(in_real);
8
9      kappa_real = tau*mean(mean(x_mag));
10     for r = 1:size(input,1)
11         for c = 1:size(input,2)
12             if(x_mag(r,c) >= kappa_real)
13                 if(in_real(r,c) < 0)
14                     in_real(r,c) = -kappa_real;
15                 else
16                     in_real(r,c) = kappa_real;
17                 end
18             end
19         end
20     end
21
22     in_imag = imag(input);
23     x_mag_i = abs(in_imag);
24     kapp_imag = tau*mean(mean(x_mag_i));
25     for r = 1:size(input,1)
26         for c = 1:size(input,2)
```

```
27                    if (x_mag_i(r,c) >= kapp_imag)
28                        if (in_imag(r,c) < 0)
29                            in_real(r,c) = -kapp_imag;
30                        else
31                            in_real(r,c) = kapp_imag;
32                        end
33                    end
34                end

36        clipped = complex(in_real,in_imag);
37  end
```

Listing B.3: Code for generating any codebook

```
 1  % FILE: generate_CodebookMain.m
 2  % AUTH: Martin Trollip
 3  % DATE: 2016/06/01
 4  % DESC: This function will return a codebook for any C_b(M,N) white N ...
        prime or non-prime
 5  function codebook = generate_CodebookMain(N,M)
 6
 7  z = M/N;%number of elements in a spectral null grouping
 8
 9  A = zeros(N,z);
10  for i = 1:N
11      k = 0;
12      while k < z
13          A(i,k+1) = (i + k*N);
14          k = k + 1;
15      end
16  end
17
18  all_permutations = generate_AllBinaryCombos(M);
19
20  if isprime(N)
```

```
21          codebook = generate_Codebook(A, all_permutations);
22  else
23      codebook = generate_CodebookNonPrime(A, all_permutations ,N);
24  end
25
26  codebook = selectZeroDisparity(codebook);
27  codebook = unique(codebook, 'rows');
```

Listing B.4: Code for genertating a codebook if N is prime

```
1  % FILE: generate_AllBinaryCombos.m
2  % AUTH: Martin Trollip
3  % DATE: 2016/06/01
4  % DESC: Generate Codebook by iterating and finding the entries of combo ...
       satiffying A
5  function codebook = generate_Codebook(A, combo)
6      [combo_r, combo_c] = size(combo);
7      [a_r, a_c] = size(A);
8
9      results = zeros(combo_r,a_r);
10
11     for combo_row = 1:combo_r
12         curr_code = combo(combo_row,:);
13         for a_row = 1:a_r
14             curr_a = A(a_row,:);
15             sum = 0;
16             for a_col = 1:a_c
17                 %add elements
18                 ind = curr_a(1,a_col);
19                 elem = curr_code(1,ind)-48;
20                 if(elem == 0)
21                     elem = -1;
22                 end
23                 sum =  elem + sum;
24                 results(combo_row,a_row) = sum;
```

```
25                end
26            end
27        end
28
29        codebook = zeros(1, combo_c);
30
31        for res_row = 1:combo_r
32            curr_res_row = results(res_row,:);
33            if range(curr_res_row) == 0 % A1 = A2 = A3 ...
34                codebook = [codebook; combo(res_row,:)];
35            end
36        end
37  end
```

Listing B.5: Code for genertating a codebook if *N* is non-prime

```
1  % FILE: generate_CodebookNonPrime.m
2  % AUTH: Martin Trollip
3  % DATE: 2016/06/01
4  % DESC: Generate a codebook in the case where N is not prime by iterating ...
        and finding all the entries in combo satisfying A
5  function codebook = generate_CodebookNonPrime(A, combo, N)
6      factN = fact(N);
7      [f_r, f_c] = size(factN);
8      [c_r, c_c] = size(combo);
9
10     codebook = zeros(1, c_c);
11     for i = 1:f_r
12         c = factN(i, 1);
13         d = factN(i, 2);
14
15         u = zeros(1,c);
16         v = zeros(1,d-1);
17
18         for j = 1:c
```

```
19                u(1,j) =  j;
20          end
21          u;
22
23          for k = 1:d-1
24              v(1,k) = k;
25          end
26          v;
27
28          [u_r, u_c] = size(u);
29          [v_r, v_c] = size(v);
30
31          sub_A = zeros(u_c, 2);
32
33          for nv = 1:v_c
34              for mu = 1:u_c
35                  sub_A(mu, 1) = u(1, mu);
36                  sub_A(mu, 2) = mu + (nv*c);
37              end
38              sub_A;
39              codebook = [codebook; generate_partialcodebook(A, sub_A, ...
                      combo)];
40          end
41      end
42  end
```

Listing B.6: Code for generatting all possible binary combinations with length n

```
1  % FILE: generate_AllBinaryCombos.m
2  % AUTH: Martin Trollip
3  % DATE: 2016/06/01
4  % DESC: Generate all possible binary combinations for codes with  a ...
        length of n
5  function A = generate_AllBinaryCombos(n)
6      try
```

```
 7            possible_codes = 2^n-1;
 8            assert(n <= ...
                  16,'generate_all_possible_binary_combo:tooBigToProcess','Please ...
                  select n <= 16');
 9          A = de2bi(0:2^n-1);
10      catch causeException
11          baseException = ...
                  addCause(MException('generate_all_possible_binary_combo
12          :tooBigToProcess','Please select n <= 16'),causeException);
13          throw(baseException)
14      end
15  end
```

Listing B.7: Code for plotting CCDF

```
 1  %% 2017/03/21
 2  %  Martin Trollip - 201174479
 3
 4  function  plot_single_CCDF(input, line)
 5      papr = 0:.25:20; % dB vector of PAPR values
 6
 7      semilogy(papr,ccdf(papr,input), line);
 8      hold on
 9
10      title('CCDF');
11      xlabel('\gamma in dB');
12      ylabel('CCDF(\xi) = Pr(\xi >\gamma )');
13      xlim([0 20])
14
15  end
16
17  function [ccdf] = ccdf(papr, input)
18      x_mag = input;
19      papr_ratio=x_mag.^2/mean(x_mag);
20      papr_ratio_dB = 10*log10(papr_ratio);
```

```matlab
21        for i = 1:length(papr)
22            y(i) = (length(find(abs(papr_ratio_dB) >= ...
                  papr(i)))/length(x_mag)); % # of samples exceeding papr(i)
23        end
24        ccdf = y;
25  end
```

Appendix C - Figures

Additional figures

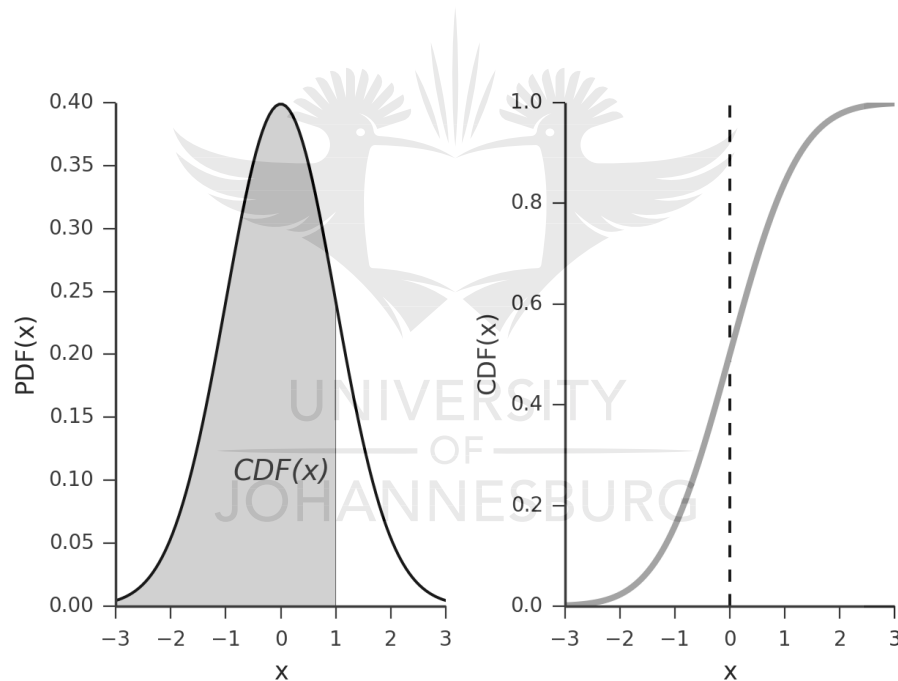This appendix provides some additional figures which was not presented in earlier chapters.

Figure C.1: CCDF and PDF

Figure C.2: Federal Communications Commission (FCC) - Radio Spectrum Allocation [4]

References

[1] A. A. Huurdeman, *The worldwide history of telecommunications.* John wiley & sons, 2003.

[2] M. Meeker, "Internet trends 2015-code conference," *Glokalde*, vol. 1, no. 3, 2015.

[3] T. Rappaport, *Wireless Communications: Principles and Practice*, 2nd ed. Upper Saddle River, NJ, USA: Prentice Hall PTR, 2001.

[4] FCC. (2017) Federal communications comission - radio spectrum allocation. [Online]. Available: https://www.fcc.gov/engineering-technology/policy-and-rules-division/general/radio-spectrum-allocation

[5] Y. S. Cho, J. Kim, W. Y. Yang, and C. G. Kang, *MIMO-OFDM wireless communications with MATLAB.* John Wiley & Sons, 2010.

[6] X. Wang, K. Kienzle, and S. t. Brink, "On spectral shaping of multicarrier waveforms employing fir-filtering and active interference cancellation," in *SCC 2017; 11th International ITG Conference on Systems, Communications and Coding*, Feb 2017, pp. 1–6.

[7] P. Anker. (2005) Tellecoms abc: Out-of-band emission. [Online]. Available: http://www.telecomabc.com/o/out-of-band.html

[8] K. S. Immink, "Spectral null codes," *IEEE Transactions on Magnetics*, vol. 26, no. 2, pp. 1130–1135, 1990.

[9] A. Batra and J. R. Zeidler, "Narrowband interference mitigation in ofdm systems," in *Military Communications Conference, 2008. MILCOM 2008. IEEE.* IEEE, 2008, pp. 1–7.

[10] M. Ndlovu and L. Cheng, "An ofdm inter-subcarrier permutation coding scheme for power-line communication," in *Proceedings of the 18th IEEE International Symposium on Power Line Communications and Its Applications*, March 2014, pp. 196–201.

[11] I. Sommerville, "Software engineering. international computer science series," *Addison Wesley*, 2004.

[12] M. Trollip, "A simulation study of ofdm robustness in wireless environments," *Mini-Dissertation, University of Johannesburg*, 2014.

[13] M. Trollip, K. Ouahada, and T. Imoto, "Narrowband signal detection in ofdm systems using spectral shaping techniques," in *Proceedings of the 13th IEEE AFRICON Conference*. IEEE, 2017, pp. 232–237.

[14] S. M. Moser and P.-N. Chen, *A student's guide to coding and information theory*. Cambridge University Press, 2012.

[15] A. Ephremides, "How information theory changed the world - a brief review of the history of the information theory society," in *2009 IEEE Conference on the History of Technical Societies*, Aug 2009, pp. 1–7.

[16] C. E. Shannon, "A mathematical theory of communication," *ACM SIGMOBILE Mobile Computing and Communications Review*, vol. 5, no. 1, pp. 3–55, 2001.

[17] H. Schulze and C. Lüders, *Theory and applications of OFDM and CDMA: Wideband wireless communications*. John Wiley & Sons, 2005.

[18] R. W. Hamming, "Error detecting and error correcting codes," *Bell Labs Technical Journal*, vol. 29, no. 2, pp. 147–160, 1950.

[19] A. Blokhuis and G. E. Moorhouse, "Some p-ranks related to orthogonal spaces," *Journal of Algebraic Combinatorics*, vol. 4, no. 4, pp. 295–316, 1995.

[20] T. K. Moon, *Error Correction Coding: Mathematical Methods and Algorithms*. Wiley-Interscience, 2005.

[21] W. C. Lee, "Estimate of channel capacity in rayleigh fading environment," *IEEE transactions on Vehicular Technology*, vol. 39, no. 3, pp. 187–189, 1990.

[22] Q. Zhang and S. A. Kassam, "Finite-state markov model for rayleigh fading channels," *IEEE Transactions on communications*, vol. 47, no. 11, pp. 1688–1692, 1999.

[23] S. C. Yang, *OFDMA system analysis and design*. Artech House, 2010.

[24] T.-D. Chiueh and P.-Y. Tsai, *OFDM baseband receiver design for wireless communications*. John Wiley & Sons, 2008.

[25] K. Fazel and S. Kaiser, *Multi-carrier and spread spectrum systems: from OFDM and MC-CDMA to LTE and WiMAX*. John Wiley & Sons, 2008.

[26] MATLAB. Find logical exclusive-or. [Online]. Available: https://www.mathworks.com/help/matlab/ref/xor.html

[27] MATLAB. Number of nonzero matrix elements. [Online]. Available: https://www.mathworks.com/help/matlab/ref/nnz.html

[28] A. Ghasemi and E. S. Sousa, "Spectrum sensing in cognitive radio networks: requirements, challenges and design trade-offs," *Communications Magazine, IEEE*, vol. 46, no. 4, pp. 32–39, 2008.

[29] M. Tripathi, "Study of spectrum sensing techniques for ofdm based cognitive radio," *International journal of technology enhancements and emerging engineering research*, vol. 2, no. 8, 2014.

[30] I. Poole. (2014) Cognitive radio spectrum sensing: an overview detailing the key techniques, technologies and methods used for spectrum sensing in cognitive radio technology. [Online]. Available: http://www.radio-electronics.com/info/rf-technology-design/cognitive-radio-cr/spectrum-sensing.phpl

[31] A. Umamaheswari, V. Subashini, and P. Subhapriya, "Survey on performance, reliability and future proposal of cognitive radio under wireless computing," in *Proceedings of the Third International Conference on Computing Communication Networking Technologies (ICCCNT)*, July 2012, pp. 1–6.

[32] J. Lunden, V. Koivunen, A. Huttunen, and H. Poor, "Spectrum sensing in cognitive radios based on multiple cyclic frequencies," in *Proceedings of the 2nd International Conference on Cognitive Radio Oriented Wireless Networks and Communications*, Aug 2007, pp. 37–43.

[33] W. Wang, "Spectrum sensing for cognitive radio," in *Proceedings of the Third International Symposium on Intelligent Information Technology Application Workshops (IITAW)*, Nov 2009, pp. 410–412.

[34] T. Yucek and H. Arslan, "A survey of spectrum sensing algorithms for cognitive radio applications," *Communications Surveys Tutorials, IEEE*, vol. 11, no. 1, pp. 116–130, First 2009.

[35] D. Cabric, S. M. Mishra, and R. W. Brodersen, "Implementation issues in spectrum sensing for cognitive radios," in *Proceedings of the thirty-eighth Asilomar conference on Signals, systems and computers*, vol. 1. IEEE, 2004, pp. 772–776.

[36] S. Bagheri and A. Scaglione, "Spatial-spectral sensing using the shrink amp; match algorithm in asynchronous mimo ofdm signals," in *Global Communications Conference (GLOBECOM), 2013 IEEE*, Dec 2013, pp. 3218–3223.

[37] H. Tang, "Some physical layer issues of wide-band cognitive radio systems," in *Proceedings of the first IEEE international symposium on New frontiers in dynamic spectrum access networks*. IEEE, 2005, pp. 151–159.

[38] P. Welch, "The use of fast fourier transform for the estimation of power spectra: A method based on time averaging over short, modified periodograms," *IEEE Transactions on Audio and Electroacoustics*, vol. 15, no. 2, pp. 70–73, Jun 1967.

[39] P. Welch, "On the variance of time and frequency averages over modified periodograms," in *Acoustics, Speech, and Signal Processing, IEEE International Conference on ICASSP '77.*, vol. 2, May 1977, pp. 58–62.

[40] T. Sanjana and M. Suma, "Combined nbi and impulsive noise cancellation in ofdm system," *International Journal of Advanced Information Science and Technology*, vol. 31, no. 31, 2014.

[41] D. Galda and H. Rohling, "Narrow band interference reduction in ofdm-based power line communication systems," in *Proceedings of the 5th IEEE International Symposium on Power Line Communications and its Applications (ISPLC), Malmo, Sweden*, 2001, pp. 345–351.

[42] T. Shongwe, V. N. Papilaya, and A. H. Vinck, "Narrow-band interference model for ofdm systems for powerline communications," in *Proceedings of the 17th IEEE International Symposium on Power Line Communications and Its Applications (ISPLC)*. IEEE, 2013, pp. 268–272.

[43] R. Nilsson, F. Sjoberg, and J. LeBlanc, "A rank-reduced lmmse canceller for narrowband interference suppression in ofdm-based systems," *IEEE Transactions on Communications*, vol. 51, no. 12, pp. 2126–2140, Dec 2003.

[44] K. Ouahada, T. G. Swart, H. Ferreira, and L. Cheng, "Spectral shaping technique for permutation distance-preserving mapping codes," in *Information Theory Workshop, 2007. ITW '07. IEEE*, Sept 2007, pp. 36–41.

[45] D. Middleton, "Canonical and quasi-canonical probability models of class a interference," *IEEE Transactions on Electromagnetic Compatibility*, vol. EMC-25, no. 2, pp. 76–106, May 1983.

[46] M. Marey and H. Steendam, "Analysis of the narrowband interference effect on ofdm timing synchronization," *IEEE Transactions on Signal Processing*, vol. 55, no. 9, pp. 4558–4566, 2007.

[47] N. Hadaschick. (2017) Techniques for uwb-ofdm. [Online]. Available: https://www.ice. rwth-aachen.de/research/algorithms-projects/entry/detail/techniques-for-uwb-ofdm/

[48] C. de Fréin, M. Flanagan, and A. Fagan, "Ofdm narrowband interference estimation using cyclic prefix based algorithm," *RTS*, vol. 6, p. 1, 2006.

[49] Z. Nikolova, G. Iliev, M. Ovtcharov, and V. Poulkov, "Narrowband interference suppression in wireless ofdm systems," *African Journal of Information and Communication Technology*, vol. 5, no. 1, pp. 30–42, 2009.

[50] D. Zhang, P. Fan, and Z. Cao, "Receiver window design for narrowband interference suppression in ieee 802.11a system," in *Joint Proceedings of the 5th International Symposium on Multi-Dimensional Mobile Communications and the 10th Asia-Pacific Conference on Communications*, vol. 2, Aug 2004, pp. 839–842 vol.2.

[51] V. Poulkov, M. Ovtcharov, G. Iliev, and Z. Nikolova, "Narrowband interference suppression in mimo systems," in *MIMO Systems, Theory and Applications*. InTech, 2011.

[52] S. Brandes, "Suppression of mutual interference in ofdm based overlay systems," Ph.D. dissertation, Universität Karlsruhe, 2009.

[53] E. Gorog, "Redundant alphabets with desirable frequency spectrum properties," *IBM Journal of Research and Development*, vol. 12, no. 3, pp. 234–241, May 1968.

[54] K. Ouahada, H. Ferreira, A. H. Vinck, A. Snyders, and T. Swart, "Combined spectral shaping codes and ofdm modulation for narrowband interference channels," 2007.

[55] M. Gao, A. Hyytinen, and O. Toivanen, "Demand for mobile internet: Evidence from a real-world pricing experiment," ETLA Discussion Papers, The Research Institute of the Finnish Economy (ETLA), Tech. Rep., 2004.

[56] H. Sampath, S. Talwar, J. Tellado, V. Erceg, and A. Paulraj, "A fourth-generation mimo-ofdm broadband wireless system: design, performance, and field trial results," *Communications Magazine, IEEE*, vol. 40, no. 9, pp. 143–149, 2002.

[57] E. Dahlman, S. Parkvall, and J. Skold, *4G: LTE/LTE-advanced for mobile broadband.* Academic press, 2013.

[58] O. Edfors, M. Sandell, J.-J. van de Beek, D. Landström, and F. Sjöberg, "An introduction to orthogonal frequency-division multiplexing," *Lulea University of Technology*, 1996.

[59] M. Engels, *Wireless OFDM Systems: How to make them work?* Springer Science & Business Media, 2002.

[60] S. Vaughan-Nichols, "Ofdm: back to the wireless future," *Computer*, vol. 35, no. 12, pp. 19–21, Dec 2002.

[61] O. Bejarano, E. W. Knightly, and M. Park, "Ieee 802.11ac: from channelization to multi-user mimo," *IEEE Communications Magazine*, vol. 51, no. 10, pp. 84–90, October 2013.

[62] M. Russell and G. Stuber, "Interchannel interference analysis of ofdm in a mobile environment," in *Vehicular Technology Conference, 1995 IEEE 45th*, vol. 2, Jul 1995, pp. 820–824 vol.2.

[63] A. R. Bahai, B. R. Saltzberg, and M. Ergen, *Multi-carrier digital communications: theory and applications of OFDM.* Springer Science & Business Media, 2004.

[64] J. Proakis, M. Salehi, and G. Bauch, *Contemporary communication systems using MATLAB.* Cengage Learning, 2012.

[65] T. Haslwanter. (2014) Thomas haslwanter lectures - statistics. [Online]. Available: http://work.thaslwanter.at/Stats/html/_images/PDF_CDF.png

[66] V. K. Ingle and J. G. Proakis, *Digital Signal Processing Using MATLAB: A Problem Solving Companion.* Cengage Learning, 2016.

[67] N. Marchetti, M. I. Rahman, S. Kumar, and R. Prasad, "Ofdm: Principles and challenges," in *New Directions in Wireless Communications Research*. Springer, 2009, pp. 29–62.

[68] H. Steendam and M. Moeneclaey, "Different guard interval techniques for ofdm: performance comparison," *Lecture Notes in Electrical Engineering*, vol. 1, p. 11, 2007.

[69] N. Robertson. Peak to average power ratio and ccdf. [Online]. Available: https://www.dsprelated.com/showarticle/962.php

[70] M. Fitz, *Fundamentals of communications systems*. Tata McGraw-Hill Education, 2007.

[71] Agilent, "Characterizing digitally modulated signals with ccdf curves," *Agilent Technologies*, p. 21, 2000.

[72] K. Sankar. Peak to average power ratio for ofdm. [Online]. Available: http://www.dsplog.com/2008/02/24/peak-to-average-power-ratio-for-ofdm/

[73] K. Mhatre and U. P. Khot, "Efficient selective mapping papr reduction technique," *Procedia Computer Science*, vol. 45, pp. 620–627, 2015.

[74] C. Nunes, B. Corrêa, and G. Cavalcante, "Matlab's solutions to reduce the papr on isdb-t's ofdm," in *Proceedings of the 7th Latin American Networking Conference*, ser. LANC '12. New York, NY, USA: ACM, 2012, pp. 67–71. [Online]. Available: http://0-doi.acm.org.ujlink.uj.ac.za/10.1145/2382016.2382028

[75] C. Kang, Y. Liu, M. Hu, and H. Zhang, "A low complexity papr reduction method based on fwft and pec for ofdm systems," *IEEE Transactions on Broadcasting*, vol. 63, no. 2, pp. 416–425, June 2017.

[76] S.-K. Lee, H.-L. Chiu, Y.-C. Tsai, and H.-Y. Chen, "Lt codes for ofdm multicast systems with papr reduction capability," in *Proceedings of the 2009 International Conference on Wireless Communications and Mobile Computing: Connecting the World Wirelessly*, ser. IWCMC '09. New York, NY, USA: ACM, 2009, pp. 348–352. [Online]. Available: http://0-doi.acm.org.ujlink.uj.ac.za/10.1145/1582379.1582456

[77] O. A. Omer and A. A. Reheem, "A novel algorithm for papr reduction in lte system," in *Proceedings of the International Conference on Advances in Computing, Communications and Informatics*, ser. ICACCI '12. New York, NY, USA: ACM, 2012, pp. 307–311. [Online]. Available: http://0-doi.acm.org.ujlink.uj.ac.za/10.1145/2345396.2345447

[78] S. H. Han and J. H. Lee, "Papr reduction of ofdm signals using a reduced complexity pts technique," *IEEE Signal Processing Letters*, vol. 11, no. 11, pp. 887–890, Nov 2004.

[79] H. Ochiai and H. Imai, "On clipping for peak power reduction of ofdm signals," in *Global Telecommunications Conference, 2000. GLOBECOM '00. IEEE*, vol. 2, 2000, pp. 731–735 vol.2.

[80] S. Albdran, A. Alshammari, and M. Matin, "Clipping and filtering technique for reducing papr in ofdm," *IOSR Journal of Engineering (IOSRJEN), vol2*, pp. 91–97, 2012.

[81] M. Phulia and O. Sahu, "Peak-to-average power ratio (papr) reduction of ofdm signals using a modified pts technique," *International Journal of Electronic and Electrical Engineering*, vol. 7, no. 1, pp. 79–84, 2014.

[82] M. Ali, R. K. Rao, and V. Parsa, "Papr reduction in ofdm systems using clipping based on symbol statistics," in *2017 IEEE 30th Canadian Conference on Electrical and Computer Engineering (CCECE)*, April 2017, pp. 1–5.

[83] D. J. MacKay, "Fountain codes," *IEE Proceedings-Communications*, vol. 152, no. 6, pp. 1062–1068, 2005.

[84] R. E. Alami, C. B. Gueye, M. Boussetta, M. Zouak, and M. Mrabti, "Bit flipping-sum product algorithm for regular ldpc codes," in *2010 5th International Symposium On I/V Communications and Mobile Network*, Sept 2010, pp. 1–4.

[85] R. Tanner, "A recursive approach to low complexity codes," *IEEE Transactions on information theory*, vol. 27, no. 5, pp. 533–547, 1981.

[86] S. H. Muller and J. B. Huber, "A comparison of peak power reduction schemes for ofdm," in *Global Telecommunications Conference, 1997. GLOBECOM'97., IEEE*, vol. 1. IEEE, 1997, pp. 1–5.

[87] R. S. Bansode, B. Mishra, and A. M. Temrikar, "Hardware implementation of ofdm system to reduce papr using selective level mapping on fpga," *IOSR Journal of Electronics and Communication Engineering*, vol. 7, pp. 05–11, 2013.

[88] S. H. Muller and J. B. Huber, "Ofdm with reduced peak-to-average power ratio by optimum combination of partial transmit sequences," *Electronics Letters*, vol. 33, no. 5, pp. 368–369, Feb 1997.

[89] L. J. Cimini and N. R. Sollenberger, "Peak-to-average power ratio reduction of an ofdm signal using partial transmit sequences," *IEEE Communications letters*, vol. 4, no. 3, pp. 86–88, 2000.

[90] A. Garg and G. Saini, "A papr reduction anaysis of various techniques in ofdm system," in *2016 International Conference on Micro-Electronics and Telecommunication Engineering (ICMETE)*, Sept 2016, pp. 349–354.

[91] N. Valliappan and R. Ganesh. Papr reduction techniques in ofdm systems. [Online]. Available: https://wirelesscommlab.wordpress.com/documentation/

[92] R. K. Singh and M. Fidele, "An efficient papr reduction scheme for ofdm system using peak windowing and clipping," in *2015 Third International Conference on Image Information Processing (ICIIP)*, Dec 2015, pp. 491–495.

[93] P. P. Ann and R. Jose, "Comparison of papr reduction techniques in ofdm systems," in *2016 International Conference on Communication and Electronics Systems (ICCES)*, Oct 2016, pp. 1–5.

[94] K. A. S. Immink, *Codes for mass data storage systems.* Shannon Foundation Publisher, 2004.

[95] K. A. S. Immink, "Reed-solomon codes and the compact disc," *Reed-Solomon codes and their applications*, pp. 41–59, 1994.

[96] S. Sivaprakasam and K. S. Shanmugan, "An equivalent markov model for burst errors in digital channels," *IEEE Transactions on Communications*, vol. 43, no. 2/3/4, pp. 1347–1355, Feb 1995.

[97] K. Sathananathan and C. Tellambura, "Forward error correction codes to reduce inter-carrier interference in ofdm," in *Proceedings of the 2001 IEEE International Symposium on Circuits and Systems*, vol. 4, May 2001, pp. 566–569 vol. 4.

[98] H. Ferreira, "On dc free magnetic recording codes generated by finite state machines," *IEEE Transactions on Magnetics*, vol. 19, no. 6, pp. 2691–2693, Nov 1983.

[99] K. A. S. Immink, "Dc-free codes of rate (n-1)/n, n odd," *IEEE Transactions on Information Theory*, vol. 46, no. 2, pp. 633–634, Mar 2000.

[100] P. Welch, "The use of fast fourier transform for the estimation of power spectra: a method based on time averaging over short, modified periodograms," *IEEE Transactions on audio and electroacoustics*, vol. 15, no. 2, pp. 70–73, 1967.

[101] N. Kaur, H. Kaur, and J. Kaur, "Power spectral density analysis of wlan based ofdm system," *International Journal of Computer Applications*, vol. 68, no. 7, 2013.

[102] P. T. Hong, *Introduction to digital signal processing: Computer musically speaking.* World Scientific, 2009.

[103] H. Yamaguchi, "Active interference cancellation technique for mb-ofdm cognitive radio," in *34th European Microwave Conference, 2004.*, vol. 2, Oct 2004, pp. 1105–1108.

[104] M. Z. Afgani, H. Haas, H. Elgala, and D. Knipp, "Visible light communication using ofdm," in *Proceedings of the 2nd International Conference on Testbeds and Research Infrastructures for the Development of Networks and Communities.* IEEE, 2006, pp. 6–pp.